

# Methane oxidation and emission in Lake Lugano (southern Switzerland)

## A lipid biomarker and isotopic approach

**Inauguraldissertation**

zur

Erlangung der Würde eines Doktors der Philosophie

vorgelegt der

Philosophisch-Naturwissenschaftlichen Fakultät

der Universität Basel

von

Hendrik Jan Reynier Blees

aus Rotterdam, Den Niederlanden

Ede (Die Niederlande), 2015

Original document stored on the publication server of the University of Basel  
**edoc.unibas.ch**

This work is licenced under the agreement „Attribution Non-Commercial No  
Derivatives – 3.0 Switzerland“ (CC BY-NC-ND 3.0 CH). The complete text may be  
reviewed here: [creativecommons.org/licenses/by-nc-nd/3.0/ch/deed.en](https://creativecommons.org/licenses/by-nc-nd/3.0/ch/deed.en)

Genehmigt von der Philosophisch-Naturwissenschaftlichen  
Fakultät auf Antrag von

Prof. Dr. M.F. Lehmann (Dissertationsleiter)

Prof. Dr. T.I. Eglinton (Korreferent)

Basel, den 18. Juni 2013

Prof. Dr. Jörg Schibler  
Dekan



**Namensnennung-Keine kommerzielle Nutzung-Keine Bearbeitung 3.0 Schweiz**  
(CC BY-NC-ND 3.0 CH)

**Sie dürfen: Teilen** — den Inhalt kopieren, verbreiten und zugänglich machen

**Unter den folgenden Bedingungen:**



**Namensnennung** — Sie müssen den Namen des Autors/Rechteinhabers in der von ihm festgelegten Weise nennen.



**Keine kommerzielle Nutzung** — Sie dürfen diesen Inhalt nicht für kommerzielle Zwecke nutzen.



**Keine Bearbeitung erlaubt** — Sie dürfen diesen Inhalt nicht bearbeiten, abwandeln oder in anderer Weise verändern.

**Wobei gilt:**

- **Verzichtserklärung** — Jede der vorgenannten Bedingungen kann aufgehoben werden, sofern Sie die ausdrückliche Einwilligung des Rechteinhabers dazu erhalten.
- **Public Domain (gemeinfreie oder nicht-schützbar Inhalte)** — Soweit das Werk, der Inhalt oder irgendein Teil davon zur Public Domain der jeweiligen Rechtsordnung gehört, wird dieser Status von der Lizenz in keiner Weise berührt.
- **Sonstige Rechte** — Die Lizenz hat keinerlei Einfluss auf die folgenden Rechte:
  - Die Rechte, die jedermann wegen der Schranken des Urheberrechts oder aufgrund gesetzlicher Erlaubnisse zustehen (in einigen Ländern als grundsätzliche Doktrin des fair use bekannt);
  - Die **Persönlichkeitsrechte** des Urhebers;
  - Rechte anderer Personen, entweder am Lizenzgegenstand selber oder bezüglich seiner Verwendung, zum Beispiel für Werbung oder Privatsphärenschutz.
- **Hinweis** — Bei jeder Nutzung oder Verbreitung müssen Sie anderen alle Lizenzbedingungen mitteilen, die für diesen Inhalt gelten. Am einfachsten ist es, an entsprechender Stelle einen Link auf diese Seite einzubinden.



# Table of contents

---

Summary	1
<b>1 Introduction</b>	
1.1 The greenhouse gas methane	5
1.2 Methane isotope geochemistry	6
1.2.1 Isotope fractionation, enrichment and the delta-notation	6
1.2.2 Carbon isotope dynamics of methane	7
1.3 The biological methane cycle – I: Sources	8
1.3.1 Sources of atmospheric methane	8
1.3.2 Microbial methanogenesis	9
1.3.3 Production of methane in oxic surface waters	11
1.4 The biological methane cycle – II: Sinks	12
1.4.1 Aerobic methane oxidation	12
1.4.2 Methane, oxygen and niches for methanotrophs	14
1.4.3 Methane monooxygenase	14
1.4.4 Anaerobic oxidation of methane	15
1.4.5 Efflux from the surface water to the atmosphere	16
1.5 Lake Lugano	18
1.5.1 Lake Lugano – a model system for the study of lacustrine methane oxidation	18

1.5.2	The meromictic northern basin	18
1.5.3	The monomictic southern basin	20
1.6	Scope and outline	21
2	Micro-aerobic bacterial methane oxidation in the chemocline and anoxic water column of deep south-Alpine Lake Lugano (Switzerland)	
2.1	Abstract	25
2.2	Introduction	26
2.3	Methods	29
2.3.1	Study site	29
2.3.2	Sampling	30
2.3.3	Hydrochemical analyses	30
2.3.4	Dissolved methane	31
2.3.5	Methane oxidation rates	32
2.3.6	Sulfate reduction rates	34
2.3.7	Flux calculations in the water column	35
2.3.8	Particulate organic carbon	36
2.3.9	Biomarker analyses	36
2.3.10	DNA extraction, polymerase chain reaction and cloning	38
2.4	Results	39
2.4.1	Physical parameters, oxygen and nutrients	39
2.4.2	Methane	40
2.4.3	Methane oxidation rates in the water column	41
2.4.4	Sulfate reduction rates in the water column	43
2.4.5	Particulate organic carbon and lipid biomarkers	43
2.4.6	Phylogenetic analyses	45

2.5	Discussion	46
2.5.1	Anoxia in the water column	46
2.5.2	Methane distribution in the hypolimnion and identification of methane sinks	47
2.5.3	MOx at the oxic-anoxic interface	49
2.5.4	Methanotrophy in the anoxic hypolimnion	53
2.5.5	MOx potential in anoxic waters	55
2.5.6	Sources of O <sub>2</sub> in the anoxic hypolimnion	56
2.5.7	Scope for true anaerobic methane oxidation and isotopic constraints	57

### 3 Bacterial methanotrophs drive the formation of a seasonal anoxic benthic nepheloid layer in an alpine lake

3.1	Abstract	63
3.2	Introduction	64
3.3	Methods	66
3.3.1	Sampling site	66
3.3.2	Sampling	67
3.3.3	Hydrochemical analyses	67
3.3.4	Dissolved methane	67
3.3.5	Methane oxidation rates	68
3.3.6	Flux calculations in the water column	70
3.3.7	Particulate organic carbon	71
3.3.8	Biomarker analyses	71
3.3.9	Cell enumeration by epifluorescence microscopy	72
3.4	Results	74
3.4.1	Mixing, stratification and the development of the BNL	74

3.4.2	Hydrochemical analyses and methane $\delta^{13}\text{C}$	74
3.4.3	Turbulent diffusive fluxes of methane and oxygen and methane oxidation rates	75
3.4.4	POC and FA biomarkers – Concentrations and C- isotopic composition	77
3.4.5	Contribution of MOB to the BNL’s FA carbon pool	78
3.4.6	Cell enumeration by fluorescence microscopy	79
3.5	Discussion	80
3.5.1	Development of the BNL by bacterial in situ production	80
3.5.2	Type I methanotrophs dominate BNL biomass	84
3.5.3	Abundance of MOB and contribution to the organic carbon pool	86
3.5.4	Methanotrophic activity and oxygen consumption within the BNL	87
4	Surface water methane super-saturation and emission in Lake Lugano, southern Switzerland	
4.1	Abstract	93
4.2	Introduction	94
4.3	Methods	96
4.3.1	Study site	96
4.3.2	Sampling	97
4.3.3	Dissolved methane	97
4.3.4	Flux calculations	98
4.4	Results	101
4.4.1	Dissolved methane concentration and stable isotope composition	101

4.4.2	CH <sub>4</sub> fluxes	104
4.5	Discussion	106
4.5.1	Modes of CH <sub>4</sub> emission	106
4.5.2	Potential sources of surface water CH <sub>4</sub>	108
4.5.3	Spatio-temporal variability in CH <sub>4</sub> concentrations in the surface mixed layer	112
4.5.4	Absence of CH <sub>4</sub> oxidation in the surface layer	113
4.5.5	Spatio-temporal variability of CH <sub>4</sub> loss from the surface mixed layer	114
4.6	Conclusion	115
5	Conclusion and outlook	
5.1	Conclusions and implications	117
5.1.1	Aerobic methane oxidation potentials in anoxic waters – implications for water column (in)stability	118
5.1.2	The distribution of methane oxidation potentials in the anoxic hypolimnion	120
5.1.3	Implications of the south basin BNL for methane emission	120
5.1.4	The lack of methane oxidation in surface waters	121
5.2	Outlook	122
	Bibliography	127
	Acknowledgments	149

## List of figures

---

1.1	Global methane sources in per cent of the total atmospheric budget	9
1.2	Map of Lake Lugano	19
2.1	Hydrochemical profiles of O <sub>2</sub> concentration, CH <sub>4</sub> concentration and $\delta^{13}\text{C}$ in the water column and sediment, potential aerobic CH <sub>4</sub> oxidation rates, and concentration and $\delta^{13}\text{C}$ of FAs and POC	42
2.2	Water column concentration profiles of Fe(II) and Fe(III), total sulfide, SO <sub>4</sub> <sup>2-</sup> , and sulfate reduction rates	44
2.3	Rayleigh plot of CH <sub>4</sub> data from the anoxic water column of August and October 2009 and August 2010	45
2.4	Neighbour joining phylogenetic tree of translated amino acid sequences of <i>pmoA</i> gene clones from the oxic-anoxic interface (135 m) and anoxic deep water (170 m)	50
3.1	Turbidity and O <sub>2</sub> profiles through the water column	76
3.2	Water column CH <sub>4</sub> concentration and $\delta^{13}\text{C}$	76
3.3	CH <sub>4</sub> oxidation rates in the water column	78
3.4	Concentration and $\delta^{13}\text{C}$ of POC and FAs in the water column	85
3.5	Cell counts of total cells and MOB	86
4.1	Surface water CH <sub>4</sub> concentration in October 2011, May 2012, and October 2012	100

4.2	Temperature and CH <sub>4</sub> concentration and δ <sup>13</sup> C profiles in the upper 40 m of the water column in the central northern basin	103
4.3	Temperature and CH <sub>4</sub> concentration and δ <sup>13</sup> C profiles in the upper 40 m of the water column in the eastern part of the northern basin	104
4.4	Temperature and CH <sub>4</sub> concentration profiles in the upper 40 m of the water column in the vicinity of Lugano	105
4.5	Diffusive fluxes across the water – air boundary layer in October 2011, May 2012, and October 2012	109



## Summary

---

Methane is an important greenhouse gas in Earth's atmosphere. The sources of atmospheric methane are largely biogenic, being produced under anoxic conditions by methanogenic *Archaea*. Wetlands, which include lakes, are important contributors to the atmospheric methane budget, since they commonly feature anoxic sediments or bottom water. Methane oxidising bacteria at the interface between oxic and anoxic sediments and water limit the efflux of methane. Furthermore, in the oceans, methane is oxidised anaerobically by *Archaea*, in a process coupled to sulfate reduction. In freshwater environments, where sulfate concentrations are orders of magnitude lower, this process is not thermodynamically favourable, and archaeal anaerobic oxidation of methane is often absent. It has been proposed in certain lake environments, however, that anaerobic oxidation of methane does take place.

One lake in which anaerobic oxidation of methane was proposed is the northern basin of Lake Lugano, southern Switzerland. Anaerobic oxidation of methane in this basin is explored in chapter 2 of this PhD thesis. Indeed we found methane concentration and  $\delta^{13}\text{C}$  profiles characteristic of methane oxidation in the anoxic hypolimnion, more than 30 m below the interface between the oxic and anoxic waters. In addition,

microbial biomass at these depths showed  $\delta^{13}\text{C}$  signatures of methane-derived carbon ( $\delta^{13}\text{C}$ -values as low as  $-70\text{‰}$  in  $\text{C}_{16:1}$  fatty acids), indicating that methane is used as a carbon source. However, no methane oxidation took place in incubation experiments under anoxic conditions. Addition of alternative potential electron acceptors did not stimulate methane oxidation, and methane oxidation was only observed in the presence of oxygen. Instead, we propose that episodic introduction of oxygenated water into the anoxic hypolimnion sustains a community of aerobic methanotrophs.

Carbon derived from methane oxidation has been shown in several studies to constitute an important carbon input to aquatic ecosystems. In the studies reported in chapters 2 and 3, compound specific stable carbon isotope analysis of lipid biomarkers was used to trace methane-derived carbon through the ecosystems at redox interfaces and in the anoxic hypolimnion of Lake Lugano. In the monomictic southern basin (chapter 3), an anoxic benthic nepheloid layer develops during the period of water column stratification. This layer was found to be derived from microbial production in the hypolimnion. Methane oxidising bacteria constituted up to 30% of total microbial cell numbers in the nepheloid layer, and 77% – 96% of the organic carbon in this layer was methane-derived. High rates of aerobic methane oxidation at the top of the anoxic nepheloid layer led to an oxygen consumption that was greater than the downward diffusion, causing the anoxic nepheloid layer to expand. Bacterial aerobic methanotrophs migrate upwards through the water column with the interface between the oxic hypolimnion and the anoxic nepheloid layer.

The extent of emission of methane to the atmosphere depends on the totality of sinks and sources in the lake basin. In both the northern and the southern basin of Lake Lugano, large amounts of methane are emitted from the sediments into the bottom water. However, consumption by aerobic methanotrophs at the oxic-anoxic redoxcline is near complete, and during stratified conditions, no methane escapes to the epilimnion. On the other hand, methane super-saturation in the surface water was observed throughout the year. Chapter 4 describes the results of three mapping campaigns of surface water methane concentrations in the northern basin of Lake Lugano, in spring and autumn. Additionally, methane concentration and carbon isotopic composition were measured on depth profiles down to 40 m depth in transects across the lake basin. Methane fluxes to the atmosphere were calculated from surface water concentration and wind speed. At a standardised wind speed of  $1.6 \text{ m s}^{-1}$  (average wind speed during the period from May until October) fluxes to the atmosphere were significantly higher in autumn (44 and  $97 \mu\text{mol m}^{-2} \text{ d}^{-1}$  in October 2011 and October 2012, respectively) than in spring ( $7 \mu\text{mol m}^{-2} \text{ d}^{-1}$ , May 2012). This difference is in part due to higher concentrations in autumn than in spring, and in part a result of a stronger dependence of the transfer velocity on buoyancy flux when the surface water cools. The source of methane in the surface water could not be determined with certainty. It is possible that internal waves at the thermocline induce friction at the sediment-water interface in the littoral zone, which leads to increased outgassing of sedimentary methane. However, the northern basin of Lake Lugano has steep shores along large parts of the basin, which offer little space for deposition of sediments, and the possibility of in situ production of methane in the water column must be considered.



## Introduction

---

### 1.1 The greenhouse gas methane

The discovery of methane is credited to Alessandro Volta, who studied marsh gas on Lago Maggiore between 1776 and 1778. Methane is the main component of natural gas. Methane is also a trace gas in Earth's atmosphere. As a long-lived greenhouse gas (GHG), it plays an important part in the temperature regulation of our planet. Atmospheric methane concentrations – reconstructed from measurements on ice cores – have fluctuated between 320 and 790 parts per billion by volume (ppbv) over the past 420,000 years (Chappellaz et al. 1990; Petit et al. 1999). However, over the past centuries this concentration has increased from a pre-industrial level of 715 ppbv to a present day level of 1865 ppbv (Canfield et al. 2005). This increase has caused a rise in radiative forcing of  $0.48 \pm 0.05 \text{ W m}^{-2}$  (Forster et al. 2007). For the sake of comparison, GHGs are assigned global warming potentials (GWPs) relative to  $\text{CO}_2$ , the most famous, and after water vapour quantitatively the most important GHG. GWPs compare the integrated radiative forcing over a specified time horizon from a unit mass emission pulse. Thereby they allow comparison of the effects of GHG emissions on climate. The GWP of

methane is 25 times that of CO<sub>2</sub>, and thus the concentration increase observed in atmospheric methane contributes comparatively strongly to the total radiative forcing (0.48 W m<sup>-2</sup>, compared to 1.66 W m<sup>-2</sup> for CO<sub>2</sub>, Forster et al. 2007), making methane second only to CO<sub>2</sub> in terms of radiative forcing. Once methane is emitted to the atmosphere, the main sink is reaction with tropospheric OH (hydroxyl) radicals. This reaction produces HO<sub>2</sub> (perhydroxyl) radicals, which eventually react with ozone (O<sub>3</sub>) (Warneck 2000), i.e. methane oxidation in the troposphere may result in a decrease in tropospheric ozone concentrations. It is therefore important to identify and quantify methane sources and sinks.

## 1.2 Methane isotope geochemistry

### 1.2.1 Isotope fractionation, enrichment and the delta-notation

The studies on methane dynamics in Lake Lugano reported here rely heavily on carbon isotope studies. Atmospheric CO<sub>2</sub> contains about 1.1% of the heavier isotope <sup>13</sup>C and 98.9% <sup>12</sup>C. (Bio)chemical processes usually discriminate between lighter and heavier isotopes of an element, resulting in isotopic fractionation between substrate and product. This discrimination occurs due to slight differences in reaction speed between the lighter and heavier versions of an element, resulting in an enrichment of the heavier isotope in one pool, and a depletion in the other pool. The fractionation that occurs can be expressed as a fractionation factor:

$$\alpha_{A-B} = \frac{R_A}{R_B}$$

where R<sub>A</sub> and R<sub>B</sub> are the isotope ratios of the rare versus the common isotope in substrate A and product B. In the case of carbon, this becomes:

$$R = \frac{^{13}\text{C}}{^{12}\text{C}}$$

Since variations in  $\alpha$  values are very small, isotope enrichment is usually expressed as an enrichment factor in per mille (‰):

$$\varepsilon_{\text{A-B}} = (\alpha_{\text{A-B}} - 1) \times 1000 [\text{‰}]$$

The fractionation that occurs during a process, and the resulting isotope enrichment in the product, lead to differences in isotope ratios between various pools. This difference in isotopic composition can be expressed in per mille relative to a standard material with a known isotope ratio as:

$$\delta R = \left( \frac{R_{\text{sample}}}{R_{\text{standard}}} - 1 \right) \times 1000 [\text{‰}]$$

In the case of carbon, the standard reference material is Vienna Pee Dee Belemnite (VPDB). By expressing the isotope ratios in samples of various pools in our system in this way, we can infer the fractionation that took place during their chemical history.

### *1.2.2 Carbon isotope dynamics of methane*

When photosynthesis binds carbon from atmospheric  $\text{CO}_2$  into plant material, this is associated with isotope fractionations. The extent of the net isotope fractionation during photosynthesis depends on the photosynthetic pathway, with  $\text{C}_3$  carbon fixation leading to stronger (net fractionation around -20‰) and  $\text{C}_4$  carbon fixation leading to less pronounced (net fractionation around -5‰)  $^{13}\text{C}$ -depletion relative to  $\text{CO}_2$ . Biomass- $\delta^{13}\text{C}$  values of primary producers therefore show a relatively

wide range between -10‰ and -33‰ (for detailed reviews see Farquhar et al. 1989; Brugnoli and Farquhar 2000). During microbial methanogenesis, additional isotope fractionation takes place, which is superimposed on the source material. For acetate fermentation the enrichment factor is on the order of -25‰ to -35‰ relative to  $\delta^{13}\text{C}_{\text{acetate}}$ . Stronger carbon isotope fractionation is found in methanogenesis by carbonate reduction, leading to a  $^{13}\text{C}$ -depletion of more than 55‰ relative to  $\delta^{13}\text{C}_{\text{CO}_2}$  (Whiticar 1999). This leads to strong  $^{13}\text{C}$ -depletion in microbial methane, and this isotope depletion can serve as a tracer in a food web. For example, the methane oxidising bacteria that use this methane as a carbon source will bear a characteristic depleted carbon isotopic composition.

## **1.3 The biological methane cycle – I: Sources**

### *1.3.1 Sources of atmospheric methane*

The global atmospheric  $\text{CH}_4$  budget is dominated by biogenic sources (Fig. 1.1). The most important among these are natural wetlands (23% of the total budget), intestines of ruminants and termites (20%), rice fields (10%), and waste water treatment and landfills (11%) (Conrad 2007, 2009). This means that about 75% of the atmospheric  $\text{CH}_4$  budget originates from production by microorganisms (section 1.2.2). Other sources are release from fossil methane reservoirs (geologic methane) (Etiope and Klusman 2002; Walter Anthony et al. 2012),  $\text{CH}_4$  production under high temperature and pressure (thermogenic methane),  $\text{CH}_4$  production under UV-light stimulation in plant material (Keppler et al. 2006; Vigano et al. 2008), and de-methylation pathways in the surface ocean (Karl et al. 2008; Damm et al. 2010).

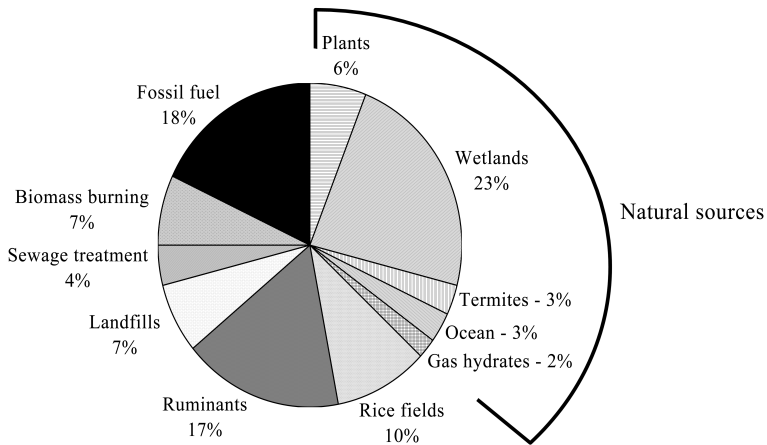


**Figure 1.1** Global methane sources in per cent of the total atmospheric budget (data from Conrad 2009).

The most important source of biogenic  $\text{CH}_4$  is methanogenesis by specialised *Archaea* in the final steps of decomposition of organic matter under anoxic conditions (Liu 2010; Sieber et al. 2010). This leads to high methane concentrations in anoxic sediments and waters. However, more than half of the biogenic  $\text{CH}_4$  produced in anoxic environments is oxidised by microbes before it reaches the atmosphere (Reeburgh 2007).

### 1.3.2 Microbial methanogenesis

Biogenic methane formation is performed by autotrophic or fermentative *Archaea*. These so-called methanogens are strict anaerobes that require redox potentials  $E_h < -200$  mV (Whiticar 1999). Their inability to tolerate higher redox potentials is mainly caused by the redox-sensitivity of the  $F_{420}$ -hydrogenase enzyme complex (Schönheit et al. 1981). Methanogens are part of a complex microbial community that

accomplishes the degradation of organic matter in several steps. Methanogens use a wide range of substrates, including CO<sub>2</sub>, acetate and methylated substrates. However, they cannot metabolise the more complex products of the primary fermentation reactions, and often rely on syntrophic microorganisms for the secondary fermentation to produce H<sub>2</sub>, CO<sub>2</sub> and acetate. These syntrophic fermenters in turn rely on methanogens to keep H<sub>2</sub> partial pressure low. A further group of fermenting bacteria, the homoacetogens, produces acetate from sugars, H<sub>2</sub> and CO<sub>2</sub>, reducing the potential for hydrogenotrophic methanogenesis. More than two thirds of the biogenic methane production in fresh water ecosystems therefore result from acetoclastic methanogenesis. In the acetoclastic methanogenesis reaction, the carboxyl group is oxidised to CO<sub>2</sub>, and the methyl group reduced to methane.

Members of only two genera are able to perform acetoclastic methanogenesis: *Methanosarcina* spp. and *Methanosaeta* spp. While *Methanosarcina* spp. are metabolically diverse, members of the genus *Methanosaeta* are specialised acetoclastic methanogens. *Methanosaeta* spp. display very high affinities for acetate, requiring minimal concentrations for growth of 7 – 70 μmol L<sup>-1</sup>. Therefore, *Methanosaeta* spp. can outcompete *Methanosarcina* spp. under low acetate conditions. The latter are often missing in lake sediments (Conrad 2007). Another important difference between the two genera lies in the energy expenditure for acetate activation. *Methanosaeta* spp. require twice the amount of energy as *Methanosarcina* spp. do for this step. This has important implications for the ecological niches, and also results in differences in isotopic fractionation (Penning et al. 2006). *Methanosaeta* spp. display smaller isotope fractionation than *Methanosarcina*, i.e. the resulting methane is isotopically relatively heavy (less negative δ<sup>13</sup>C) than

in other methanogenic pathways. The methane encountered in waters close to the sediment in Lake Lugano had a  $\delta^{13}\text{C}$  of about -70‰. This is on the light (more  $^{13}\text{C}$ -depleted) side of acetoclastic methanogenesis (Whiticar 1999). The methane in Lake Lugano may thus be a combination of acetoclastic and carbonate reduction, similar to the findings of Nüsslein et al. (2001), who reported a combination of acetoclastic and hydrogenotrophic methanogenesis in Lake Kinneret.

Methanogenesis is relatively more important in fresh water environments than in the marine realm. In marine waters and sediments, with higher sulfate concentrations, sulfate reducing bacteria can outcompete methanogens for  $\text{H}_2$  and acetate (Kristjansson et al. 1982). Although this has similarly been reported for  $\text{H}_2$  in freshwater environments (Lovley and Klug 1983), concentrations of  $\text{H}_2$  and acetate, released by fermentation, are generally high enough to support methanogenesis.

### *1.3.3 Production of methane in oxic surface waters*

A conundrum in the methane cycle is the widespread super-saturation of methane in surface waters, relative to atmospheric equilibrium (e.g. Lamontagne et al. 1973; Karl and Tilbrook 1994). The source of  $\text{CH}_4$  in oxygenated surface waters remains unclear. In coastal areas of oceans, and in lakes with extensive littoral sediments, sediment-derived  $\text{CH}_4$  may spread out in plumes through the surface water. However, this cannot explain  $\text{CH}_4$  super-saturation in open ocean environments, and some lakes lack littoral sedimentary environments that may act as a source for  $\text{CH}_4$ . This is especially the case in lakes with steep shores, such as the fjord-like drowned glacial valleys in alpine environments. It was therefore

hypothesised that methane may be produced in the surface water. However, the high redox potential of oxygenated waters poses a problem within the classical view of methanogenesis. Several mechanisms have been proposed, which fall into two categories: 1) production through canonical methanogenesis in anoxic microenvironments (Sieburth and Donaghay 1993; Karl and Tilbrook 1994; Rusanov et al. 2004), and 2) breakdown of methylated molecules under oxic conditions, resulting in the liberation of methane. The latter includes de-methylation of dimethylsulfoniopropionate (DMSP) (Damm et al. 2010) and methylphosphonates (MPn) (Karl et al. 2008). However, DMSP is a metabolite of marine phytoplankton and sea weeds, and it is not commonly found in fresh water environments. Furthermore, DMSP was found to promote CH<sub>4</sub> production under NO<sub>3</sub><sup>-</sup>-depleted conditions (Damm et al. 2010), which are less likely to occur in eutrophic lakes. The use of MPn as an alternative source of phosphorus could be important during P-limitation in the surface water during phytoplankton blooms. A potential pathway for the formation of MPn was recently described (Metcalf et al. 2012), but the organisms described are marine, rather than fresh-water species. CH<sub>4</sub> production was also shown to proceed in oxygenated fresh water (Grossart et al. 2011), but the pathway of formation of this CH<sub>4</sub> still awaits elucidation, and the environmental significance of all potential in situ pathways of CH<sub>4</sub> production is still unclear.

## **1.4 The biological methane cycle – II: Sinks**

### *1.4.1 Aerobic methane oxidation*

Methane oxidising bacteria (MOB), the so-called methanotrophs (Hanson and Hanson 1996), oxidise methane under oxic conditions. Most

methanotrophs are members of the alpha and gamma subdivisions of the *Proteobacteria* (Hanson and Hanson 1996). They are unique in their ability to use methane as their sole source of carbon and energy. Traditionally the methanotrophs are separated into two assemblages: type I and type II methanotrophs. The two types were originally distinguished based on morphological and physiological differences, formation of resting stages, and pathways of carbon assimilation (Whittenbury et al. 1970). Type I methanotrophs utilise the ribulose monophosphate (RuMP) pathway for assimilation of formaldehyde, while type II methanotrophs employ the serine pathway. A third type (type X) utilises the RuMP pathway, but also contains low levels of enzymes of the serine pathway, and ribulose-1,5-biphosphate carboxylase/oxygenase (RuBisCo), an enzyme involved in carbon fixation in the Calvin-Benson cycle. An important difference between type I, type II and type X methanotrophs is the composition of their cell membranes: the dominant fatty acid (FA) composition in type I and type X methanotrophs is of 16-carbon chain length, whereas type II methanotrophic membranes contain predominantly 18-carbon FAs. Most methanotrophs have dominant mono-unsaturated FAs, e.g. C<sub>16:1 $\omega$ 8</sub> (*Methylomonas* spp., *Methylobacter tundripaludum*), C<sub>16:1 $\omega$ 7</sub> (*Methylobacter* spp.) or C<sub>18:1 $\omega$ 8</sub> (type II methanotrophs) (Hanson and Hanson 1996; Wartiainen et al. 2006). *Methylococcus capsulatus* strains (type X) form an exception, containing primarily C<sub>16:0</sub> (Hanson and Hanson 1996).

Phylogenetically, the proteobacterial methanotrophs are further subdivided among six genera: *Methylococcus*, *Methylomicrobium*, *Methylobacter*, *Methylomonas* (the family *Methylococcaceae*), *Methylocystis* and *Methylosinus*. The type I group of methanotrophs contains species belonging to the *Methylococcaceae*, and the genera *Methylocystis* and *Methylosinus* belong to the type II methanotrophs.

#### *1.4.2 Methane, oxygen and niches for methanotrophs*

Type II methanotrophs are often absent from lake sediments and water column redox transition zones, where they are outcompeted by type I methanotrophs, which have a higher affinity for methane (Hanson and Hanson 1996). Methanotrophs in lakes are usually found to inhabit a narrow niche between oxic and anoxic environments, where O<sub>2</sub> and methane come together (e.g. Rudd et al. 1974). The lack of methane oxidation potential sometimes observed in more oxic environments (e.g. Rudd et al. 1976; Schubert et al. 2006) may be traced back to competition with heterotrophs (Van Bodegom et al. 2001). These have higher half saturation constants for O<sub>2</sub>, but also higher specific growth rates, and therefore methanotrophs can only compete with them at low O<sub>2</sub> concentrations. The low half saturation constant of methanotrophs for O<sub>2</sub>, combined with a lower specific growth rate, helps to explain their preference for low O<sub>2</sub> concentrations. However, the occurrence of aerobic methane oxidising bacteria on the anoxic side of the oxic-anoxic transition (e.g. Schubert et al. 2006), rather than on the sub-oxic side, is striking. This is explored further in chapter 2. Another unresolved question concerns the lack of methane oxidation in photic zone waters, even if these exhibit strong methane super-saturation (Murase and Sugimoto 2005), as also observed in chapter 4.

#### *1.4.3 Methane monoxygenase*

The first step in aerobic methane oxidation is catalysed by methane monoxygenases (MMOs) (Hanson and Hanson 1996). Monoxygenases are a specific group of oxidoreductases, i.e. enzymes that facilitate the electron transfer in biological redox reactions. More specifically, monoxygenases split the O=O bond in O<sub>2</sub>. One O-atom is reduced to

form water, and the other is incorporated into a hydroxyl group, forming methanol (CH<sub>3</sub>OH). There are two forms of methane monooxygenase: a soluble (sMMO) and a particulate, membrane bound form (pMMO). Since nearly all known methanotrophs, with the exception of the genus *Methylocella* (Dedysh et al. 2000), contain pMMO, the gene encoding the alpha subunit of pMMO, *pmoA*, can be used to construct phylogenetic relations between methanotrophs (Costello and Lidstrom 1999).

Despite their functional similarity, sMMO and pMMO show no structural homology (Holmes et al. 1995). An important difference lies in the elemental composition of their active sites. The functional centre of pMMO contains copper, in a mononuclear and a dinuclear centre (Lieberman and Rosenzweig 2005), whereas sMMO has a di-iron centre. With the exception of *Methylocella* spp. (Dedysh et al. 2000), all known methanotrophic bacteria contain pMMO. On the other hand, not all methanotrophs are able to synthesise sMMO (Hanson and Hanson 1996). In copper-rich environments, the production of sMMO is suppressed. Conversely, in copper-deficient environments sMMO is preferred (Conrad 2007). In natural systems, copper limitation may arise when communities grow to high cell densities (e.g. in the benthic nepheloid layer of the southern basin of Lake Lugano, chapter 3). This can have important implications for the isotope signature in the biomass, since sMMO expresses a smaller isotope fractionation than pMMO (Jahnke et al. 1999).

#### *1.4.4 Anaerobic oxidation of methane*

Around 5 – 20% of the methane flux from anoxic sediments, corresponding to  $20 - 100 \times 10^{12} \text{ g yr}^{-1}$ , is consumed by the process of anaerobic oxidation of methane (AOM) in marine sediments (Valentine

and Reeburgh 2000). The process of AOM has been elusive for decades. The ability of methanogens to oxidise methane besides producing it was documented early on (Zehnder and Brock 1979), and this was confirmed with laboratory studies, which showed that bacterial sulfate reduction could lower pore water  $H_2$  concentrations sufficiently for reverse hydrogenotrophic methanogenesis to be thermodynamically favourable, and net methane oxidation to occur (Hoehler et al. 1994). At the turn of the century it was shown that a consortium of methane oxidising *Archaea* and sulfate reducing bacteria mediate the anaerobic oxidation of methane (Hinrichs et al. 1999; Boetius et al. 2000a), but the obligate syntrophy was recently called into question (Milucka et al. 2012). Archaeal AOM is common in marine sediments, but reports of its occurrence in freshwater environments are scarce (Eller et al. 2005b; Schubert et al. 2011; Deutzmann and Schink 2011). Nitrite-dependent AOM by *Bacteria* of the NC10 phylum (Ettwig et al. 2008) acts as a methane sink in anoxic eutrophic environments, but its environmental significance is still unclear. Alternative electron acceptors besides sulfate and nitrate include iron and manganese (Beal et al. 2009; Crowe et al. 2010). However, the occurrence of AOM in lakes is still a topic of debate.

#### *1.4.5 Efflux from the surface water to the atmosphere*

The fate of methane in oxic surface waters is uncertain. It has been observed that aerobic methane oxidation is inhibited by sunlight (e.g. Murase and Sugimoto 2005), which correlates with the absence of methane oxidation in the photic zone, even if these have high methane concentrations (Murase et al. 2005). The only remaining ‘sink’ for methane in the lake surface water that escapes oxidation is efflux to the

atmosphere. The efflux (in  $\text{mmol m}^{-2} \text{d}^{-1}$ ) is determined by the difference between the methane concentration ( $\text{mmol m}^{-3}$ ) in the surface layer ( $C_w$ ) and the equilibrium concentration ( $C_{eq}$ ), and by the transfer velocity,  $k$  (Liss and Slater 1974):

$$F = k (C_w - C_{eq})$$

The equilibrium concentration is the concentration we would find in the water if it were allowed to equilibrate completely with the atmosphere above the lake, and depends on the atmospheric concentration and the water temperature. The transfer velocity, in  $\text{m d}^{-1}$ , is a measure for the depth of water that equilibrates with the surface layer per unit time (Cole et al. 2010). Traditionally,  $k$  is assumed to depend mainly on the wind speed above the water (e.g. Cole and Caraco 1998; Crusius and Wanninkhof 2003). However, other processes also contribute to the transfer velocity, and it is increasingly being recognised that the buoyancy flux ( $\beta$ ) plays an important role (MacIntyre et al. 2001). The buoyancy flux can be pictured as rising and sinking of parcels of water in response to changes in buoyancy, which may arise from temperature changes in the surface layer. For example, cooling of the surface layer increases its density, which causes the underlying water to rise to the surface and replace it. MacIntyre et al. (2010) found that  $k$  was independent of  $\beta$  when  $\beta$  was positive, and negatively correlated when  $\beta$  was negative. In practical terms this means that when the lake surface is cooling, the flux across the air – water interface increases, because the thermal stratification becomes unstable, and renewal of water in the boundary layer is increased. On the other hand, thermal stratification becomes increasingly stable in a heating lake, and therefore buoyancy no longer has a positive influence on the gas efflux.

## 1.5 Lake Lugano

### 1.5.1 Lake Lugano – a model system for the study of lacustrine methane oxidation

The following chapters will focus on methane consumption in the water column (chapters 2 and 3) and emission from the surface waters (chapter 4) of Lake Lugano. Lake Lugano is a south-alpine lake located on the Swiss-Italian border, at an elevation of 271 m above sea level. It consists of two basins, separated by a natural dam (Fig. 1.2) – the terminal moraine of glaciated times. The connection between the basins is narrow and shallow, and the two basins can be regarded as separate lakes. The northern and southern basins have different mixing regimes, making Lake Lugano an ideal model system for studying the influence of deep water processes on methane oxidation. The upper water layer (epilimnion) in the southern basin mixes with the lower water layer (hypolimnion) once a year, i.e. the basin is *monomictic* (“once-mixing”). In contrast, the epilimnion and hypolimnion of the northern basin do not mix, and the lake is said to be *meromictic* (from Greek μέρος, meaning “part”).

### 1.5.2 The meromictic northern basin

The northern basin is a drowned glacial valley. This is reflected in the bathymetry: due to the typical U-shaped glacial valley morphology, the shores are steep, especially in the central part of the basin. As a result there is little space for deposition of sediments along the shores. The deepest point in the northern basin has a water depth of 288 m. The water input by tributaries is relatively small, resulting in a long mean hydrological residence time of around 12 years (Aeschbach-Hertig et al.

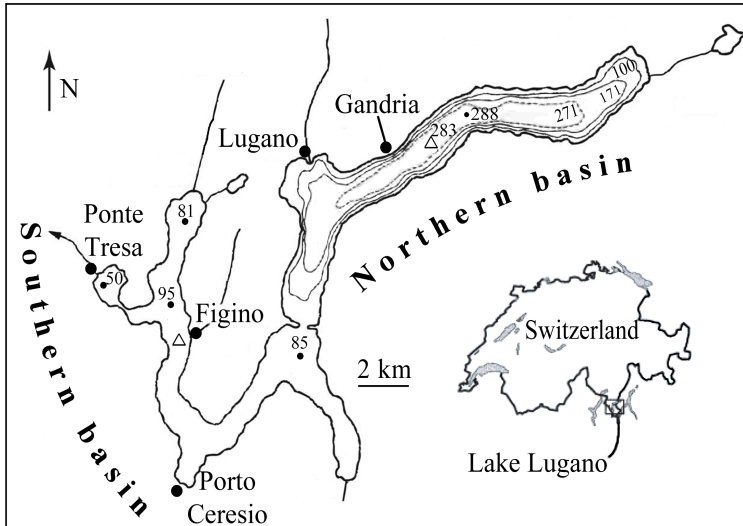


**Figure 1.2** Map of Lake Lugano. The sampling sites in the northern and southern basins are indicated by triangles. Water depths are shown in m (map adapted from Barbieri and Polli (1992))

2007). During the 20<sup>th</sup> century the lake has been subject to intense eutrophication (Barbieri and Simona 2001). The trophic evolution of the lake has been studied in detail through efforts of the Swiss Federal Institute of Aquatic Science and Technology (EAWAG), the Istituto Italiano di Idrobiologia, the International Commission for the protection of Italian-Swiss waters, and since 1980 the Laboratorio Studi Ambientali (LSA) of the environmental department of the canton Ticino and the University of Applied Sciences and Arts of Southern Switzerland (SUPSI). Studies performed in the 1940s and 1950s reported low oxygen concentrations of 1-3 mg L<sup>-1</sup> in the bottom water (Barbieri and Simona 2001). Furthermore, decreasing nitrate and increasing ammonium concentrations were reported, and the meromictic character of the lake

was first described. Oxygen in the deep water (below 100 m) disappeared entirely in 1960-1961. From 1967 until 2005 no oxygen was found in the deep water (Barbieri and Mosello 1992; SUPSI unpublished data).

Following two consecutive cold winters in 2005 and 2006 the northern basin experienced a complete overturn, with water renewal down to the bottom water (Holzner et al. 2009). The associated introduction of oxygen to the hypolimnion led to the complete oxidation of reducing compounds – notably ammonium and methane (SUPSI unpublished data). Anoxia re-established below 135 m in 2007.

### *1.5.3 The monomictic southern basin*

The southern basin of Lake Lugano is located on the downstream side of the old terminal moraine. This former pro-glacial valley is less deep than the northern basin (95 m), and it has a mixing period in mid to late winter, between January and March. During the summer months a layer of increased particle load develops in the bottom waters. Such a layer, often detected through the increase in optical backscatter it causes, is termed a nepheloid layer, after the Greek word νέφος (nephos), meaning “cloud”, for its cloud-like appearance of floating particles. Since the nepheloid layer in the southern basin of Lake Lugano develops from the bottom sediment up, it is called a *benthic* nepheloid layer (BNL). This layer is anoxic, and the organic carbon in the BNL is strongly carbon-isotopically depleted, as described by Lehmann et al. (2004), which indicates that methanotrophs may play an important role in carbon cycling within the BNL.

## 1.6 Scope and outline

The following chapters address two important elements of the lacustrine “methane cycle”: microbial oxidation, and emission from the surface water to the atmosphere. As outlined in the preceding sections, this is only part of the path of methane through natural systems, sandwiched between methanogenesis (section 1.2) and the atmospheric transformations (section 1.1). However, since more than half of the methane produced in deep lake sediments is oxidised by microbial methane oxidation (Bastviken et al. 2008), this represents an important constraint on the efflux to the atmosphere. Lake Lugano represents an excellent model system to study methane oxidation under different mixing regimes. The questions that motivated the studies presented here were:

- Does a methane sink exist within the anoxic hypolimnion of the northern basin of Lake Lugano?
- If so, does this sink represent archaeal AOM, bacterial AOM, or an as yet unidentified methane sink in anoxic waters?
- Which organisms mediate methane oxidation in the northern and southern basins of Lake Lugano?
- To what extent do methanotrophs provide a carbon source for the ecosystem in the benthic nepheloid layer of the southern basin of Lake Lugano?
- How efficient is the microbial methane filter in the meromictic northern and monomictic southern basins of Lake Lugano?
- Does Lake Lugano represent a source of atmospheric methane, and does this source undergo seasonal variability?

**Chapter 2** describes methane oxidation in the deep hypolimnion of the northern basin of Lake Lugano. Methane diffusing from the sediments is oxidised at the permanent redoxcline in 135 m water depth. However, early observations of methane distribution in the water column (Liu et al. 1996) indicated a potential sink for methane in the anoxic water. Similar observations were made after anoxia re-established in the water column following the turnover in 2005. Initially, AOM was proposed as a methane sink in the anoxic hypolimnion (Liu et al. 1996). However, in this chapter arguments against AOM in the water column of Lake Lugano are discussed. Instead, an aerobic methanotrophic community resides deep within the formally anoxic water column.

**Chapter 3** presents a seasonally recurring chemocline and layer of increased microbial abundance in the bottom water of the southern basin of Lake Lugano. This layer, characterised by high concentrations of suspended organic matter, is anoxic, and grows throughout the period of water column stratification. Methane oxidation at the top of this layer is the primary sink for  $O_2$  in the bottom water. Since  $O_2$  consumption proceeds faster than the downward diffusive flux can sustain, the methanotrophic ecosystem at the redoxcline migrates upwards through the water column.

**Chapter 4** deals with methane super-saturation in the surface water of the northern basin, and emission to the atmosphere. Methane concentrations were found to be within a typical range for lake surface waters, but variable in space and time. In spring, concentrations were low, with an average of  $16 \text{ nmol L}^{-1}$ . In autumn, we found higher concentrations, with averages of  $57 \text{ nmol L}^{-1}$  and  $45 \text{ nmol L}^{-1}$  in two

consecutive years. At these concentrations the surface water was always supersaturated with respect to atmospheric equilibrium. In this chapter calculations of the diffusive flux of methane to the atmosphere are presented, with consideration of the changing buoyancy flux in response to the seasonally changing thermal stratification of the surface water. The results identify Lake Lugano as a seasonally variable source of atmospheric methane. Furthermore, no biological methane sink in the form of methane oxidation was found within the surface mixed layer, indicating that the fate of the entire surface water methane inventory is ultimately emission to the atmosphere. The results of this study show that even though nearly the entire methane flux from the deep water is oxidised within the hypolimnion, Lake Lugano does present a source of atmospheric methane. It is therefore important to consider both surface and deep water processes in the study of lacustrine methane dynamics.

---

Chapter 2 was published in *Limnology & Oceanography*:

Blees, Jan, Helge Niemann, Christine B. Wenk, Jakob Zopfi, Carsten J. Schubert, Mathias Kirf, Mauro L. Veronesi, Carmen Hitz and Moritz F. Lehmann. Micro-aerobic bacterial methane oxidation in the chemocline and anoxic water column of deep south-Alpine Lake Lugano (Switzerland). *Limnol. Oceanogr.* **59**: 311–324. doi: 10.4319/lo.2014.59.2.0311

## Micro-aerobic bacterial methane oxidation in the chemocline and anoxic water column of deep south-Alpine Lake Lugano (Switzerland)

---

### 2.1 Abstract

We measured seasonal variations in the vertical distribution of methane concentration, methane oxidation rates, and lipid biomarkers in the northern basin of Lake Lugano. Methane consumption below the oxic-anoxic interface co-occurred with concentration maxima of  $^{13}\text{C}$ -depleted  $\text{C}_{16}$  fatty acid biomarkers (with  $\delta^{13}\text{C}$ -values as low as  $-70\text{‰}$ ) in the anoxic water column, as well as characteristic  $\delta^{13}\text{CCH}_4$  profiles. Although we cannot rule out potential anaerobic oxidation of methane, we argue that the conspicuous methane concentration gradients are primarily driven by (micro-)aerobic methane oxidation (MOx) below the chemocline. We measured a strong MOx potential throughout the anoxic water column, while MOx rates at in situ  $\text{O}_2$  concentration  $>10 \text{ nmol L}^{-1}$  were undetectable. Similarly, we found MOx-related biomarkers and gene sequences encoding the particulate methane monooxygenase (*pmoA*) in the anoxic, but not in the oxic water. The mechanism of (episodic) oxygen supply sustaining the MOx community in anoxic waters is still uncertain. Our results indicate that a bacterial methanotrophic community is

responsible for the methane consumption in Lake Lugano, without detectable contribution from archaeal methanotrophs. Bacterial populations that accumulated both at the suboxic-anoxic interface and in the deeper anoxic hypolimnion, where maximum potential MO<sub>x</sub> rates were observed throughout the year (1.5 to 2.5  $\mu\text{mol L}^{-1} \text{d}^{-1}$ ) were mainly related to *Methylobacter* sp. Close relatives are found in lacustrine environments throughout the world, and their potential to thrive under micro- and anoxic conditions in Lake Lugano may imply that micro-aerobic methane oxidation is important in methane cycling and competition for methane and oxygen in stratified lakes worldwide.

## 2.2 Introduction

The concentration of atmospheric methane (CH<sub>4</sub>) has increased dramatically since pre-industrial times, from ~700 parts per billion volume (ppbv) to ~1700 ppbv (IPCC 2007). On a per-mol basis and on a 100-year time horizon, CH<sub>4</sub> is a 25 times more efficient greenhouse gas than CO<sub>2</sub>, contributing ~18% to the total radiative forcing of long-lived greenhouse gases (IPCC 2007). Consequently, an in-depth knowledge of the CH<sub>4</sub> cycle is paramount to the assessment of present-day and future climate change. Natural CH<sub>4</sub> sources to the atmosphere are very important, constituting about 30% of total CH<sub>4</sub> emissions (Chen and Prinn 2006). Particularly wetlands and lakes are major CH<sub>4</sub> emitters, of which the latter contribute up to 16% of total natural sources (Bastviken et al. 2004). CH<sub>4</sub> is produced by specialized *Archaea* (methanogens) in anoxic environments, such as lacustrine sediments, where it typically accumulates to high concentrations. In well-mixed lakes, a significant fraction of CH<sub>4</sub> is subsequently consumed with oxygen at the sediment-

water interface (Bastviken et al. 2002). During stratified conditions, however, the flux of oxygen across density gradients in the water column is hindered, so that aerobic processes lead to oxygen depletion in bottom waters (Diaz and Rosenberg 2008; Zaikova et al. 2010). Consequently, CH<sub>4</sub> is liberated into the water column, where it may accumulate. In lakes, density stratification is typically interrupted by one or two mixing events a year (mono- or dimictic regimes, respectively). Alternatively, lakes can exhibit permanent stratification (meromixis) with a stable chemocline. Particularly narrow and deep lakes, with a low surface to volume ratio, or systems experiencing little physical disturbance (e.g. wind stress) are prone to developing meromixis.

In contrast to the marine realm, where anaerobic oxidation of CH<sub>4</sub> (AOM) coupled to sulfate (SO<sub>4</sub><sup>2-</sup>) reduction (S-AOM) is an efficient sink for CH<sub>4</sub> (Knittel and Boetius 2009), the S-AOM CH<sub>4</sub> filter does not work in sulfate-depleted freshwater reservoirs, and CH<sub>4</sub> was long thought to be oxidized exclusively by aerobic methane oxidizing bacteria (MOB) (Hanson and Hanson 1996; Trotsenko and Murrell 2008). Indeed, maximum MOB abundances and highest rates of aerobic methanotrophy (MOx) are found at oxic-anoxic interfaces in sediments and water columns (Rudd et al. 1976). Yet biogeochemical indications of CH<sub>4</sub> consumption in anoxic freshwater environments exist (Panganiban et al. 1979; Schubert et al. 2010; Crowe et al. 2010). To some degree, this could be attributed to S-AOM operating at relatively low SO<sub>4</sub><sup>2-</sup> concentrations. However, the recent discovery of anaerobic CH<sub>4</sub> oxidizing bacteria utilizing molecular oxygen from the conversion of NO<sub>2</sub><sup>-</sup> to N<sub>2</sub> and O<sub>2</sub> (Ettwig et al. 2009, 2010) and, so far unidentified, microbial communities utilizing Fe or Mn as an electron acceptor for CH<sub>4</sub> oxidation (Beal et al. 2009; Crowe et al. 2010; Sivan et al. 2011) raise the question

whether CH<sub>4</sub> stored in these water bodies may be consumed through processes other than S-AOM and MOx. Finally, if MOB in fresh water bodies rely on O<sub>2</sub> as the oxidant, it remains uncertain to which extent aerobic MOB are able to survive, and possibly thrive, under micro-oxic or anoxic conditions.

Possible differences between the isotope effects of (micro-)aerobic and anaerobic CH<sub>4</sub> oxidation may result in distinct shifts in the isotopic composition of residual CH<sub>4</sub>, which can in turn be used diagnostically to distinguish the methanotrophic modes at work. While the C-isotopic fractionation of MOx has been the subject of intensive field and laboratory studies (Whiticar and Faber 1986; Jahnke et al. 1999), the isotope effects of AOM, or the isotopic expression of MOx under micro-oxic conditions or severe substrate limitation are not well constrained.

The northern basin of Lake Lugano provides a natural laboratory to study CH<sub>4</sub> oxidation under different redox regimes in a freshwater environment, as it is characterized by meromixis and features a CH<sub>4</sub>-rich hypolimnion (Barbieri and Mosello 1992; Barbieri and Simona 2001). Previous work in the northern basin of Lake Lugano (Liu et al. 1996) has shown deep hypolimnetic CH<sub>4</sub> concentration profiles and enrichment of <sup>13</sup>C in the residual CH<sub>4</sub> pool, suggesting a CH<sub>4</sub> sink well within the anoxic part of the water column. In this study, we question whether this apparent CH<sub>4</sub> sink represents AOM, or rather micro-aerobic CH<sub>4</sub> oxidation at sub-micromolar O<sub>2</sub> concentrations that are undetectable by traditional O<sub>2</sub> concentration measurement techniques. We applied an interdisciplinary approach that combines lipid biomarker, stable and radioactive isotope methods, and we made use of a newly developed O<sub>2</sub> sensing system that allows determination of sub-micromolar O<sub>2</sub> concentration. The aims of this study were 1) to quantify rates of CH<sub>4</sub> oxidation in the epi-, meta- and

hypolimnion of the lake's northern basin and thus to evaluate the importance of potential modes of CH<sub>4</sub> oxidation, 2) to identify the methanotrophic community, and 3) to study the effect of micro-aerobic CH<sub>4</sub> consumption on the C-isotopic composition of the hypolimnetic CH<sub>4</sub> and organic carbon pools. We show that, despite seemingly clear indications of AOM in the geochemical profiles, micro-aerobic CH<sub>4</sub> oxidation is the prime mode of CH<sub>4</sub> oxidation in the northern basin of Lake Lugano.

## **2.3 Methods**

### *2.3.1 Study site*

Lake Lugano is a south-alpine lake located on the Swiss-Italian border, at an elevation of 271 m above mean sea level. It consists of two basins, separated by a natural dam. The northern basin is a former glacial valley with a fjord-like bathymetry, surrounded by steep mountains. The maximum water depth is 288 m. The water input by tributaries is relatively small, resulting in a long mean hydrological residence time of ~12 years (Aeschbach-Hertig et al. 2007). A small surface to volume ratio, low average wind speeds, and ongoing eutrophication have led to the development of meromixis, with a permanent chemocline in intermediate water depths and an anoxic hypolimnion since the early 1960s (Barbieri and Mosello 1992; Aeschbach-Hertig et al. 2007). The sole exception to this was a brief period of deep water ventilation in 2005 and 2006 (Holzner et al. 2009), after which the chemocline re-established at 135 m water depth.

### 2.3.2 Sampling

Sampling campaigns were conducted during different seasons in April 2008, March, June, August, October 2009, January, August 2010, September, October 2011, and January and May 2012 (Table 2.1). All sampling casts were performed in the middle of the lake's northern basin (46.01°N, 9.02°E). Temperature, conductivity, O<sub>2</sub> concentration, pH, and turbidity were measured with a conductivity, temperature and depth (CTD) device (Idronaut Ocean Seven 316 Plus, Idronaut). O<sub>2</sub> concentration measurements of the CTD's O<sub>2</sub> sensor were calibrated against Winkler titration measurements, and the detection limit was determined at 1 μmol L<sup>-1</sup>. In addition, high-resolution O<sub>2</sub> concentration measurements with nanomolar sensitivity were performed across the oxic-anoxic interface using highly amplified amperometric sensors and oxygen optodes (Kirf et al. 2014). The in situ detection limit (2 × standard deviation) of the amperometric oxygen microsensor was 4.5 ± 0.7 nmol L<sup>-1</sup>. Water samples were collected in 5 or 10 L Niskin bottles, and subsamples were taken directly from the Niskin bottle through silicon tubing. A sediment core was collected with a gravity corer in April 2008. Sediments for CH<sub>4</sub> analyses were extracted from the core liner through pre-drilled holes, using cut-off syringes, at a 5 cm resolution.

### 2.3.3 Hydrochemical analyses

Samples for Fe(II) and total sulfide were fixed on board, and concentrations were determined photometrically. Dissolved Fe(II) was quantified using the 'bipyridine method' (Hill 1930). Additional unfiltered water samples were collected for determination of total Fe through reduction of oxidized Fe-species with hydroxylamine

hydrochloride prior to the analysis of the evolved Fe(II) with the bipyridine method. Fe(III) concentration was then calculated as the difference between Fe(II) and total Fe. Samples for total sulfide were fixed in aqueous zinc acetate solution (1% final concentration) and subsequently analysed using the ethylene blue method (Rees et al. 1971).  $\text{SO}_4^{2-}$  samples were measured by ion chromatography.

#### *2.3.4 Dissolved methane*

Water column samples for the determination of  $\text{CH}_4$  concentration and its stable C-isotopic composition were collected in 500 mL glass bottles, which were immediately sealed with thick butyl rubber stoppers. Subsequently, a 10 mL headspace was introduced, and 10 mL of aqueous NaOH solution (50%, w:v) were added in exchange with sample in order to stop microbial activity and to expel dissolved  $\text{CH}_4$  into the headspace. For concentration and  $\delta^{13}\text{C}$ - $\text{CH}_4$ -measurements in the sediment, samples were amended immediately with 5 mL NaOH (2.5%, w:v) in 20 mL butyl rubber-sealed glass vials.  $\text{CH}_4$  concentrations were determined with a gas chromatograph (GC, Agilent 6890N) equipped with a 30 m Supelco Carboxen 1010 porous layer open tubular (PLOT) column (0.53 mm inner diameter) and a flame ionization detector (FID).  $^{13}\text{C}$ : $^{12}\text{C}$  ratios were analysed with an isotope ratio mass spectrometer (IRMS, Isoprime) subsequently to gas chromatography (Isoprime TraceGas) and pre-concentration with a cryo-trap. Corrections were made for linearity effects and instrument drift. Stable C isotope ratios are reported in the conventional  $\delta$ -notation (in ‰) relative to Vienna Pee Dee Belemnite (VPDB).  $\text{CH}_4$   $\delta^{13}\text{C}$ -values reported here have an analytical error of  $\pm 1\%$ .

Apparent kinetic isotope enrichment factors were calculated using a closed system approach (Mariotti et al. 1981):

$$\varepsilon_{\text{closed}} = \frac{10^3 \ln \frac{10^{-3} \delta_s + 1}{10^{-3} \delta_{s,0} + 1}}{\ln f} \quad \text{Eq. 2.1}$$

and according to an open system approach (Sigman et al. 2003):

$$\varepsilon_{\text{open}} = \frac{\delta_s - \delta_{s,0}}{1 - f} \quad \text{Eq. 2.2}$$

where  $\varepsilon$  is the enrichment factor (in ‰) between product and substrate,  $\delta_s$  and  $\delta_{s,0}$  are the  $\delta^{13}\text{C}$ -values of  $\text{CH}_4$  at a considered depth and the  $\delta^{13}\text{C}$  of the source  $\text{CH}_4$ , respectively, and  $f$  is the fraction of  $\text{CH}_4$  remaining.

### 2.3.5 Methane oxidation rates

Triplicate samples for methane oxidation rate (MOR) measurements were collected in 25 mL crimp top serum vials. Immediately after sampling, the vials were capped bubble-free with grey bromo-butyl stoppers (Helvoet Pharma, Belgium). Samples were stored cooled (4°C) for transport to the laboratory. Radio-tracer was added about 24 h after sampling by injecting a 10  $\mu\text{L}$  bubble of  $^{14}\text{CH}_4\text{:N}_2$  gas (~10 kBq). The bubble dissolved within an hour. Samples were incubated at in situ temperature. Time series of up to 4.5 days (time points at 10, 30, 50, 72, 104 hours after incubation start) were performed on two depths in each profile in order to determine linearity of  $\text{CH}_4$  turnover, and single end point measurements were used for the remaining depths. All samples were incubated in triplicate. Killed controls were analysed for each

profile. Similar to CH<sub>4</sub> concentration measurements, the incubation was terminated by fixing the samples with 0.5 mL of aqueous NaOH solution and introducing 5 mL headspace. CH<sub>4</sub> concentration in the headspace was quantified by GC-FID. Separation of remaining <sup>14</sup>CH<sub>4</sub> in the headspace and the produced <sup>14</sup>CO<sub>3</sub><sup>2-</sup> in the aqueous phase of the fixed sample was achieved by flushing the headspace with a continuous stream of air (30 mL min<sup>-1</sup>, for 30 min). The stripped <sup>14</sup>CH<sub>4</sub> was further transported through an oxidation reactor (quartz tubing filled with CuO at 850°C), where it was transformed into <sup>14</sup>CO<sub>2</sub>, which was then trapped in a methoxyethanol:phenylethylamine (7:1 v:v, 8 mL) solution (Treude et al. 2003). The alkaline water phase was subsequently acidified to pH <1, in order to shift the carbonate equilibrium towards CO<sub>2</sub>. The liberated <sup>14</sup>CO<sub>2</sub> was then purged and trapped as described above. <sup>14</sup>C-activity was analysed by liquid scintillation counting. Recovery was >95%, as determined with synthetic H<sup>14</sup>CO<sub>3</sub><sup>-</sup>. Finally, any remaining <sup>14</sup>C-activity in the (acidified) water was determined in an 8 mL aliquot by liquid scintillation counting.

The first order rate constant (*k*) was calculated from the activity of the three carbon pools:

$$k = \frac{A_{\text{CO}_2} + A_{\text{R}}}{A_{\text{CH}_4} + A_{\text{CO}_2} + A_{\text{R}}} \times \text{d}^{-1} \quad \text{Eq. 2.3}$$

where A<sub>CH<sub>4</sub></sub>, A<sub>CO<sub>2</sub></sub>, and A<sub>R</sub> represent the radioactivity of CH<sub>4</sub>, CO<sub>2</sub> and the remaining radioactivity (which includes biomass and metabolic intermediates), respectively. Potential CH<sub>4</sub> oxidation rates (MOR) were then calculated assuming first order kinetics:

$$\text{MOR} = k \times [\text{CH}_4], \text{ in } \mu\text{mol L}^{-1} \text{ d}^{-1} \quad \text{Eq. 2.4}$$

where  $[CH_4]$  is the  $CH_4$  concentration at the start of incubation, calculated from the concentration at the end of the incubation period and from the turnover fraction. Even in originally anoxic samples, minor  $O_2$  contamination took place during tracer injection and diffusion of trace amounts of  $O_2$  from the butyl elastomer could not be prevented, so that incubations essentially took place under micro-oxic or suboxic conditions. Therefore, and since our analyses revealed the presence of aerobic methanotrophic communities, but not of microbes known to be involved in anaerobic modes of methane oxidation (see discussion below), reported rates should consequently be considered as potential aerobic MOR.

#### *2.3.6 Sulfate reduction rates*

Samples for sulfate reduction rate (SRR) measurements were collected as described for MOR incubations. Incubations were amended with 10  $\mu$ L aqueous  $^{35}SO_4^{2-}$  solution (100 kBq) and incubated for up to 24 days at in situ temperature. All samples were incubated in triplicate. Incubations were terminated and produced sulfide was fixed by addition of 15 mL aqueous zinc acetate solution (20%, w:v) in 50 mL centrifuge tubes. Artificial sediment (kaolinite) was then added to facilitate precipitation of zinc sulfide, and samples were stored at  $-20^\circ C$  until further analysis. Sulfate reduction rates were determined via single-step cold chromium distillation and liquid scintillation counting of reduced  $^{35}S$  compounds and remaining  $^{35}SO_4^{2-}$  tracer according to Kallmeyer et al. (2004). Rates were calculated analogously to the approach described for  $CH_4$  oxidation rates (Eqs. 2.3 and 2.4).

### 2.3.7 Flux calculations in the water column

Vertical turbulent-diffusive fluxes of solutes in the water column were calculated as:

$$F_z = -K_z \frac{dC}{dz} \quad \text{Eq. 2.5}$$

where  $F_z$  is the vertical flux of the solute,  $K_z$  is the vertical eddy diffusivity, and  $dC/dz$  is the solute concentration gradient over depth interval  $z$ . For August 2010,  $K_z$  was estimated for the depth interval between 135 and 145 m water depth by dividing the  $\text{CH}_4$  flux through the horizontal section (from methane oxidation rate measurements, under the simplified assumption of a 1 m thick reaction zone) by the  $\text{CH}_4$  concentration gradient (Zopfi et al. 2001). The estimated value of  $3.3 \times 10^{-5} \text{ m}^2 \text{ s}^{-1}$  agrees well with previously reported values for the northern basin of Lake Lugano (Wüest et al. 1992).  $K_z$  varies with depth. It depends on the buoyancy frequency, and can be expressed as (Gargett 1984):

$$K_z = a_0 \times \left( \frac{-g}{\rho_z} \times \frac{d\rho}{dz} \right)^{-0.5} \quad \text{Eq. 2.6}$$

where  $g$  is the standard gravity,  $\rho_z$  is the density at depth  $z$  (145 m), and  $d\rho/dz$  is the density gradient between 135 and 145 m water depth. We then solved Eq. 2.6 for  $a_0$  and obtained an  $a_0$  of  $3.2 \times 10^{-8} \text{ m}^2 \text{ s}^{-2}$ , which is characteristic for restricted basins (Gargett 1984). The factor  $a_0$  is a system-specific constant, which we then used to calculate  $K_z$  at other depths, based on density profiles alone, allowing calculation of the turbulent-diffusive flux of  $\text{CH}_4$  and  $\text{O}_2$  towards the chemocline throughout the year.

### 2.3.8 Particulate organic carbon

Particulate organic carbon (POC) was analysed from lake water samples (~5 L) filtered through pre-combusted glass fiber filters (GF-F, Whatman) by applying a gentle vacuum ( $\sim 0.5 \times 10^5$  Pa). Filters were then wrapped in aluminium foil and stored frozen ( $-20^\circ\text{C}$ ). Bulk stable carbon isotopic composition of POC was determined on filter pieces of  $1\text{ cm}^2$ , which had been decarbonated in a desiccator with fumes of concentrated HCl. The remaining organic carbon was combusted to  $\text{CO}_2$  in a Flash EA elemental analyser (Flash EA 1112, Thermo Finnigan), and the  $\delta^{13}\text{C}$  of the  $\text{CO}_2$  was determined online on a Delta V Advantage isotope ratio mass spectrometer (IRMS, Thermo Finnigan). POC  $\delta^{13}\text{C}$ -values reported here have an analytical error of  $<0.2\%$ .

### 2.3.9 Biomarker analyses

*Extraction and derivatisation* – Lipid biomarkers were extracted according to (Elvert et al. 2003). Briefly, a total lipid extract (TLE) was obtained by ultrasonication of filter samples with solvents of decreasing polarity: (1) dichloromethane (DCM):methanol (MeOH) 1:2; (2) DCM:MeOH 2:1; and (3,4) DCM. Further separation into polar lipid-derived fatty acid (FA), hydrocarbon, ketone, and alcohol fractions, as well as derivatisation of FAs and alcohols into fatty acid methyl esters (FAMES) and trimethylsilyl (TMS) ethers, respectively, was carried out according to previous works (Elvert et al. 2003; Niemann et al. 2005). In short, the TLE was saponified with methanolic KOH. The neutral fraction, comprising hydrocarbons, ketones and alcohols, was then extracted from the saponified TLE with hexane. The remaining TLE containing the FAs was then acidified, and the protonated FAs were

extracted with hexane and methylated with methanolic  $\text{BF}_3$ . Double bond positions were determined through analysis of their dimethyl-disulfide adducts (Nichols et al. 1986; Moss and Lambert-Fair 1989). Hydrocarbons, ketones and alcohols were separated over a SiOH glass cartridge. Alcohols were subsequently methylated with bis(trimethylsilyl)trifluoroacetamide.

*Quantification, identification and stable carbon isotope composition* – Individual compounds were separated by gas chromatography (Trace GC Ultra, Thermo Scientific equipped with a split-splitless injector operated in splitless mode at  $300^\circ\text{C}$ ), over a capillary column (Rxi®-5ms, 60 m x 0.25 mm inner diameter) with a constant He flow of  $1 \text{ mL min}^{-1}$  using the following temperature program: initial oven T was  $50^\circ\text{C}$ , held for 2 min and then increased to  $140^\circ\text{C}$  at  $10^\circ\text{C min}^{-1}$ , then to  $300^\circ\text{C}$  with  $4^\circ\text{C min}^{-1}$  and finally held at  $300^\circ\text{C}$  for 63 min. The abundance of individual compounds was quantified by flame ionization detection (FID). Concentrations were calculated against an internal standard and corrected for introduction of carbon atoms. Identification of single compounds was achieved by GC-mass spectrometry with electron ionization (GC-MS, Thermo Scientific DSQ II Dual Stage Quadrupole). Acquired mass spectra were identified through comparison with known standards and published data. Compound-specific stable carbon isotope ratios were determined using a GC-IRMS (Delta V Advantage, Thermo Scientific). As with concentrations,  $\delta^{13}\text{C}$ -values were corrected for introduced carbon atoms. Reproducibility was monitored by repeated injections and monitoring of internal standards. Reported  $\delta^{13}\text{C}$ -values have an analytical error of  $\pm 1\%$ .

### 2.3.10 DNA extraction, polymerase chain reaction and cloning

Particulate matter for phylogenetic analyses was collected by filtering 500 mL of lake water through 0.2  $\mu\text{m}$  polycarbonate membrane filters (Cyclopore, Whatman). Filters were frozen immediately and stored at  $-70^{\circ}\text{C}$  until extraction of desoxyribonucleic acid (DNA), using a FastDNA<sup>®</sup> SPIN Kit for Soil (MP Biomedicals). In order to analyse the phylogeny of bacterial methanotrophs, the gene coding for particulate methane mono-oxygenase (pMMO) was targeted. Polymerase chain reaction (PCR) of the alpha subunit of the pMMO gene (*pmoA*) was performed using primers A189f (5'GGNGACTGGGACTTCTGG3') (Holmes et al. 1995) and mb661r (5'CCGGMGCAACGTCYTTACC3') (Costello and Lidstrom 1999). Reactions were carried out in 50  $\mu\text{L}$  (total volume) mixtures following a protocol adapted from Shrestha et al. (2008). Reaction mixtures contained 5  $\mu\text{L}$  of 1:10 diluted template DNA, 10  $\mu\text{L}$  5 $\times$  Phusion<sup>®</sup> HF buffer (Finnzymes, Thermo Fisher Scientific), 200  $\mu\text{mol L}^{-1}$  of each dNTP, 0.2  $\mu\text{mol L}^{-1}$  of each primer, 3% dimethyl sulfoxide (DMSO) (final concentration) and 1 unit of Phusion<sup>®</sup> High-Fidelity DNA polymerase (Finnzymes, Thermo Fisher Scientific). PCR conditions were as follows: initial denaturation at  $98^{\circ}\text{C}$  for 2 min, then 30 cycles of 30 s denaturation at  $98^{\circ}\text{C}$ , 30 s primer annealing at  $57^{\circ}\text{C}$  and 30 s elongation at  $72^{\circ}\text{C}$ , followed by a final elongation step of 10 min at  $72^{\circ}\text{C}$ . PCR products of four separate 50  $\mu\text{L}$  reactions were combined and concentrated to 25  $\mu\text{L}$  using a Wizard SV PCR clean-up kit (Promega). Amplicon length was checked on a 1.2% agarose gel. Clone libraries of samples from 135 and 170 m water depth (August 2009) were constructed using the Zero Blunt<sup>®</sup> TOPO<sup>®</sup> PCR Cloning Kit (Invitrogen). Restriction digestion analysis using *MspI* (Costello and Lidstrom 1999; Busmann et

al. 2006) was performed in order to assess the number of phylotypes. The obtained DNA sequences, as well as the most closely related representatives retrieved from the National Center for Biotechnology Information (NCBI) database, were translated into their amino acid sequences and aligned by the Muscle implementation in MEGA5 (Tamura et al. 2011). Phylogenetic trees were constructed in MEGA5 using the neighbour-joining algorithm, and evolutionary distances were calculated using the Poisson correction method. Sequences reported in this study were deposited in the European Molecular Biology Laboratory (EMBL) Bank under the accession numbers HF674401-9.

## **2.4 Results**

### *2.4.1 Physical parameters, oxygen and nutrients*

A strong thermocline developed at 20 m water depth in the northern basin of Lake Lugano in spring. Density stratification at the thermocline prevented exchange of water from the epilimnion and the hypolimnion. Below ~50 m water depth, the temperature remained stable at 5.7°C throughout the year. In late winter, cooling of surface waters destabilized the thermocline, leading to ventilation of the metalimnion (20 – 50 m water depth). The water body below ~50 m depth, however, remained stratified throughout the whole duration of our study. The lack of water exchange deeper than 50 m is evidenced by decreasing O<sub>2</sub> concentration below this depth (Fig. 2.1a). During the sampling campaigns between March 2009 and May 2012, the oxic-anoxic interface, as determined with the CTD oxygen sensor ( $[O_2] < 1 \mu\text{mol L}^{-1}$ , here defined as the CTD-O<sub>2</sub>-zero), was stable at 125 to 130 m water depth (Fig. 2.1a). O<sub>2</sub> concentration data obtained with the combined amperometric O<sub>2</sub> sensor

and O<sub>2</sub> optode showed that the oxic-anoxic interface, defined as [O<sub>2</sub>] < 10 nmol L<sup>-1</sup>, was located between 125.6 and 128.2 m water depth (Fig. 2.1a), i.e. within the range reported by the CTD-O<sub>2</sub>-sensor. The sub-micromolar zone, where [O<sub>2</sub>] ranged between 1000 and 10 nmol L<sup>-1</sup>, had a thickness of 1.55 ± 0.36 m (3 casts). This indicates that in the northern basin of Lake Lugano the CTD-O<sub>2</sub>-zero approximates the true O<sub>2</sub>-zero. In the oxic hypolimnion above the chemocline, NO<sub>3</sub><sup>-</sup> was present, and decreased linearly towards the chemocline (Wenk et al. 2013). No NO<sub>3</sub><sup>-</sup> was detected below 150 m water depth. NH<sub>4</sub><sup>+</sup> was absent in the oxygenated hypolimnion, but its concentration increased below the redox transition zone to >20 μmol L<sup>-1</sup> in the bottom water. There, Fe(II) accumulated to 8 μmol L<sup>-1</sup> (Fig. 2.2a). Fe(III) concentrations were consistently below 0.5 μmol L<sup>-1</sup> throughout the water column (and undetectable between 135 and 80 m depth), with the exception of the upper 20 m of the water column, where concentrations of ~1 μmol L<sup>-1</sup> were observed (Fig. 2.2b). Sulfide was detected at depths >140 m, and increased to 11.2 μmol L<sup>-1</sup> in the bottom water (Fig. 2.2c).

#### 2.4.2 Methane

CH<sub>4</sub> concentrations in the sediment below 20 cm depth were stable at ~5 mmol L<sup>-1</sup>, and decreased towards the sediment-water interface, yet without any discernable shift in δ<sup>13</sup>CCH<sub>4</sub> (Fig. 2.1b,c). Within the anoxic hypolimnion the CH<sub>4</sub> concentration continued to decrease from the near-bottom water (40 – 160 μmol L<sup>-1</sup>) upwards towards the chemocline (Fig. 2.1b). Interestingly, the CH<sub>4</sub> concentration did not decrease linearly within the deep hypolimnion, and the convex profile well below the chemocline suggests non-conservative behaviour – possibly consumption

– within the anoxic water column. Moreover, the non-linear concentration decrease between 220 and 135 m water depth was accompanied by a  $^{13}\text{C}$ -isotopic enrichment in the residual  $\text{CH}_4$  pool, from -70‰ in the deep water to -40‰ at the oxic-anoxic boundary, with a robust closed system apparent C-isotope effect ( $\varepsilon_{\text{closed}}$ ) of -7‰ to -9‰ (Fig. 2.3). Using an open-system model, on the other hand (Eq. 2.2), the observational data could not be fitted, i.e. no single  $\varepsilon$  value could reproduce the observed relationship between  $\delta^{13}\text{C}$  and  $[\text{CH}_4]$ . Below 220 m, only minor C-isotope ratio changes were observed (Fig. 2.1c). The concentration directly above the top of the anoxic hypolimnion (usually  $<20 \text{ nmol L}^{-1}$ ) was only a small fraction of the deep-water concentration just above the sediment during all sampling campaigns.

#### 2.4.3 Methane oxidation rates in the water column

We observed two distinct and (apparently) temporally stable peaks of potential aerobic  $\text{CH}_4$  turnover rates: one at 145 m and a second at 175 m (Fig. 2.1d).  $k$ -values at these depths were comparably high in August 2010 ( $0.71 \pm 0.02$  and  $0.27 \pm 0.05 \text{ d}^{-1}$ , respectively), and slightly lower in January 2010 ( $0.21 \pm 0.03$  and  $0.07 \pm 0.01$ , respectively). These  $k$ -values translate into a MOR of  $2.31 \pm 0.34$  and  $4.63 \pm 0.81 \mu\text{mol L}^{-1} \text{ d}^{-1}$  in August and  $1.07 \pm 0.16$  and  $1.47 \pm 0.12$  in January. Above, towards the oxic-anoxic interface, potential aerobic MOR decreased to  $1 \mu\text{mol L}^{-1} \text{ d}^{-1}$ , and dropped below the detection limit in the oxic water column. Similarly, MOR decreased with depth below 175 m but remained significant down to near-bottom waters, where they approached the detection limit. In all incubations with measurable  $\text{CH}_4$  turnover, a residual activity was found after extraction of the carbonate phase. This

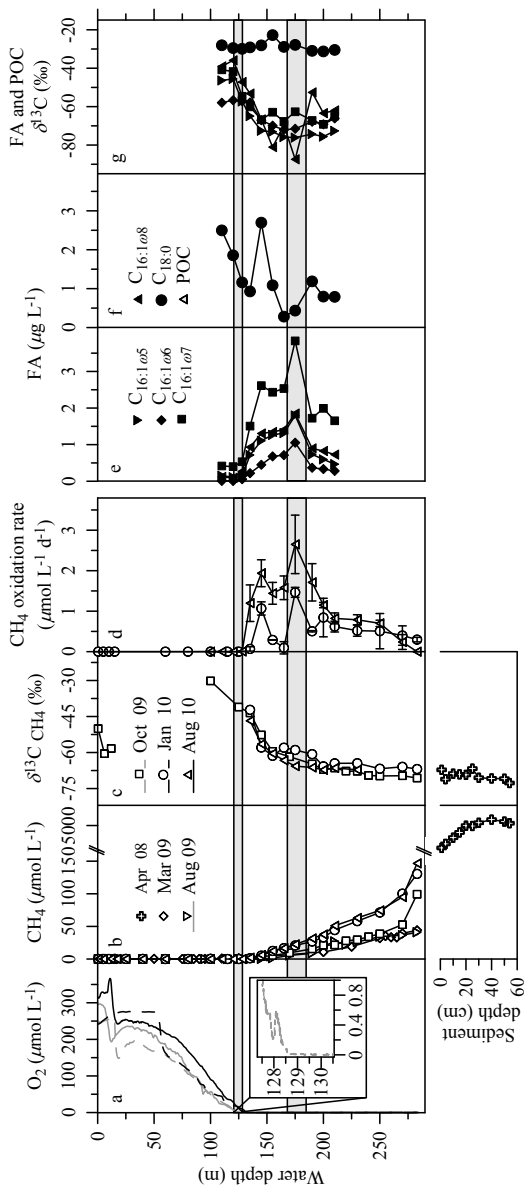


**Figure 2.1** Hydrochemical profiles of (a)  $O_2$  concentration, with a magnification of the sub-micromolar zone in October 2009 (inset), (b)  $CH_4$  concentration, (c)  $CH_4$   $\delta^{13}C$  in the water column and sediment, and (d) potential aerobic  $CH_4$  oxidation rates. Months are indicated in the legend in (b). Concentration of (e)  $C_{16:1,6,5-8}$  and (f)  $C_{18:0}$  FAs from August 2010 and (g)  $\delta^{13}C$  of  $C_{16:1,6,5-8}$  and  $C_{18:0}$  FAs from August 2009, October 2009, January 2010, and August 2010 (grey, 1 standard deviation error bars). The oxic-anoxic interface is indicated by the narrow upper grey bar. The lower grey bar indicates the putative  $CH_4$  sink within the anoxic water column, where potential MOR and methanotrophic biomass concentration are highest, and the isotope shift in methanotrophic biomarkers is most pronounced.

residual activity was on average  $70 \pm 20\%$  of the turnover into bicarbonate. Since it constitutes a significant fraction of the  $^{14}\text{CH}_4$  oxidation, it has been included in the MOR calculation (see Eq. 2.3). The residual  $^{14}\text{C}$  pool was suspended and/or water-soluble at low pH, and may have comprised biomass and metabolic intermediates not liberated by acidification. If this residual activity were not included in the MOR calculation, the MOR would be underestimated.

#### *2.4.4 Sulfate reduction rates in the water column*

SRR in the hypolimnion was very low, with values of  $7.29 \pm 2.69 \text{ nmol L}^{-1} \text{ d}^{-1}$  at 175 m water depth and up to  $37 \text{ nmol L}^{-1} \text{ d}^{-1}$  close to the sediment in January 2010 (Fig. 2.2e). Sulfide accumulated in the deep water, with up to  $11.2 \text{ } \mu\text{mol L}^{-1}$  close to the sediment (Fig. 2.2c). However, the decline in  $\text{SO}_4^{2-}$  concentration into the bottom water was significantly greater than the accumulation of sulfide ( $95 \text{ } \mu\text{mol L}^{-1} \text{ SO}_4^{2-}$  in bottom waters, compared to  $120 \text{ } \mu\text{mol L}^{-1}$  in the oxic water column, Fig. 2.2d). The discrepancy between apparent sulfate consumption and sulfide production is best explained by the co-precipitation of sulfide with iron, but this aspect was not further investigated.

#### *2.4.5 Particulate organic carbon and lipid biomarkers*

$\delta^{13}\text{C}$ -values of POC in the oxic water column were about  $-34\text{‰}$  (Fig. 2.1g). Below the oxycline, POC showed significant  $^{13}\text{C}$ -isotopic depletion, with  $\delta^{13}\text{C}$  values as low as  $-47\text{‰}$ . Concentration of four mono-unsaturated  $\text{C}_{16}$  FAs (with double bonds at positions  $\omega 5$ ,  $\omega 6$ ,  $\omega 7$ , and  $\omega 8$ ) increased with depth below the oxic-anoxic interface, paralleling the depth distribution of MOR (Fig. 2.1e), with two temporally stable

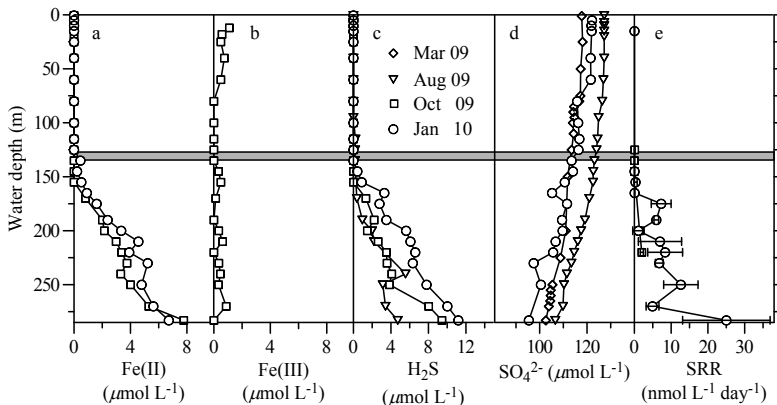


**Figure 2.2** Water column concentration profiles of (a) Fe(II) and (b) Fe(III), (c) total sulfide, (d)  $\text{SO}_4^{2-}$ , and (e) sulfate reduction rates. The oxic-anoxic interface is indicated by a grey bar.

concentration maxima; one at 145 m and one at 175 m. The distributions of other bacterial biomarkers such as  $iC_{15}$  and  $aiC_{15}$  displayed similar, yet much less pronounced peaks at the same depths (data not shown). In August 2010 the four  $C_{16:1}$  lipids accounted for 64% of total FAs at 175 m. The  $C_{16:1\omega7}$  concentration strongly increased from  $0.4 \mu\text{g L}^{-1}$  just above the oxic-anoxic interface to  $>1.5 \mu\text{g L}^{-1}$  in the deep hypolimnion, with a concentration maximum of  $3.8 \mu\text{g L}^{-1}$  at 175 m water depth. The concentration of other FAs did not increase significantly with depth, except for concentration peaks at the redoxcline at 145 m (e.g.  $C_{12:0}$ ,  $C_{14:0}$ ,  $C_{15:0}$ ,  $C_{16:0}$ ). The four mono-unsaturated  $C_{16:1}$  FA biomarkers were markedly more depleted in  $^{13}\text{C}$  than other FAs. The most abundant of the four FAs,  $C_{16:1\omega7}$ , displayed a  $\delta^{13}\text{C}$  as low as  $-74.2\text{‰}$  (at 175 m) (Fig. 2.1g). Other lipids displayed ‘normal’ values of about  $-30\text{‰}$  to  $-40\text{‰}$ . We also investigated other lipid fractions (hydrocarbons and alcohols, the latter typically comprising ether lipids; data not shown). However, none

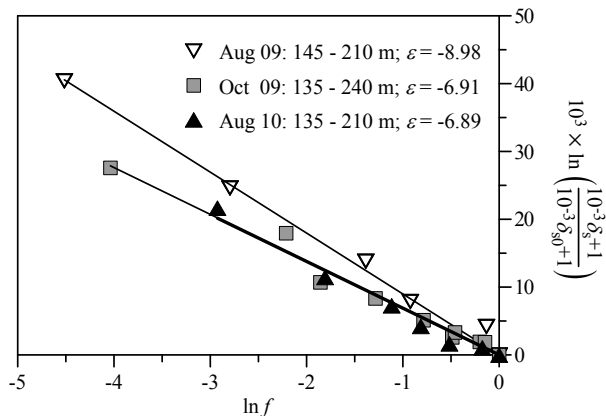


**Figure 2.3** Rayleigh plot of CH<sub>4</sub> data from the anoxic water column of August and October 2009 and August 2010. Linear regressions are plotted through the three data sets, and the slope is equivalent to the isotope enrichment factor. Depth intervals of the linear ranges and their slopes are indicated in the legend.

of the analysed compounds displayed the same conspicuous concentration peaks and characteristic <sup>13</sup>C-isotopic depletion between 145 and 175 m water depth. Notably no archaeal lipids typical for S-AOM (e.g. archaeol, *sn*2-hydroxyarchaeol, pentamethylcosane (PMI) or crocetane (Niemann and Elvert 2008)) or lipids diagnostic of the recently described bacterial AOM by “*Candidatus Methyloirabilis oxyfera*” (e.g. 10-methylhexadecanoic acid (Kool et al. 2012)) were detected during any of the sampling campaigns.

#### 2.4.6 Phylogenetic analyses

Sequences of *pmoA* could be amplified from all samples collected at the oxic-anoxic interface and in deeper water layers, but not from the oxic water column. After restriction fragment length analysis of MspI-digested

inserts of 47 clones, 4 representatives from 135 m and 5 representatives from 170 m were selected for sequencing. The clones belonged to 7 phylotypes, with two phylotypes represented by two clones each. One phylotype was represented by two clones from 170 m, and another by one clone from 135 m and one from 170 m. The phylogenetic relationship of *pmoA* sequences from 135 and 170 m water depth in August 2009 is shown in Fig. 2.4. They form four clusters within the type I MOB and are closely related to uncultured representatives from oxic environments in Lake Constance (Deutzmann et al. 2011), Lake Washington (Nercessian et al. 2005) and Lake Mizugaki (Tsutsumi et al. 2011). Closest cultured relatives are *Methylobacter* sp. No sequences of alphaproteobacterial MOB were found.

## 2.5 Discussion

### 2.5.1 Anoxia in the water column

Well-constrained information about the geometry of the redox transition zone, and hence the redox state of various levels in the water column, is fundamental for identifying the modes of CH<sub>4</sub> oxidation in a water body. While the extreme end-members of the water column redox spectrum – fully oxygenated and sulfidic – are easily characterized, precise identification of the transition from oxic to hypoxic and finally to truly anoxic conditions is challenging. Trace levels of O<sub>2</sub> may escape detection because most oxygen sensors have a detection limit of around 1 μmol L<sup>-1</sup> (Revsbech et al. 2009), and even Winkler titration measurements have uncertainties of ~5 μmol L<sup>-1</sup> or more (Jalukse et al. 2008). In Lake Lugano, the depth interval between the supposed onset of anoxia and the first appearance of sulfide differed by 10 to 35 m. Therefore, we

investigated the sub-micromolar O<sub>2</sub> zone in high resolution and with nanomolar sensitivity using highly amplified amperometric O<sub>2</sub> sensors and O<sub>2</sub> optodes (Table 2.1, Fig. 2.1a inset, Kirf et al. 2014) in order to validate O<sub>2</sub> data measured with the CTD-device. These measurements showed that the sub-micromolar O<sub>2</sub> zone was relatively thin ( $1.55 \pm 0.36$  m) and the true oxic-anoxic interface (i.e. O<sub>2</sub> < 10 nmol L<sup>-1</sup>) fluctuated between 125.6 and 128.2 m, i.e. within 5 m of the CTD-O<sub>2</sub>-zero. In fact, throughout our sampling campaigns we never measured O<sub>2</sub> at depths below 135 m.

### *2.5.2 Methane distribution in the hypolimnion and identification of methane sinks*

The water column CH<sub>4</sub> concentration profiles show highly similar trends of decreasing concentration from the bottom waters towards the oxycline (Fig. 2.1b), indicating production of CH<sub>4</sub> in the sediments and its turbulent diffusive flux through the deep hypolimnion. Based on the concentration and  $\delta^{13}\text{C}$  distribution of the sedimentary and water column CH<sub>4</sub>, four zones are defined for the following discussion:

1) *Sediment porewater* - Stable CH<sub>4</sub> concentrations in the sediment below 20 cm and the concentration gradient towards the top of the sediment and into the water column indicate CH<sub>4</sub> production below 20 cm and the diffusive flux of CH<sub>4</sub> out of the sediment. The absence of a C-isotope shift in the residual CH<sub>4</sub> across the sediment-water interface argues against CH<sub>4</sub> oxidation in the sediment porewater, since biological CH<sub>4</sub> oxidation results in isotope fractionation, in contrast to turbulent diffusive transport only.

2) *283 - 220 m* - In the deep hypolimnion, the CH<sub>4</sub> concentration

profiles display a convex shape that may indicate CH<sub>4</sub> consumption in this water layer. However, these non-linear concentration changes are not paired with a substantial C-isotope shift, which argues against a biogeochemical CH<sub>4</sub> sink within this depth interval. Although we cannot completely rule out an anaerobic mode of CH<sub>4</sub> oxidation within the deep anoxic hypolimnion, we argue that the shapes of the CH<sub>4</sub> concentration and  $\delta^{13}\text{C}$  profiles by themselves do not provide conclusive evidence for such a CH<sub>4</sub> sink. We further allege that the CH<sub>4</sub> concentration in the water column below ~100 m water depth was not in steady state prior to 2010. Our (Fig. 2.1b) and unpublished data (University of Applied Sciences of Southern Switzerland (SUPSI) unpubl.) show that CH<sub>4</sub> concentrations in the hypolimnion have increased since the holomixis in 2005 and 2006 (Holzner et al. 2009); i.e. from ~40  $\mu\text{mol L}^{-1}$  in spring 2008 to ~160  $\mu\text{mol L}^{-1}$  in 2010. After the mixing events, stratification re-established and the lower hypolimnion became anoxic again in early 2008 (SUPSI unpubl.). However, steady state with regard to the methane distribution in the water column was not reached at that time. Sediment-derived CH<sub>4</sub>, liberated into the water column, is transported through the anoxic hypolimnion by turbulent diffusion, and the decreasing water column concentration with distance from the sedimentary source is due to source dilution and mixing with ambient water. The convex-shaped CH<sub>4</sub> distributions between 220 m water depth and the sediment can be explained as being the expression of a non-steady state situation, in which the slow vertical transport of CH<sub>4</sub> after re-establishment of full meromixis led to a delayed CH<sub>4</sub> accumulation in the upper portions of the anoxic hypolimnion.

3) 220 – 135 m - The water column between 220 m and the oxic-anoxic interface at 135 m is also characterized by a weakly convex CH<sub>4</sub> concentration profile (Fig. 2.1b). In contrast to the lower anoxic

hypolimnion, however, we observed a clear  $^{13}\text{C}$ -enrichment in the residual  $\text{CH}_4$  pool, suggesting a consumption process in the anoxic water column, tens of meters below the oxic-anoxic interface.

4) *The oxic-anoxic interface* –  $\text{CH}_4$  concentrations of  $<20 \text{ nmol L}^{-1}$  immediately above the oxic-anoxic interface indicate that very little  $\text{CH}_4$  escaped from the deep hypolimnion across the chemocline. This underscores the importance of the oxic part of the redox transition zone as an efficient  $\text{CH}_4$  filter preventing  $\text{CH}_4$  emissions to the atmosphere.

### 2.5.3 *MOx at the oxic-anoxic interface*

Steep gradients in both  $\text{CH}_4$  concentration and  $\delta^{13}\text{C}$  across the oxic-anoxic interface, which indicate a flux of  $1.7 - 3.0 \text{ mmol m}^{-2} \text{ d}^{-1}$  over the depth range between 190 and 135 m, provide evidence for a strong aerobic  $\text{CH}_4$  sink in Lake Lugano. The zone of sub-micromolar  $\text{O}_2$  concentrations is  $\sim 1.5 \text{ m}$  thick, and no  $\text{CH}_4$  oxidation took place at depths with in situ  $\text{O}_2$  concentration  $> 1 \mu\text{mol L}^{-1}$ . If we assume an MOx reaction zone with a thickness of  $1.5 \text{ m}$ , the calculated  $\text{CH}_4$  flux translates into a  $\text{CH}_4$  consumption rate of  $1.1 - 2.0 \mu\text{mol L}^{-1} \text{ d}^{-1}$ , in agreement with the rates obtained from ex situ MOR incubations. Assuming a uniform  $\text{CH}_4$  flux throughout the northern basin of Lake Lugano, with a surface area of  $17 \text{ km}^2$  at 135 m depth (SUPSI), and uniform  $\text{CH}_4$  oxidation at the redoxcline, the total  $\text{CH}_4$  consumption rate at the oxic-anoxic interface amounts to  $10 - 19 \times 10^6 \text{ mol yr}^{-1}$ , i.e.  $127 - 224 \times 10^3 \text{ kg C yr}^{-1}$ .

High MORs cause a complete consumption of oxygen, creating seemingly anoxic conditions at the depth of highest potential aerobic  $\text{CH}_4$  oxidation (135 – 145 m), and possibly driving niche specialization of

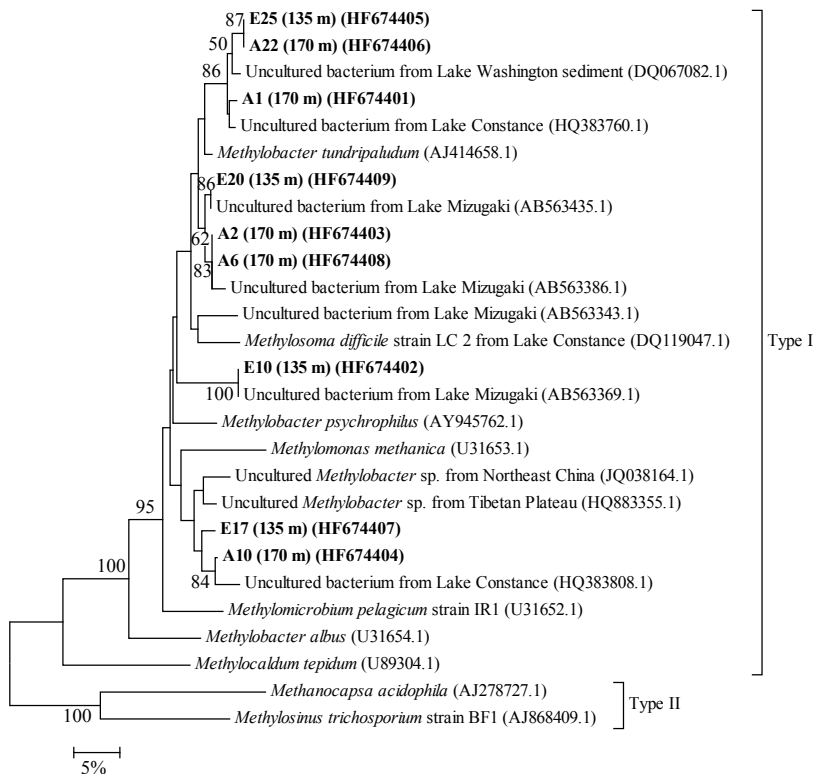


**Figure 2.4** Neighbour joining phylogenetic tree of translated amino acid sequences of *pmoA* gene clones from the oxic-anoxic interface (135 m) and anoxic deep water (170 m). Lake Lugano clones are indicated in bold. 27 amino acid sequences were used for the analysis. Bootstrap values >50% (1000 replications) are shown at branch nodes. Closely related sequences from Lakes Mizugaki, Constance and Washington, and two *Methylobacter* sp. sequences from wetlands are shown for comparison.

**Table 2.1** Overview of measured parameters and incubations

Date	Depth interval (m)	Parameters measured	Incubations (depth, m)
Apr 2008	Sediments	[CH <sub>4</sub> ], δ <sup>13</sup> CH <sub>4</sub> , lipid biomarkers	
Mar 2009	0 – 283	CTD, pH, O <sub>2</sub> ; [CH <sub>4</sub> ], δ <sup>13</sup> CH <sub>4</sub> , SO <sub>4</sub> <sup>2-</sup> , total sulfide, lipid biomarkers, DNA	
Jun 2009	0 – 283	CTD, pH, O <sub>2</sub> ; [CH <sub>4</sub> ], δ <sup>13</sup> CH <sub>4</sub> , SO <sub>4</sub> <sup>2-</sup> , total sulfide, lipid biomarkers, DNA	SRR (0 – 283)
Aug 2009	0 – 283	CTD, pH, O <sub>2</sub> , sub-micromolar O <sub>2</sub> , [CH <sub>4</sub> ], δ <sup>13</sup> CH <sub>4</sub> , SO <sub>4</sub> <sup>2-</sup> , total sulfide, Fe(II) and Fe(III), lipid biomarkers, DNA, clone libraries	SRR (0 – 283)
Oct 2009	0 – 283	CTD, pH, O <sub>2</sub> , sub-micromolar O <sub>2</sub> , [CH <sub>4</sub> ], δ <sup>13</sup> CH <sub>4</sub> , SO <sub>4</sub> <sup>2-</sup> , total sulfide, Fe(II) and Fe(III), lipid biomarkers, DNA	MOR, SRR (125 – 145, 200, 220)
Jan 2010	0 – 283	CTD, pH, O <sub>2</sub> ; [CH <sub>4</sub> ], δ <sup>13</sup> CH <sub>4</sub> , SO <sub>4</sub> <sup>2-</sup> , total sulfide, Fe(II) and Fe(III), lipid biomarkers, DNA	MOR, SRR (0 – 283)
Aug 2010	0 – 283	CTD, pH, O <sub>2</sub> ; [CH <sub>4</sub> ], δ <sup>13</sup> CH <sub>4</sub> , SO <sub>4</sub> <sup>2-</sup> , total sulfide, lipid biomarkers, DNA	MOR (0 – 283)
Sep 2011	175	CTD, pH, O <sub>2</sub>	<i>e</i> <sup>-</sup> -acceptor (175)
Oct 2011	175	CTD, pH, O <sub>2</sub>	<i>e</i> <sup>-</sup> -acceptor (175)
Jan 2012	175	CTD, pH, O <sub>2</sub>	MOR (175)
May 2012	175	CTD, pH, O <sub>2</sub>	MOR (175)

MOB towards micro-oxic conditions (Tavormina et al. 2013). Assuming a  $\text{CH}_4:\text{O}_2$  stoichiometry of MOx of 1:1.8 (Naguib 1976) our  $\text{CH}_4$  oxidation rates translate into  $\text{O}_2$  consumption rates of up to  $3.5 \mu\text{mol L}^{-1} \text{d}^{-1}$ . The  $\text{O}_2$  consumption in suboxic incubations of  $4 \mu\text{mol L}^{-1} \text{d}^{-1}$ , determined with a switchable trace oxygen (STOX) sensor (data not shown), supports this value. Based on the  $\text{O}_2$  concentration profiles, the flux of  $\text{O}_2$  from the upper hypolimnion towards the oxic-anoxic interface ranged between 4.3 and  $15 \text{ mmol m}^{-2} \text{d}^{-1}$ , or between 2.9 and  $10 \mu\text{mol L}^{-1} \text{d}^{-1}$  in a 1.5 m reaction zone. Micro-aerobic MOx is thus responsible for more than one third of the  $\text{O}_2$  consumption at the redoxcline in the northern basin of Lake Lugano, and is therefore an important constraint on the depth of the oxic-anoxic interface.

Further evidence for an MOx-community at these depths is indicated by biomarker and phylogenetic data. We found an increase of  $^{13}\text{C}$ -depleted FAs at the oxic-anoxic interface, indicating incorporation of  $\text{CH}_4$ -derived carbon into lipid biomass. The  $^{13}\text{C}$ -isotopic depletion within  $\text{C}_{16}$  (particularly  $\text{C}_{16:1\omega7}$ ) rather than  $\text{C}_{18}$  FAs compared to other lipids (Fig. 2.1g) indicates a dominance of type I methanotrophs (Bowman et al. 1993; Hanson and Hanson 1996). Moreover, the fractional abundances of the  $\text{C}_{16:1\omega5-8}$  FAs correspond to those reported for *Methylobacter* sp. (Hanson and Hanson 1996). A dominance of type I methanotrophs is further confirmed by the sole presence of sequences clustering within the type I MOB related to the *Methylobacter* sp. in our *pmoA* clone libraries (Fig. 2.4). In contrast to the anoxic water column, we could not detect the above-mentioned diagnostic biomarkers or *pmoA* sequences above the oxic-anoxic interface, further supporting that the  $\text{CH}_4$  sinks are restricted to waters at or below the oxic-anoxic interface.

The absence of MOB above the oxic-anoxic interface agrees well with

the fact that ex situ CH<sub>4</sub> turnover was only observed in incubations from a depth of 128 m or below (Fig. 2.1d). At the depth of maximum potential CH<sub>4</sub> turnover (145 m), the in situ O<sub>2</sub> concentration was always <10 nmol L<sup>-1</sup>. Very low O<sub>2</sub> concentrations have been found to constitute the preferred niche for some aerobic methanotrophs in lakes (Rudd et al. 1976). On the other hand, in incubations of water from the anoxic hypolimnion we did not observe an inhibitory effect of high O<sub>2</sub> concentrations (~100 μmol L<sup>-1</sup>) on MOx (data not shown), which indicates that high O<sub>2</sub> is not the direct cause of the absence of MOx. Studies on CH<sub>4</sub>-starvation in MOB have shown that recovery is significantly faster and more successful when starvation occurred under anoxic conditions rather than under oxic conditions (Roslev and King 1994). Under oxic conditions MOB were shown to degrade protein during C-starvation, potentially hampering their subsequent ability to oxidize CH<sub>4</sub> again, whereas under anoxic conditions only low-molecular-weight compounds were oxidized (Roslev and King 1995). This implies that for MOB, O<sub>2</sub>-starvation is preferable to CH<sub>4</sub>-starvation under oxic conditions. In dynamic systems with spatio-temporal variations of the redoxcline, this may drive MOB towards the anoxic side of the anoxic-oxic continuum, providing protection against the detrimental effects of CH<sub>4</sub>-starvation under oxic conditions.

#### *2.5.4 Methanotrophy in the anoxic hypolimnion*

While the CH<sub>4</sub> profiles in the water column between 220 m and the oxic water leave some ambiguity with regard to the water depth where CH<sub>4</sub> oxidation takes place, and particularly its mode, the lipid biomarker data from the Lake Lugano North Basin provide additional indication for

a CH<sub>4</sub> oxidation potential below the oxic-anoxic interface. The temporally stable concentration maximum of <sup>13</sup>C-depleted C<sub>16:1ω5-8</sub> FAs at ~175 m water depth (Fig. 2.1e) implies the presence of methanotrophic biomass in anoxic water masses. The dominance of the four C<sub>16:1</sub> FAs and the absence of <sup>13</sup>C-depleted archaeal lipids (e.g. isoprenoidal ether lipids or alkanes; Niemann and Elvert 2008) underscores that *Bacteria*, and not *Archaea* drive CH<sub>4</sub> oxidation in the northern basin of Lake Lugano. However, lipids characteristic of the recently described “*Candidatus Methyloirabilis oxyfera*”, like 10-MeC<sub>16:0</sub> and 10-MeC<sub>16:1ω9</sub> (Kool et al. 2012) were also absent, suggesting no significant contribution of a bacterial pathway of AOM in Lake Lugano. As is the case with the oxic-anoxic interface, only type I MOB related to *Methylobacter* sp. were found in the *pmoA* clone libraries (Fig. 2.4). The absence of a clear distinction between *pmoA*-phylogenies at 135 and 170 m, and the occurrence of an identical clone at both depths, suggests a high similarity between the bacterial methanotrophic communities.

Accumulation of methanotrophic bacterial biomass in the anoxic vicinity of the chemocline has been described in other systems (Schubert et al. 2006), but not as far as 40 m below the oxic water column. The methanotrophic biomass can originate from in situ production, but it may also have been ‘scavenged’ and carried down from the oxic-anoxic interface by sedimenting phyto-detritus. Such a flux of sinking organic matter would be highest after the phytoplankton blooms in March and September. However, the depth of the CH<sub>4</sub> oxidation maxima (145 and 175 m; Fig. 2.1d) appeared to be temporally stable, thus arguing against such a gravity-driven downward transport of MOB from the oxic-anoxic interface. Moreover, we did not observe biomass concentration peaks at other depths, and only the concentration of MOB-derived lipids increased

at 175 m, representing further evidence for a selective increase of MOB at this depth, and possibly in situ activity.

#### *2.5.5 MOx potential in anoxic waters*

Corresponding to the concentration peak of  $^{13}\text{C}$ -depleted  $\text{C}_{16:1\omega5-8}$  FAs, a local potential MOx rate maximum was found at about 175 m water depth (Fig. 2.1d). At this depth, permanent presence of  $\text{O}_2$  can be excluded as no  $\text{O}_2$  was detected with the  $\text{O}_2$  sensors and substantial concentrations of reduced compounds (sulfide,  $\text{NH}_4^+$ , and Fe(II); Fig. 2.2) act as a natural  $\text{O}_2$  buffer. Incubation experiments used for MOx rate determination had initial  $\text{O}_2$  concentrations of around  $10 \mu\text{mol L}^{-1}$ . Hence, the obtained potential rates do not reflect methane oxidation under in situ conditions, but they highlight the important potential for aerobic  $\text{CH}_4$  oxidation in anoxic water masses, well below the oxic-anoxic interface. In fact, high MOx potentials were not only measured at 175 m, but throughout the anoxic water column (Fig. 2.1d). Thus, if oxygen were mixed into the anoxic hypolimnion, high aerobic  $\text{CH}_4$  oxidation rates are expected, limited only by the availability of  $\text{O}_2$ . We performed incubations with various oxygenation conditions. Most intriguingly, potential methane oxidation rates under oxic conditions ( $> 100 \mu\text{mol L}^{-1}$ ) were similar to the rates in micro-oxic ( $< 5 \mu\text{mol L}^{-1}$ ) incubations. This argues against detrimental effects of high  $\text{O}_2$  concentrations on MOx (Rudd et al. 1976). Rather, it suggests that the methanotrophic community has adapted to trace levels of  $\text{O}_2$ , reaching maximum turnover at low  $\text{O}_2$  concentrations (Ren et al. 1997), with half saturation rate constants possibly below micromolar  $\text{O}_2$  levels (Tiano 2013).

The MOR discussed above were obtained under (micro-)oxic

conditions, and therefore only reflect in situ  $\text{CH}_4$  oxidation when  $\text{O}_2$  is mixed into the deep anoxic hypolimnion. The actual in situ MOR depends on the frequency and amount of  $\text{O}_2$  supply. With the data in hand it is impossible to estimate the time-integrated or sporadic  $\text{O}_2$  availability below the redox transition zone. In any case, the potential rates shown in Fig. 2.1d are almost certainly an overestimate, and may be representative for the in-situ conditions only when sufficient  $\text{O}_2$  is mixed into the deep water.

#### *2.5.6 Sources of $\text{O}_2$ in the anoxic hypolimnion*

We were unable to detect  $\text{O}_2$  in the water column below 135 m. However, it should be noted that the density stratification in the northern basin of Lake Lugano has been weakened since the overturn events during the winters of 2005 – 2006 and 2006 – 2007 (Holzner et al. 2009). Even though wind energy input and surface water cooling are not sufficient to induce a full overturn of the water column, oxygen-rich cold water masses may episodically and locally sink into the anoxic hypolimnion. For example, injections of  $\text{O}_2$  into hypolimnetic waters have been reported for Lake Maggiore, where sinking of cold fluvial water led to measurable  $\text{O}_2$  intrusions along the lakes' side walls to depths below 200 m (Ambrosetti et al. 2010). Moreover, as a result of flood events in tributaries, turbidity currents from the surface waters that reach the bottom waters of the northern basin of Lake Lugano have been observed (Lavelli et al. 2002). However,  $\text{O}_2$  from episodic inputs is most likely consumed quickly and would likely not be detected by our sampling regime. Yet its consumption during  $\text{MOx}$  would lead to a decrease in  $\text{CH}_4$  concentration, coupled to  $^{13}\text{C}$ -enrichment in the residual  $\text{CH}_4$  pool, as

observed in this study and previously by Liu et al. (1996). More importantly, it could be a plausible explanation for the presence of aerobic CH<sub>4</sub> oxidizers in ‘stand-by mode’ in the upper anoxic hypolimnion.

Relatively low potential MOx rates were also observed below 200 m (Fig. 2.1d), where the CH<sub>4</sub> concentration decrease is not coupled to a CH<sub>4</sub>-isotope shift. We putatively attribute the discrepancy between our measurements of potential MOR and the lack of expression in the geochemical environment to the presence of viable MOB in the lower water column (as indicated by low concentrations of <sup>13</sup>C-depleted FAs, Fig. 2.1e,f), possibly carried down from the oxycline by sinking particles. These MOB likely recover quickly from O<sub>2</sub> starvation once O<sub>2</sub> is introduced in laboratory incubations (Roslev and King 1994), resulting in measurable potential MOx rates. However, based on the reduced expression of geochemical signatures diagnostic of in situ MOx (CH<sub>4</sub> concentration and δ<sup>13</sup>C, Fig. 2.1b,c), the lower concentrations of MOx-specific FAs, (Fig. 2.1e,f) and the lower potential aerobic MOR (Fig. 2.1d) below 200 m water depth, we argue that any in situ population of aerobic methane oxidizing bacteria in ‘stand-by mode’, as postulated for the upper anoxic hypolimnion, is small in the deeper parts of the hypolimnion. This conclusion also seems consistent with our notion that the likelihood of O<sub>2</sub> reaching the deeper parts of a strongly stratified water body decreases significantly with water depth, particularly in a setting where MOB higher up in the water column are likely to consume O<sub>2</sub> in sinking water masses rapidly.

#### *2.5.7 Scope for true anaerobic methane oxidation and isotopic constraints*

As discussed in the previous section, episodic micro-aerobic methane

oxidation in otherwise anoxic waters can explain the occurrence of aerobic methanotrophs and the high potential for MOx in the anoxic hypolimnion. However, since no clear density stratification exists within the anoxic hypolimnion, it is difficult to explain the distinct vertical distribution of methanotrophs in the water column (e.g. the peak at 175 m water depth). This in turn begs the question of whether a true anaerobic mode of methane oxidation may be part of the hypolimnetic methane filter. The results of incubation experiments under anoxic conditions remained ambiguous. We aimed at testing the potential for AOM in Lake Lugano's northern basin by incubating water samples from 175 m for time periods of up to 7 days. In some of the anoxic incubations, no CH<sub>4</sub> oxidation took place. In other incubations, even when an O<sub>2</sub> scavenger (15 μmol L<sup>-1</sup> H<sub>2</sub>S) was used, we found persistent CH<sub>4</sub> turnover after several days. As is the case for any elastomer, there is no material that is totally diffusion tight. However, we monitored O<sub>2</sub> leakage through the bromobutyl stopper in parallel incubations with MilliQ water. Over 30 days, we measured a sulfide concentration decrease of 0.15 μmol L<sup>-1</sup> d<sup>-1</sup>, which translates to an influx of O<sub>2</sub> of ~0.3 μmol L<sup>-1</sup> d<sup>-1</sup>, under the conservative assumption that sulfide is completely oxidized to SO<sub>4</sub><sup>2-</sup>. The O<sub>2</sub> leakage-flux is thus > 5-fold lower than required if the late-stage CH<sub>4</sub> turnover were due to MOx. Still, we cannot offer an explanation with respect to a potential, alternative electron acceptor for CH<sub>4</sub>-oxidation. Sulfate reduction could not account for the observed CH<sub>4</sub> oxidation, given that the ex situ SRR was 100-fold lower than CH<sub>4</sub> oxidation (Figs. 2.2e, 2.1d). Similarly, concentrations of other potential electron acceptors such as NO<sub>3</sub><sup>-</sup> or NO<sub>2</sub><sup>-</sup> (Wenk et al. 2013) or Fe(III) (Fig. 2.2b) were too low (< 1 μmol L<sup>-1</sup>) to account for the observed CH<sub>4</sub> turnover. Further investigations are required to ascertain potential anaerobic modes of CH<sub>4</sub>

oxidation in Lake Lugano's anoxic hypolimnion.

Biochemical processes impose an isotopic fractionation on the substrate that can be intrinsic to the enzymatic pathway. A characteristic  $\delta^{13}\text{C}$ -to- $\text{CH}_4$  concentration relationship (constrained by a characteristic  $\epsilon$ ) may help to diagnose the pathway of methane oxidation better. MOx is typically associated with  $\epsilon$  values between -15‰ and -30‰, with pMMO-based  $\text{CH}_4$  oxidation leading to larger fractionation (Jahnke et al. 1999). In contrast to an open-system model, a closed-system Rayleigh model described the Lake Lugano data quite well, yet the resulting apparent  $^{13}\text{C}$  isotope effect for methane oxidation in the hypolimnion (Eq. 2.1) ranged between -6.9‰ and -9.0‰ (Fig. 2.3). This is significantly lower than the organism-level  $\epsilon$  values expected for MOx. An anaerobic  $\text{CH}_4$  oxidation process with lower C-isotope fractionation could be invoked to explain the low  $\epsilon$  values. However, estimates for  $\epsilon$  values of known modes of AOM are scarce and rather indistinct (with values between -12‰ and -39‰; Holler et al. 2009), so that they do not serve as robust point of comparison to diagnose AOM in Lake Lugano unambiguously. We also recognize that the closed system approach may not be fully appropriate for this system. The isotope effects assessed on the ecosystem level may be lower by several per mille compared to the biological isotope effect at the cellular level, especially in the case of complete substrate consumption (see Thunell et al. 2004 and Lehmann et al. 2007 for a discussion on  $\epsilon$ -suppression). In contrast to  $\text{CH}_4$  oxidation at the oxycline,  $\text{CH}_4$  occurs in micromolar concentrations throughout large parts of the water column where potential methane turnover is observed (between 220 m and 145 m), arguing against a substrate limitation-driven suppression of  $\epsilon$ . However, in case of a temporally discontinuous process, in which periods of MOx with large fractionation alternate with periods without

consumption, mixing along the concentration gradient dampens the expression of  $\varepsilon$  in the ambient water, possibly leading to the observed lowered  $\varepsilon$  values. In conclusion, the apparent, or ecosystem-scale C-isotope effects for Lake Lugano determined here most likely do not represent C-isotope fractionation at the enzyme level and are hence of limited use for pinpointing the dominant mode of methane oxidation.

Our study provides the first in situ geochemical evidence of aerobic CH<sub>4</sub> oxidation at nanomolar O<sub>2</sub> concentrations, below detection limit of common O<sub>2</sub>-sensors, in a lacustrine environment. Micro-aerobic CH<sub>4</sub> oxidation is responsible for CH<sub>4</sub> consumption at the oxic-anoxic interface on the order of 1.7 – 3.0 mmol CH<sub>4</sub> m<sup>-2</sup> d<sup>-1</sup>, amounting to a total annual turnover of 127 – 224 × 10<sup>3</sup> kg C. Our data also suggest CH<sub>4</sub> consumption within the anoxic hypolimnion. The concentration and  $\delta^{13}\text{C}$  depth-distributions of CH<sub>4</sub> and lipid biomarkers in the anoxic hypolimnion of Lake Lugano's northern basin could (possibly erroneously) be interpreted as AOM. However, the evidence for AOM in Lake Lugano remains ambiguous. We provide multiple lines of evidence for micro-aerobic methane oxidation (MOx) even 40 m below the chemocline. MOB appear to survive prolonged periods of O<sub>2</sub>-starvation in a state of anaerobic dormancy, but rapidly resume micro-aerobic MOx upon episodic introduction of O<sub>2</sub>. This adaptation may represent an efficient strategy to avoid the detrimental effects of CH<sub>4</sub>-starvation under oxic conditions and escape grazing pressure in more oxygenated water. The long-term presence of potentially active MOB deep within the anoxic water column implies that O<sub>2</sub>-rich water is downwelled episodically, yet the exact mechanisms that induce O<sub>2</sub> injection and lead to the apparent blurring of anoxic and suboxic ecological regimes requires further investigation.

Micro-aerobic CH<sub>4</sub> oxidation both well below and at the oxic-anoxic interface make the hypolimnion of the Lake Lugano North Basin an efficient CH<sub>4</sub> filter, preventing export of CH<sub>4</sub> to the upper hypolimnion and epilimnion, and ultimately preventing emission to the atmosphere.

---

Chapter 3 was published in *Limnology & Oceanography*:

Blees, Jan, Helge Niemann, Christine B. Wenk, Jakob Zopfi, Carsten J. Schubert, Joël S. Jenzer, Mauro Veronesi, and Moritz F. Lehmann. Bacterial methanotrophs drive the formation of a seasonal anoxic benthic nepheloid layer in an alpine lake. *Limnol. Oceanogr.* **59**: 1410–1420. doi: 10.4319/lo.2014.59.4.1410

## Bacterial methanotrophs drive the formation of a seasonal anoxic benthic nepheloid layer in an alpine lake

---

### 3.1 Abstract

We investigated the formation and microbial composition of a seasonal benthic nepheloid layer (BNL) in the eutrophic, monomictic southern basin of Lake Lugano. During stratification, a BNL developed at the sediment – water interface and progressively expanded 20 – 30 m into the water column, following the rising oxic-anoxic interface. The dominance of the fatty acids  $C_{16:1\omega5}$ ,  $C_{16:1\omega6}$ ,  $C_{16:1\omega7}$  and  $C_{16:1\omega8}$ , with  $\delta^{13}C$  values between  $-62\text{‰}$  ( $\omega6$ ) and  $-80\text{‰}$  ( $\omega7$ ), suggests that the BNL was composed primarily of Type I aerobic methane oxidizing bacteria (MOB). Indeed, MOB contributed  $>75\%$  to the fatty acid carbon pool in the fully developed BNL, with cell densities up to  $8.5 \times 10^5$  cells  $mL^{-1}$ . In ex situ incubation experiments,  $CH_4$  turnover rate coefficients were up to  $2.1 d^{-1}$ , which translates into potential  $CH_4$  oxidation rates as high as  $20 \text{ mmol } m^{-3} d^{-1}$  under in situ  $CH_4$  concentrations.  $CH_4$  oxidation was limited by the diffusive supply of  $O_2$ , and  $O_2$  consumption by aerobic  $CH_4$  oxidation (up to  $13.1 \text{ mmol } m^{-2} d^{-1}$ ) appears to be the primary driver of the seasonal

growth of the BNL and expansion of the hypolimnetic anoxic zone. Methanotrophic activity at the interface between oxic and anoxic water masses can actuate the formation of a BNL, which in turn functions as an effective microbial CH<sub>4</sub> filter in the water column, preventing CH<sub>4</sub> transport to surface waters and evasion to the atmosphere. In situ biomass production by methanotrophic bacteria may represent, in addition to sediment resuspension and detritus trapping, a novel BNL formation mechanism.

### **3.2 Introduction**

Benthic nepheloid layers (BNLs), i.e. layers of increased suspended particle load, are a common feature in bottom waters of both lakes and oceans (McCave 1986). As a result of elevated organic matter and nutrient content, they are often hotspots for microbial activity, characterized by elevated microbial cell numbers and metabolic turnover rates (Guo and Santschi 2000; Boetius et al. 2000b). Most studies to date have focused on BNLs in ocean basins (Hunkins et al. 1969; Spinrad et al. 1983; McCave 1986), and the few studies dealing with BNLs in lake systems were carried out in very large lakes (e.g. Lake Ontario, Lake Michigan, Lake Superior), approaching inland seas in size (Hawley and Murthy 1995; Hawley and Muzzi 2003; Hicks et al. 2004). The exact controls on the formation of lacustrine BNLs remain enigmatic. In most cases, they have been attributed to physical processes, e.g. resuspension of sediments in high-energy environments or transport of sediment-laden water (i.e. sediment focusing or density currents) (Guo and Santschi 2000; Wieland et al. 2001). Laboratory and field tests have indicated significant resuspension of both sediment and bacteria at shear velocities exceeding

1 cm s<sup>-1</sup> (Wainright 1990), supporting the resuspension hypothesis in most cases. However, this mechanism fails to explain the formation of BNLs in stagnant and/or stratified water bodies with low physical disturbance in the vicinity of the sediment-water interface. Moreover, most reported BNLs occur in oxygenated water columns, without O<sub>2</sub> depletion prior to development of the BNL.

Lacustrine systems are thought to be important sources of atmospheric CH<sub>4</sub>, estimated to contribute up to 16% of natural CH<sub>4</sub> emissions (Bastviken et al. 2004, 2011). CH<sub>4</sub> is produced by methanogenic *Archaea* in anoxic sediments, where it typically accumulates to high concentrations. Under oxic bottom water conditions, a significant fraction of CH<sub>4</sub> is consumed at the sediment-water interface (Bastviken et al. 2002). During periods of water column stratification, however, the diffusive supply of oxygen across density gradients in the water column is hindered, and aerobic respiratory processes, including aerobic methane oxidation (MOx), lead to oxygen depletion and potentially anoxia in the hypolimnion (Diaz and Rosenberg 2008; Zaikova et al. 2010). In lakes, such seasonal density stratification is common, and it is typically interrupted by one or two mixing events per year (mono- or dimictic regimes, respectively), which replenish O<sub>2</sub> in the deep water. CH<sub>4</sub> can therefore accumulate periodically in the bottom water, providing a habitat for aerobic methane oxidizing bacteria (MOB) at the interface between CH<sub>4</sub>-rich and O<sub>2</sub>-replete water masses. Such redox interfaces may thus provide an ideal niche for the development of ‘bacterial clouds’ of methanotrophs (Lehmann et al. 2004). CH<sub>4</sub> dynamics in seasonally stratified lakes have been studied previously (Rudd et al., 1976; Bastviken et al., 2008), but the contribution of MOB to the development of anoxia

during water column stratification, as well as their potential role in the formation of BNLs, remains poorly constrained.

In this study we investigated the mechanisms of formation of the seasonal BNL in the monomictic southern basin of Lake Lugano. Using lipid biomarker, stable isotope and rate measurements, we focused particularly on the origin of (bacterial) particles forming the BNL, and the CH<sub>4</sub> and O<sub>2</sub> dynamics that lead to the development of anoxia in the BNL. We demonstrate that the BNL in Lake Lugano consists primarily of aerobic MOB, likely without significant contribution of resuspended sediments.

### **3.3 Methods**

#### *3.3.1 Sampling site*

Lake Lugano is a south-alpine lake on the Swiss-Italian border at an elevation of 271 m above mean sea level. The lake consists of a southern and northern basin, which are separated from each other by a natural dam. The narrow southern basin, the focus of this study, is monomictic and has a maximum water depth of 95 m. During the summer months a pronounced thermocline develops. The southern basin experiences a complete water column turnover in late January or early February, when the surface water temperature is lowered enough to allow vertical mixing. Previous work has reported on the development of a near-bottom zone of high suspended particle density during the stratified period, providing the first putative evidence (e.g. low C:N ratios, strong <sup>13</sup>C<sub>org</sub>-isotopic depletion) for a methanotrophic origin of the BNL (Lehmann et al. 2004).

### 3.3.2 Sampling

Sampling campaigns were conducted in 2009 (February, March, June, August, October) and 2010 (January, August, October). All sampling casts were performed in the middle of the lake's southern basin (45.95 °N, 8.90 °E). Temperature, conductivity, O<sub>2</sub> concentration, pH and turbidity were measured with a conductivity, temperature and depth (CTD) instrument (Idronaut Ocean Seven 316 Plus, Idronaut). O<sub>2</sub> concentration measurements were calibrated against Winkler titration measurements, and a detection limit of 1 μmol L<sup>-1</sup> was determined. Water samples were collected in 5 L Niskin bottles, and subsamples were taken directly from the Niskin bottle through silicon tubing.

### 3.3.3 Hydrochemical analyses

Samples for NH<sub>4</sub><sup>+</sup>, total sulfide (hereafter 'H<sub>2</sub>S') and Fe<sup>2+</sup> were fixed on board, and concentrations were determined photometrically using the indophenol blue (NH<sub>4</sub><sup>+</sup>), bipyridine (Fe<sup>2+</sup>) and methylene blue (H<sub>2</sub>S) methods (Grasshoff et al. 1999). Additional water samples were collected for determination of total Fe through reduction of oxidized Fe species with hydroxyl ammonium chloride prior to determination of evolved Fe<sup>2+</sup> with the bipyridine method. Fe<sup>3+</sup> concentration was then calculated as the difference between Fe<sup>2+</sup> and total Fe. H<sub>2</sub>S samples were fixed with 20% zinc acetate (1% final concentration).

### 3.3.4 Dissolved methane

Samples for the determination of CH<sub>4</sub> concentration and δ<sup>13</sup>CCH<sub>4</sub> were collected in 500 mL glass bottles and immediately sealed with thick black butyl rubber stoppers. On board, a 10 mL air headspace was added and 10

mL 50% NaOH was introduced in exchange with sample to liberate dissolved CH<sub>4</sub> into the headspace. CH<sub>4</sub> samples were stored inverted until analysis. In the laboratory, an additional 40-mL N<sub>2</sub> headspace was introduced. CH<sub>4</sub> concentrations were determined in duplicate on a gas chromatograph (GC, Agilent 6890N) equipped with a 30 m Supelco Carboxen 1010 porous layer open tubular (PLOT) column (0.53 mm inner diameter (i.d.)) and a Flame Ionization Detector (FID). <sup>13</sup>C:<sup>12</sup>C ratios were analysed with an isotope ratio mass spectrometer (TraceGas, Isoprime) with a pre-concentration cryo-trap (PreCon, Thermo Scientific). Corrections were made for linearity effects and instrument drift. Stable C-isotope values are reported in the conventional δ-notation (in ‰) relative to the Vienna Pee Dee Belemnite standard (V-PDB). CH<sub>4</sub> δ<sup>13</sup>C values have an analytical error of ± 1‰. Apparent kinetic isotope enrichment factors were calculated according to Mariotti et al. (1981):

$$\varepsilon_{p/s} = \frac{10^3 \ln \frac{10^{-3} \delta_s + 1}{10^{-3} \delta_{s,0} + 1}}{\ln f} \quad \text{Eq. 3.1}$$

where  $\varepsilon_{p/s}$  is the enrichment factor (in ‰) between product and substrate,  $\delta_s$  and  $\delta_{s,0}$  are the δ<sup>13</sup>C-values of CH<sub>4</sub> at a given depth and the δ<sup>13</sup>C of the source CH<sub>4</sub>, respectively, and  $f$  is the fraction of CH<sub>4</sub> remaining, calculated as the ratio of [CH<sub>4</sub>] at the considered depth and [CH<sub>4</sub>] at the sediment – water interface.

### 3.3.5 Methane oxidation rates

Methane oxidation rate (MOR) incubations were performed in triplicate throughout the water column as described previously (Mau et al.

2013; Bles et al. 2014a, see chapter 2). Briefly, discrete 25 mL samples from 84 m water depth were incubated with  $^{14}\text{CH}_4$  (10  $\mu\text{L}$ , 1 kBq) for periods of 5, 10, 17 and 24 h. The time series measurements were used to confirm linearity of turnover, and subsequently 10 h incubation periods were used for the other sampled depths. Incubations were terminated by addition of 0.5 mL NaOH (50% v:v). Residual  $^{14}\text{CH}_4$  was extracted, combusted to  $^{14}\text{CO}_2$ , and the activity was measured by liquid scintillation counting. Incubation water was then acidified for the assessment of the activity of  $^{14}\text{CO}_2$  from  $\text{CH}_4$  oxidation. Finally, the residual activity was measured from an aliquot of remaining incubation water. The first order rate constant ( $k$ ) was calculated from the activity of the three carbon pools:

$$k = \frac{A_{\text{CO}_2} + A_{\text{R}}}{A_{\text{CH}_4} + A_{\text{CO}_2} + A_{\text{R}}} \times \text{d}^{-1} \quad \text{Eq. 3.2}$$

where  $A_{\text{CH}_4}$ ,  $A_{\text{CO}_2}$  and  $A_{\text{R}}$  represent the radioactivity of  $\text{CH}_4$ ,  $\text{CO}_2$  and the residual radioactivity, respectively.  $k$  values in the time series were constant over an incubation time range up to 10 h, and subsequently decreased with increasing degree of consumption.  $\text{CH}_4$  oxidation rates (MOR) were then calculated assuming first order kinetics:

$$\text{MOR} = k \times [\text{CH}_4], \text{ in } \text{mmol m}^{-3} \text{ d}^{-1} \quad \text{Eq. 3.3}$$

where  $[\text{CH}_4]$  is the  $\text{CH}_4$  concentration. We used the  $\text{CH}_4$  concentration at the start of incubation for the calculation of the ex situ turnover rate ( $\text{MOR}_{\text{ex situ}}$ ). It is important to note, however, that the concentration at the start of the incubation was lower than the in situ concentration at the time of sampling due to on-going  $\text{CH}_4$  consumption between sampling and

start of the incubation experiments. The CH<sub>4</sub> concentration at the start of the experiments was calculated from the concentration measured in each incubation by gas chromatography at the end of the incubation period, corrected for CH<sub>4</sub> turnover during incubation.

### 3.3.6 Flux calculations in the water column

Vertical turbulent-diffusive fluxes of solutes in the water column ( $F_z$ ) were calculated from the vertical eddy diffusivity ( $K_z$ ) and the concentration gradient ( $dC/dz$ ):

$$F_z = -K_z \frac{dC}{dz} \quad \text{Eq. 3.4}$$

$K_z$  depends on the buoyancy frequency and varies with depth. It can be expressed as (Gargett 1984):

$$K_z = a_0 \times \left( \frac{-g}{\rho_z} \times \frac{d\rho}{dz} \right)^{-0.5} \quad \text{Eq. 3.5}$$

where  $g$  is the standard gravity,  $\rho_z$  is the density at depth  $z$ , and  $d\rho/dz$  is the density gradient, calculated from temperature and conductivity data. The factor  $a_0$  is a system-specific constant, which describes the amplitude of the response of  $K_z$  to changes in the buoyancy frequency, and which was determined to be  $1.4 \times 10^{-8} \text{ m}^2 \text{ s}^{-2}$  for the southern basin of Lake Lugano during stratified conditions at the sediment – water interface (Wenk et al. 2013). This value is representative for restricted basins (Gargett 1984).  $K_z$  values for the water column above and below the oxic-anoxic interface were calculated from density profiles in October 2009 and 2010 (Eq. 3.5). During the sampling in 2009,  $K_z$  values were  $8.0 \times 10^{-6}$

$\text{m}^2 \text{s}^{-1}$  above (50 – 76 m), and  $5.5 \times 10^{-6} \text{ m}^2 \text{ s}^{-1}$  within (79 – 90 m) the BNL. In October 2010 calculated  $K_z$  values were  $1.5 \times 10^{-5} \text{ m}^2 \text{ s}^{-1}$  above (50 – 80 m), and  $6.2 \times 10^{-6} \text{ m}^2 \text{ s}^{-1}$  within (82 – 90 m) the BNL.

### 3.3.7 *Particulate organic carbon*

Particulate organic carbon (POC) was collected from lake water samples (~5 L) by filtration through pre-combusted glass fibre filters (GF/F, Whatman). Filters were stored frozen (-20°C) in aluminium foil. For the bulk concentration and stable carbon isotopic analysis of POC, filter pieces of  $1.5 \text{ cm}^2$  were de-carbonated in a desiccator with fumes of concentrated HCl for more than 24 h. The remaining organic carbon was combusted to  $\text{CO}_2$  and the  $^{12}\text{C}:^{13}\text{C}$  ratio analysed using a Sercon Integra2 elemental analyser coupled to an isotope ratio mass spectrometer (EA-IRMS). POC  $\delta^{13}\text{C}$ -values reported here have an analytical error of <0.2‰.

### 3.3.8 *Biomarker analyses*

*Extraction and derivatisation* – Lipid biomarkers were extracted according to Elvert et al. (2003). Briefly, a total lipid extract (TLE) was obtained by ultrasonication of filter samples with solvents of decreasing polarity: (1) dichloromethane (DCM):methanol (MeOH) 1:2; (2) DCM:MeOH 2:1; and (3,4) DCM. Further separation into a polar lipid-derived fatty acid (FA) and an apolar fraction, as well as derivatisation of FAs into fatty acid methyl esters (FAMES) was carried out according to previous work (Elvert et al. 2003; Niemann et al. 2005). Double bond positions were determined through analysis of their dimethyl-disulfide adducts (Nichols et al. 1986; Moss and Lambert-Fair 1989).

*Quantification, identification and stable carbon isotope composition* – Individual FAs were separated by gas chromatography (Trace GC Ultra, Thermo Scientific equipped with a split-splitless injector operated in splitless mode at 300°C), over a capillary column (Rxi®-5ms, 60 m x 0.25 mm i.d., 0.25 µm film thickness) with a constant He flow of 1 mL min<sup>-1</sup> using the following temperature program: initial oven T was 50°C, held for 2 min and then increased to 140°C at 10°C min<sup>-1</sup>, then to 300°C with 4°C min<sup>-1</sup> and finally held at 300°C for 63 min. The abundance of individual compounds was quantified by flame ionization detection (FID). Concentrations were calculated through calibration with an internal standard and corrected for the introduction of carbon atoms. Identification of single compounds was achieved by GC-mass spectrometry (GC-MS) with electron ionization (Thermo Scientific DSQ II). Acquired mass spectra were identified through comparison with known standards and published data. Compound-specific stable carbon isotope ratios were determined using a GC-IRMS (Delta V Advantage, Thermo Scientific). As with concentrations,  $\delta^{13}\text{C}$ -values were corrected for introduced carbon of known  $\delta^{13}\text{C}$ .  $\delta^{13}\text{C}$  values of FA biomarkers and their percentage contributions to the total FA pool in a profile through the fully developed BNL in October 2010 are listed in Table 3.1. Reproducibility was monitored by repeated injections and monitoring of internal standards. Reported  $\delta^{13}\text{C}$ -values have an analytical error of  $\pm 1\%$ .

### 3.3.9 Cell enumeration by epifluorescence microscopy

40 mL of water column sample were fixed with 4 mL paraformaldehyde (1% final concentration) and stored cooled in the dark for about 7 h. Aliquots of 10 mL and 30 mL were subsequently filtered

onto polycarbonate membrane filters (0.2  $\mu\text{m}$  pore size, Whatman), which were then dried at room temperature and stored at  $-20^{\circ}\text{C}$ . Fluorescence in situ hybridization (FISH) analysis of the filter samples was used to determine cell numbers of methanotrophs. 6-carboxyfluorescein (6-FAM) labelled probes (Biomers) for Type I (Mg84 and Mg705) and Type II (Ma450) methanotrophic bacteria were applied (Eller et al. 2001) following the standard SILVA protocol for FISH with fluorescently monolabelled oligonucleotide probes ([www.arb-silva.de](http://www.arb-silva.de)). Counterstaining of FISH preparations was done with  $1 \mu\text{g mL}^{-1}$  final concentration of 4',6-diamidino-2-phenylindole (DAPI) in 1:5 phosphate buffered saline (PBS):Citifluor antifadent AF1. FISH and DAPI stained cells were counted using 1000X magnification and epifluorescence microscopy (Leica DM2500 with an external ultraviolet light source EL6000).

Average cell sizes were assessed on digital photographs of FISH- (methanotrophic cells) and DAPI- (non-methanotrophic cells) stained filters. Cell volumes were then calculated according to:

$$V_B = \left( \frac{W^3}{6} \times \pi \right) + (L - W) \times \left( \frac{W^2}{4} \times \pi \right) \quad \text{Eq. 3.6}$$

(Posch et al. 2001), where  $V_B$  is the cellular volume and  $W$  and  $L$  are the width and length of the cells, respectively. Subsequently, carbon content was calculated, using the equation:

$$CC_B = 218 \times V_B^{0.86} \quad \text{Eq. 3.7}$$

(Posch et al. 2001). Finally, the total biomass carbon per litre was then obtained through multiplication of  $CC_B$  by the cell number. Cell sizes and biomass concentrations are listed in Table 3.2.

## 3.4 Results

### 3.4.1 *Mixing, stratification and the development of the BNL*

Following fully mixed conditions (late winter to early spring; Fig. 3.1a,f), a thermocline started to develop in spring in about 15 – 20 m water depth, with surface water temperatures reaching  $> 25^{\circ}\text{C}$  in late August. The water mass below 35 m retained the winter surface water temperature of  $5.5 - 5.9^{\circ}\text{C}$  throughout the year. Net  $\text{O}_2$  consumption in the stagnant deep water was indicated by a decreasing  $\text{O}_2$  inventory below the thermocline (Fig. 3.1). During early summer of both sampling years, anoxia developed first in the bottom water and then expanded progressively into the hypolimnion (up to  $\sim 15$  m above the lake floor in winter 2009 – 2010, and  $\sim 30$  m in winter 2008 – 2009). At all times, the depth of the oxic-anoxic interface corresponded to increased conductivity and turbidity (Fig. 3.1), indicating the presence of a BNL. The upper boundary of the turbid layer, while following the redox transition zone, never expanded into the fully oxygenated hypolimnion, but was always constrained to  $\text{O}_2$  concentrations  $< 1 \mu\text{mol L}^{-1}$ . Complete turnover of the water column between January and early March, after surface-water cooling to  $< 6^{\circ}\text{C}$ , led to ventilation of the deep water, the collapse of solute concentration and temperature gradients (Fig. 3.1e), and ultimately to the disappearance of the BNL (Fig. 3.1a,f).

### 3.4.2 *Hydrochemical analyses and methane $\delta^{13}\text{C}$*

During water column stratification,  $\text{NH}_4^+$  accumulated to concentrations of  $70 \mu\text{mol L}^{-1}$  in the bottom water. Similarly, bottom water concentrations of total Fe increased to up to  $10 \mu\text{mol L}^{-1}$ , but  $\text{Fe}^{2+}$

concentration remained below  $1 \mu\text{mol L}^{-1}$ .  $\text{H}_2\text{S}$  concentration remained below detection limit (data not shown).

During the mixing period in late winter,  $\text{CH}_4$  concentrations in the oxygenated water column were  $<1 \mu\text{mol L}^{-1}$ , but increased in bottom waters with development of anoxia during early summer (Fig. 3.2). Maximum  $\text{CH}_4$  concentrations of up to  $\sim 100 \mu\text{mol L}^{-1}$  were detected in the anoxic BNL just above the sediment-water interface in October 2010 (Fig. 3.2).  $\text{CH}_4$  concentration decreased towards the oxic-anoxic interface, where concentrations dropped below  $100 \text{ nmol L}^{-1}$ . Associated with the  $\text{CH}_4$  concentration decrease was an increase in  $\delta^{13}\text{CH}_4$ , from  $-70\text{‰}$  directly above the sediment to  $-50\text{‰}$  at the oxic-anoxic interface. The apparent C-isotope enrichment factor calculated for  $\text{CH}_4$  consumption within the BNL in October 2010, over the depth range between 90 m and 82 m, was  $-2.8\text{‰}$ .

### *3.4.3 Turbulent diffusive fluxes of methane and oxygen and methane oxidation rates*

Concentration gradient-based  $\text{CH}_4$  fluxes from the sediment-water interface towards the oxic-anoxic interface were  $6.8$  and  $7.3 \text{ mmol m}^{-2} \text{ d}^{-1}$  in October 2009 and 2010, respectively. The corresponding  $\text{O}_2$  fluxes from mid water depths towards the BNL were  $5.7$  and  $10.7 \text{ mmol m}^{-2} \text{ d}^{-1}$ , respectively. Methane oxidation rate measurements performed in January and October 2010 indicated high potential MORs in a narrow band at the oxic-anoxic interface, i.e. the upper boundary of the BNL (Fig. 3.3). In October 2010,  $k$  values reached  $0.09 \text{ h}^{-1}$  ( $2.1 \text{ d}^{-1}$ ), which translates into a  $\text{MOR}_{\text{ex situ}}$  of  $1.8 \text{ mmol m}^{-3} \text{ d}^{-1}$  ( $[\text{CH}_4]: < 1 \text{ mmol m}^{-3}$ ) (Fig. 3.3). MOR was insubstantial in the oxygenated water above the

BNL. Similarly, within the BNL, MOR dropped below detection limit within  $\sim 2$  m below the oxic-anoxic interface.

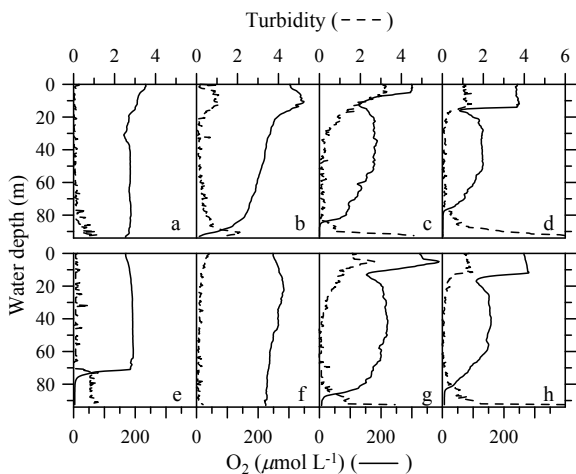


**Figure 3.1** Turbidity (dotted lines) and  $\text{O}_2$  (solid lines) profiles through the water column of (a) March 2009, (b) June 2009, (c) August 2009, (d) October 2009, (e) January 2010, (f) March 2010, (g) August 2010, and (h) October 2010.

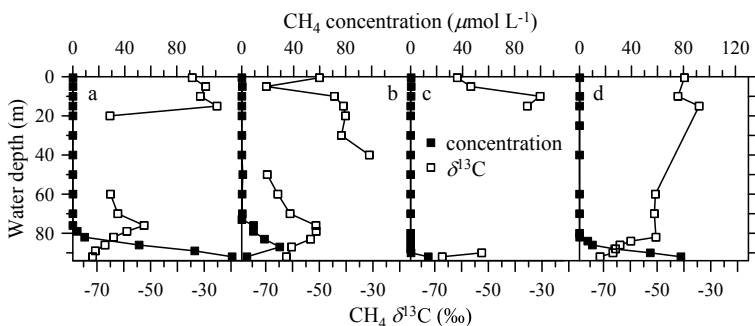


**Figure 3.2** Water column  $\text{CH}_4$  concentration and  $\delta^{13}\text{C}$  for (a) October 2009, (b) January 2010, (c) August 2010, and (d) October 2010.

### 3.4.4 POC and FA biomarkers – Concentrations and C-isotopic composition

In October 2010, the POC concentration increased from  $\sim 100 \mu\text{g L}^{-1}$  in the oxic water column to  $> 500 \mu\text{g L}^{-1}$  in the BNL (Fig. 3.4a). Similar to POC, the concentration of lipids increased sharply at the top of the anoxic BNL. Four mono-enoic  $\text{C}_{16}$  FAs ( $\omega 5$ ,  $\omega 6$ ,  $\omega 7$  and  $\omega 8$ ) constituted 70% of the total FA pool within the BNL in October 2010 (Table 3.1). The most abundant of the four FAs was  $\text{C}_{16:1\omega 7}$ , which increased from  $0.9 \mu\text{g L}^{-1}$  in the oxic water column above the BNL (70 m water depth) to  $15 \mu\text{g L}^{-1}$  in the BNL (Fig. 3.4d). The greatest concentration increase from oxic to suboxic and anoxic waters was observed in  $\text{C}_{16:1\omega 6}$ , followed by  $\text{C}_{16:1\omega 7}$  and  $\text{C}_{16:1\omega 8}$  (30-, 19- and 16-fold concentration increase, respectively). However, also other FAs displayed a significant concentration increase, such as  $\text{C}_{12:0}$  (15-fold) and  $i\text{C}_{15:0}$  (10-fold). Conversely,  $\text{C}_{18}$  FAs increased less than 3-fold, and remained at relatively low concentrations within the BNL (Fig. 3.4b).

POC in the BNL was strongly  $^{13}\text{C}$ -depleted relative to background POC in the oxic water column, with  $\Delta\delta^{13}\text{C}$  of about -10‰ to -20‰ ( $\Delta\delta_{\text{POC}} = \delta^{13}\text{C}_{\text{POC\_BNL}} - \delta^{13}\text{C}_{\text{POC\_60m}}$ , Fig. 3.4e). Similarly, a  $^{13}\text{C}$  depletion was found in all analysed FAs within the BNL except  $\text{C}_{18:2}$  and  $\text{C}_{18:0}$ . The most pronounced  $^{13}\text{C}$  depletion was found in the following fatty acids:  $\text{C}_{12:0}$ ,  $\text{C}_{14:0}$ ,  $\text{C}_{15:0}$ ,  $\text{C}_{16:1\omega 5}$ ,  $\text{C}_{16:1\omega 7}$ ,  $\text{C}_{16:1\omega 8}$  and  $\text{C}_{16:0}$  (Fig. 3.4g,h), with  $\Delta\delta^{13}\text{C}$  values (86 m vs. 60 m water depth) between -19‰ and -33‰.  $\Delta\delta^{13}\text{C}$  increased with depth within the BNL. Very close to the sediment – water interface (92 m water depth), the most abundant FA,  $\text{C}_{16:1\omega 7}$ , reached a  $\delta^{13}\text{C}$  value of -82‰ in October 2010 (i.e.  $\Delta\delta^{13}\text{C}_{92-60}$  -38‰), still 20‰ lower than the bulk POC isotope signature at the same depth. This

indicates strong C-isotope partitioning within the BNL organic matter pool.

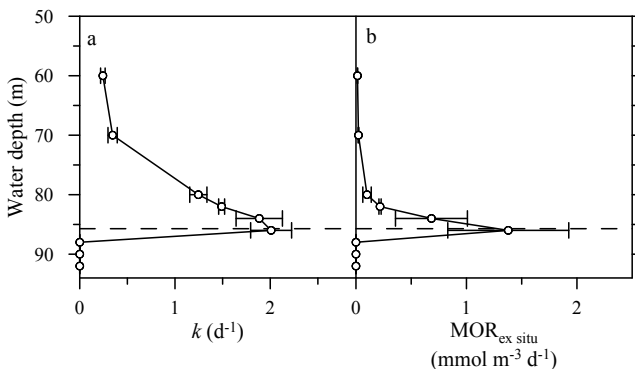


**Figure 3.3** CH<sub>4</sub> oxidation rates with standard deviations of parallel incubations in the water column of October 2010: (a)  $k$  values, (b) MOR<sub>ex situ</sub>. The dashed line indicates the interface between oxic and anoxic water.

### 3.4.5 Contribution of MOB to the BNL's FA carbon pool

The contribution of methane-derived FA carbon to the BNL's carbon pool was estimated using a simple C-isotope end-member approach (Bianchi and Canuel 2011):

$$C_{\text{CH}_4\text{-derived}} = \frac{\delta^{13}\text{C}_{\text{FA}} - \delta^{13}\text{C}_{\text{non-CH}_4\text{-derived}}}{\delta^{13}\text{C}_{\text{CH}_4\text{-derived}} - \delta^{13}\text{C}_{\text{non-CH}_4\text{-derived}}} \quad \text{Eq. 3.8}$$

where  $C_{\text{CH}_4\text{-derived}}$  is the fraction of CH<sub>4</sub>-derived carbon in the FA pool,  $\delta^{13}\text{C}_{\text{FA}}$  is the C-concentration-weighted average  $\delta^{13}\text{C}$  of the FA pool,  $\delta^{13}\text{C}_{\text{CH}_4\text{-derived}}$  is the  $\delta^{13}\text{C}$  of CH<sub>4</sub>-derived FAs, and  $\delta^{13}\text{C}_{\text{non-CH}_4\text{-derived}}$

is the  $\delta^{13}\text{C}$  of non- $\text{CH}_4$ -derived FA carbon (i.e. algal, detrital, sedimentary). Photosynthetic FA carbon (e.g.  $\text{C}_{18:0}$ ) from the oxic water column has a well-constrained value of  $-30\text{‰}$  (Fig. 3.4f). On the other hand, the most  $^{13}\text{C}$ -depleted lipids at the redoxcline in October 2010 ( $\text{C}_{16:1\omega5-8}$ ; Table 3.1) displayed  $\delta^{13}\text{C}$  values between  $-62\text{‰}$  and  $-71\text{‰}$  (Table 3.1; Fig. 3.4h), consistent with a substrate methane  $\delta^{13}\text{C}$  of approximately  $-60\text{‰}$  and a relatively low apparent C-isotope enrichment factor ( $\varepsilon = -2.8\text{‰}$ ). The reduced expression of the biological isotope fractionation at the ecosystem level is common in environments where substrate supply is diffusion-limited and consumption is complete (Thunell et al. 2004; Lehmann et al. 2007; Wenk et al. 2014). Based on Eq. 3.8, a concentration-weighted mean  $\delta^{13}\text{C}_{\text{FA}}$  of about  $-60\text{‰}$  (considering all FAs in the top 4 m of the BNL) then yields  $\text{CCH}_4$ -derived values of  $77\% - 96\%$ . That is, more than three quarters of the FA carbon in the BNL is derived from  $\text{MOx}$ , directly by methanotrophic bacteria, or indirectly by syntrophic microorganisms.

### 3.4.6 Cell enumeration by fluorescence microscopy

Total cell numbers through the water column above the BNL in October 2009 ranged between  $1.6 \times 10^6 \text{ mL}^{-1}$  and  $2.2 \times 10^6 \text{ mL}^{-1}$ , and increased slightly to  $2.6 \times 10^6 \text{ mL}^{-1}$  in the BNL (Fig. 3.5a, Table 3.2). MOB-specific FISH revealed that almost all MOB in the southern basin of Lake Lugano belonged to the Type I subgroup, corroborating the results from our lipid biomarker analyses (Fig. 3.5b). Furthermore, MOB cell numbers varied through the BNL in a manner similar to the concentration of  $\text{C}_{16:1}$ , displaying a distinct maximum of  $8.6 \times 10^5 \text{ cells mL}^{-1}$  at 90 m depth (Fig. 3.5a). The Type I MOB thus accounted for up to

30% of all bacterial cells, whereas Type II MOB typically contributed < 1%. The methanotrophic cells were significantly larger than non-methanotrophic cells in the BNL (Table 3.2) but fall well within the size range reported for laboratory pure cultures of *Methylobacter* (Bowman 2006). Methanotrophic biomass estimated from the calculated cell volumes contributed up to 77% to the total bacterial biomass, which is in good agreement with the CH<sub>4</sub>-derived fraction of FA biomass calculated from the FA isotope balance (Eq. 3.8).

## 3.5 Discussion

### 3.5.1 Development of the BNL by bacterial *in situ* production

The steep decline of the O<sub>2</sub> concentration to low suboxic levels (< 1 μmol L<sup>-1</sup>) at the top of the BNL, and below detection limit of the CTD-O<sub>2</sub>-sensor within the BNL, indicates that O<sub>2</sub> consumption takes place to a large part at the top of the BNL (Fig. 3.1). The parallel spatio-temporal evolution of the BNL and the oxic-anoxic interface – i.e. the progressive vertical expansion of the BNL accompanying the rise of the redoxcline throughout the period of water column stratification – strongly suggests that development of the BNL and anoxia in the lower water column are closely coupled. However, it is unclear whether BNL development follows the movement of the redox transition zone or vice versa. To answer this question, we first need to understand the mechanism of formation, and therefore the composition of the BNL. A BNL is a layer of increased particle load close to the bottom of a water body, which may form through resuspension and transport of sediments or sinking of particulate matter from above in the water column (McCave 1986; Hawley and Murthy 1995; Boetius et al. 2000b). However, resuspension

and sediment focusing induced by turbulence or currents seem unlikely in the southern basin of Lake Lugano during the stratified period, as this would also lead to an episodic collapse of the density stratification and introduce O<sub>2</sub> into the BNL. Moreover, the marked discrepancy between the δ<sup>13</sup>C of both the sediments (-28.9‰ to -30.9‰; Lehmann et al. 2002) and the sinking particulate matter flux from the oxic water column (about -30‰) on the one hand, and the strongly <sup>13</sup>C-depleted isotopic signature of organic matter in the BNL on the other, argues against any significant role of allochthonous or resuspended organic matter during BNL formation. As an alternative, we suggest that the BNL develops as a result of in situ organic matter production. The FA content of the BNL in Lake Lugano, and particularly the dominance of unusual FAs C<sub>16:1ω5</sub>, C<sub>16:1ω7</sub> and C<sub>16:1ω8</sub> (Table 3.1, Fig. 3.4d,h), strongly suggests a bacterial origin of a large part of the BNL biomass. A mainly bacterial origin is further indicated by low C:N ratios (Lehmann et al. 2004). Moreover, both FAs and POC carried a characteristically low <sup>13</sup>C-isotope signature, which clearly points to a CH<sub>4</sub>-derived carbon source. In situ biosynthesis of bacterial methanotrophs, growing on a low δ<sup>13</sup>C substrate (with additional discrimination against <sup>13</sup>C during biosynthesis), hence best explains the observed C-isotope and geochemical signatures reported here for BNL organic matter. The close coupling between the dynamics of CH<sub>4</sub>, O<sub>2</sub> and the BNL provide further evidence for aerobic MOB playing a driving role in the formation of the BNL. The fact that the anoxic BNL grows upwards suggests that the downward O<sub>2</sub>-flux through the stratified water column is insufficient to counter the upward flux of CH<sub>4</sub> (and other reduced substances, e.g. NH<sub>4</sub><sup>+</sup>). As the redoxcline progresses upwards with the expansion of the anoxic water layer during summer and fall, new MOx biomass is produced. MOB then remain suspended in the anoxic BNL

**Table 3.1** Percentage of total  $C_{12} - C_{20}$  FA biomarkers (upper numbers) and  $\delta^{13}C$  (lower numbers) of FAs,  $\delta^{13}C$  of POC in a profile through the fully developed BNL in October 2010. The transition from the oxic water to the anoxic BNL at 84 m water depth is indicated in boldface.

Depth (m)	Fatty acids															POC
	$C_{12:0}$	$C_{14:0}$	$iC_{15:0}$	$aiC_{15:0}$	$C_{15:0}$	$C_{16:1o8}$	$C_{16:1o7}$	$C_{16:1o6}$	$C_{16:1o5}$	$C_{16:0}$	$C_{17:0}$	$C_{18:2}$	$C_{18:1o9}$	$C_{18:1o7}$	$C_{18:0}$	
60																
%	0.8	4.6	0.8	1.1	3.3	5.2	16.2	0.8	4.9	25.9	0.0	1.4	7.6	14.1	13.1	
$\delta^{13}C$	-24.7	-31.6	-33.1	-32.9	-31.8	-45.5	-43.6	-50.9	-46.3	-27.6	-21.7	-28.3	-28.1	-21.7	-26.1	-31
70																
%	0.8	6.4	1.3	1.3	1.2	4.9	14.6	2.2	4.6	25.5	0.6	1.5	13.5	5.3	16.3	
$\delta^{13}C$	-25.4	-35.1	-33.5	-36.2	-32.9	-33.9	-48.5	-46.9	-49.0	-29.8	-21.5	-29.6	-31.2	-30.7	-25.7	-33
80																
%	1.2	3.3	1.2	1.0	0.9	14.8	22.1	4.3	11.0	15.9	0.6	0.6	3.4	11.4	8.4	
$\delta^{13}C$	-41.9	-43.5	-40.7	-38.3	-38.0	-45.9	-59.7	-60.1	-61.7	-32.2	-28.7	-31.2	-33.4	-25.2	-28.6	-40
82																
%	<b>1.2</b>	<b>3.8</b>	<b>1.4</b>	<b>1.1</b>	<b>1.0</b>	<b>15.9</b>	<b>23.0</b>	<b>4.7</b>	<b>12.0</b>	<b>16.4</b>	<b>0.7</b>	<b>0.8</b>	<b>3.2</b>	<b>6.4</b>	<b>8.3</b>	
$\delta^{13}C$	<b>-39.1</b>	<b>-48.0</b>	<b>-43.6</b>	<b>-42.1</b>	<b>-43.8</b>	<b>-59.0</b>	<b>-59.6</b>	<b>-63.3</b>	<b>-62.6</b>	<b>-36.2</b>	<b>-25.1</b>	<b>-33.1</b>	<b>-34.2</b>	<b>-30.6</b>	<b>-29.4</b>	<b>-41</b>
84																
%	<b>1.7</b>	<b>3.5</b>	<b>1.2</b>	<b>0.8</b>	<b>0.9</b>	<b>19.5</b>	<b>32.2</b>	<b>5.5</b>	<b>13.7</b>	<b>11.4</b>	<b>0.3</b>	<b>0.7</b>	<b>2.0</b>	<b>1.7</b>	<b>4.9</b>	
$\delta^{13}C$	<b>-54.4</b>	<b>-60.2</b>	<b>-47.6</b>	<b>-45.0</b>	<b>-52.0</b>	<b>-71.5</b>	<b>-67.9</b>	<b>-63.5</b>	<b>-69.3</b>	<b>-47.4</b>	<b>-39.6</b>	<b>-36.7</b>	<b>-38.3</b>	<b>-41.9</b>	<b>-28.1</b>	<b>-48</b>
86																
%	2.0	3.3	1.1	0.8	0.8	18.0	34.6	5.0	11.7	12.8	0.0	0.4	1.8	2.6	5.1	
$\delta^{13}C$	-57.6	-57.9	-47.4	-44.7	-50.9	-65.7	-65.5	-62.0	-68.4	-47.2	-36.7	-30.1	-35.4	-30.2	-28.8	-50
88																
%	2.2	2.9	1.2	0.8	0.8	18.8	36.9	4.2	8.8	13.6	0.0	0.4	1.8	4.0	3.7	
$\delta^{13}C$	-59.2	-58.9	-45.8	-43.8	-50.1	-64.0	-68.2	-63.8	-70.0	-48.6	-33.6	-33.2	-37.7	-30.5	-29.9	-53



and/or sink slowly to the bottom, explaining the accumulation of particulate matter towards the lake bottom.

### 3.5.2 Type I methanotrophs dominate BNL biomass

The predominance of  $^{13}\text{C}$ -depleted  $\text{C}_{16}$  rather than  $\text{C}_{18}$  FAs suggests a methanotrophic community composed mainly of Type I MOB (Hanson and Hanson 1996). The FA fingerprint of the methanotrophic community was dominated by  $\text{C}_{16:1\omega5-8}$  (Fig. 3.4d). This pattern, and especially the strong  $^{13}\text{C}$  depletion in the most abundant FA,  $\text{C}_{16:1\omega7}$ , was similar to the isotope-geochemical fingerprint of the methanotrophic community in the adjacent northern basin of Lake Lugano, which we identified through phylogenetic analyses as *Methylobacter* sp. (Blees et al. 2014a, see chapter 2). The BNL FA fingerprint is furthermore consistent with reports by Bowman et al. (1995), who found  $\text{C}_{16:1\omega7c}$  dominating the lipid composition of *Methylobacter* sp., making up 57% of its total FA pool. The FA data reported here are also in agreement with our microscopic observations using Type I and II-specific FISH probes, which provide evidence for a methanotrophic community dominated by Type I MOB, with minor contribution of Type II methanotrophs. Based on our microscopic analyses and the close match of the  $^{13}\text{C}$  depleted FAs in both basins, we argue that Type I methanotrophs, likely related to *Methylobacter* sp., dominate the methanotrophic community in the BNL of the southern basin of Lake Lugano.

Several other FAs made a substantial contribution to the BNL FA pool, namely  $\text{C}_{16:0}$ ,  $\text{C}_{18:1\omega9}$ ,  $\text{C}_{18:1\omega7}$  and  $\text{C}_{18:0}$  (Table 3.1). The  $\text{C}_{18}$  FAs did not display C-isotope ratios that appear to be diagnostic for methanotrophy (i.e. low  $\delta^{13}\text{C}$ ) (Table 3.1, Fig. 3.4f), suggesting neither

direct, nor indirect involvement in CH<sub>4</sub> cycling. The C<sub>16:0</sub> FA pool seems to contain some CH<sub>4</sub>-derived (i.e. low δ<sup>13</sup>C) carbon. Given, however, that the relative contribution of C<sub>16:0</sub> to the total FA pool decreases from the oxygenated water to the BNL (Table 3.1), and that C<sub>16:0</sub> is not a methanotroph-specific FA, it is reasonable to assume that it is partially derived from other, potentially syntrophic organisms. The FAs C<sub>12:0</sub>, C<sub>14:0</sub> and C<sub>15:0</sub>, which occurred in relatively low concentrations (Table 3.1, Fig. 3.4c), also displayed increasing <sup>13</sup>C depletion with depth through the BNL (Table 3.1, Fig. 3.4g), which may also be due to syntrophy in the BNL carbon cycling.

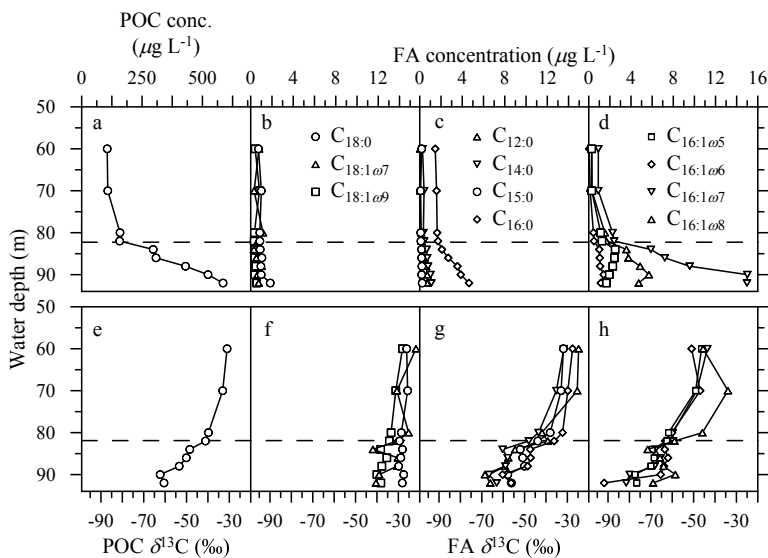


**Figure 3.4** (a-d) Concentration (conc.) and (e-h) δ<sup>13</sup>C of POC and FAs in the water column of October 2010. The top of the anoxic BNL is indicated by a dashed line. Legends in (b – d) also apply to (f – h).

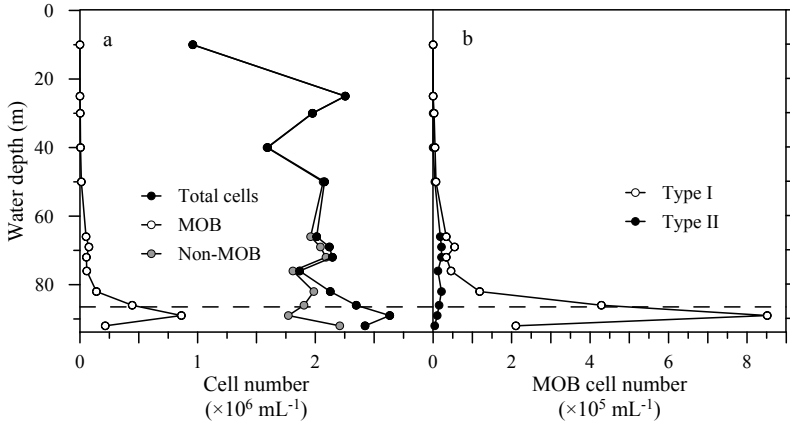


**Figure 3.5** Cell counts of (a) total cells as determined by DAPI staining, total MOB number by MOB-FISH, and total non-methanotrophic cells (non-MOB), calculated from DAPI counts minus FISH counts, and (b) counts of Type I and Type II MOB in October 2009. The dashed line indicates the depth of the chemocline.

### 3.5.3 Abundance of MOB and contribution to the organic carbon pool

The strong increase in Type I methanotrophic cell numbers below the oxic-anoxic interface (Fig. 3.5), accounting for up to 30% of total cells, shows that these bacteria constitute an important part of the microbial biomass forming the BNL. Indeed, the increase in total cell numbers is mainly due to the increase in the methanotrophic cell fraction, with the abundance of other (non-methanotrophic) cells staying almost constant through the BNL (Fig. 3.5). Whereas with regards to cell numbers, MOB already play an important role for the BNL microbial community, their role in terms of microbial biomass is even more significant. Comparison with the percentage of methane-derived FA carbon in the BNL biomass,

calculated from the  $\delta^{13}\text{C}$  end member model, suggests that 30% of the total cell number makes up more than three-quarters of the biomass. This estimate compares well with our microscopy-based biomass estimates (Table 3.2). The MOB cells observed by FISH cell-counting were larger than their non-MOB counterparts (Table 3.2), which may in part be a result of heavy investment in internal membrane synthesis in active MOB expressing particulate methane monooxygenase (pMMO) (Prior and Dalton 1985). In conclusion, two independent lines of evidence indicate that at least in terms of biomass the organic matter within the BNL consists mainly (i.e. > 75%) of Type I methanotrophic bacteria.

#### *3.5.4 Methanotrophic activity and oxygen consumption within the BNL*

The observed methane concentration gradients, the  $^{13}\text{C}$ -enrichment of residual  $\text{CH}_4$  at the water column redox transition relative to the sedimentary source (Fig. 3.2), as well as the biomarker signatures (Fig. 3.4) provide strong evidence of MOx activity at the top of the BNL. More quantitative insight with regard to the actual methane turnover in association with BNL formation is gained from the radioisotope assays. The MOR measurements indicate strong  $\text{CH}_4$  oxidation at the top of the BNL, while  $\text{CH}_4$  oxidation within the anoxic interior of the BNL is insubstantial during stratified conditions (Fig. 3.3).  $k$  values between  $0.07\text{ h}^{-1}$  and  $0.09\text{ h}^{-1}$  (between  $1.8\text{ d}^{-1}$  and  $2.1\text{ d}^{-1}$ ) at the top of the BNL translate into  $\text{MOR}_{\text{ex situ}}$  of  $0.8 - 1.8\text{ mmol m}^{-3}\text{ d}^{-1}$ . Based on the range of calculated MOB cell numbers in the BNL ( $[1.2 - 8.5] \times 10^5\text{ cells mL}^{-1}$ ) and the range of  $\text{MOR}_{\text{ex situ}}$  estimates, we assessed cell-specific rates in the BNL between  $97 \times 10^{-18}$  and  $281 \times 10^{-18}\text{ mol cell}^{-1}\text{ h}^{-1}$ . These rates are high, but fall within the range of previous MOR estimates in culture and

soil studies (Dunfield and Conrad 2000; Kolb et al. 2005), indicating that the high CH<sub>4</sub> oxidation potential in the BNL is likely the result of a high density of methanotrophs, rather than exceptionally high cellular CH<sub>4</sub> oxidation rates.

The high ex situ turnover rates persisted over a depth range of ~ 4 m (Fig. 3.3), which integrates to an apparent MOR in the water column of 5.1 mmol m<sup>-2</sup> d<sup>-1</sup>, provided that both CH<sub>4</sub> and O<sub>2</sub> are available. All incubations were performed under micro-oxic conditions, but the O<sub>2</sub> concentrations in the incubations may have been higher than in situ, especially towards the bottom of the 4-meter depth interval where potential ex situ CH<sub>4</sub> turnover was observed. The estimates of CH<sub>4</sub> consumption in the water column may thus be somewhat overestimated. On the other hand, the integrated rate reported above stands in good agreement with the calculated turbulent-diffusive flux of CH<sub>4</sub> towards the top of the BNL of 4.6 – 7.3 mmol m<sup>-2</sup> d<sup>-1</sup>. The highest ex situ turnover rates we observed were at the bottom of the CH<sub>4</sub> oxidation zone (86 m water depth). Since the CH<sub>4</sub> oxidation potential stops abruptly below this depth, this may correspond to the depth of the lowest O<sub>2</sub> concentrations the methanotrophs in situ can cope with.

Assuming a CH<sub>4</sub>:O<sub>2</sub> stoichiometry between 1:1.4 – 1:1.8 (Naguib 1976) for MOx, the consumption-driven CH<sub>4</sub> flux translates into an O<sub>2</sub>-consumption of 6.4 – 13.1 mmol m<sup>-2</sup> d<sup>-1</sup> in October 2010. The downward flux of O<sub>2</sub> ranged between 6.6 and 10.7 mmol m<sup>-2</sup> d<sup>-1</sup> in October 2010, suggesting that the O<sub>2</sub>-flux was balanced by the O<sub>2</sub> consumption through CH<sub>4</sub> oxidation. In October 2009, however, the O<sub>2</sub>-flux reached a maximum of 5.7 mmol m<sup>-2</sup> d<sup>-1</sup> only, significantly lower than the calculated O<sub>2</sub>-requirement by MOx of 12.2 mmol m<sup>-2</sup> d<sup>-1</sup>. We therefore argue that MOx at the top of the BNL is O<sub>2</sub>- rather than CH<sub>4</sub>-limited,

particularly in light of the fact that O<sub>2</sub>-consuming processes other than MOx, e.g. NH<sub>4</sub><sup>+</sup> oxidation and aerobic heterotrophic processes, likely contribute to the O<sub>2</sub> consumption. It appears that the O<sub>2</sub> requirement from oxidation of CH<sub>4</sub> alone exceeds the diffusive O<sub>2</sub> supply, driving the oxic-anoxic interface upwards through the water column, and with it the 'bacterioclinal' – i.e. the upper boundary of the BNL. The growing anoxic zone is thus tightly coupled to the metabolic requirements of MOB and the production of methanotrophic biomass.

We present biomarker, isotopic and microscopic evidence for a mostly methanotrophic origin of biomass in an annually forming BNL in the southern basin of Lake Lugano. With ongoing stratification, MOx (together with other aerobic processes) exceeds the oxygen supply, thereby leading to an upward movement of the oxic-anoxic interface in the water column, in close association with the expansion of the BNL. The MOB community at the top of the BNL thus drives carbon cycling in a temporally and spatially dynamic ecosystem that is supported by, and migrates in response to, its own O<sub>2</sub> consumption.

This novel mechanism of BNL formation is likely to be important also in other eutrophic lakes, where thermal stratification leads to development of anoxia. Our study demonstrates that a bacterial BNL – in addition to acting as an effective sink for biogenic CH<sub>4</sub> from lacustrine sediments, as a modulator for the development of anoxia in bottom waters, and as a significant source of organic matter to the sediments – can also have important implications for early diagenetic reactions within the sediments and the degradation of sedimented organic matter. By shielding the sediments from oxygenated water throughout most of the year, bacterial BNL formation provides a strong basis for methanogenesis, creating a

positive feedback on water column anoxia during stratification, and thus on organic matter preservation.



---

Chapter 4 has been submitted to Aquatic Sciences:

Blees, Jan, Helge Niemann, Markus Erne, Jakob Zopfi, Carsten J. Schubert and Moritz F. Lehmann. Surface water methane super-saturation and emission in Lake Lugano, southern Switzerland.

## Surface water methane super-saturation and emission in Lake Lugano, southern Switzerland

---

### 4.1 Abstract

We measured methane concentrations in the surface water of the northern basin of Lake Lugano in spring (May 2012) and autumn (October 2011, 2012), and calculated turbulent diffusive methane fluxes to the atmosphere. Surface water methane concentrations were highly variable in space and time but always exceeded atmospheric equilibrium. Methane concentrations were significantly lower in spring (on average 16 nmol L<sup>-1</sup>) than during the autumn sampling campaigns (on average 57 nmol L<sup>-1</sup> in 2011 and 45 nmol L<sup>-1</sup> in 2012). This suggests methane accumulation in the surface mixed layer during the summer productive season. The origin of the methane in the lake's surface waters requires further assessment, but the observed concentration profiles indicate that the excess methane originates from a near-surface source, and not from the large deep-water methane pool in the anoxic monimolimnion. As a consequence of the higher surface water methane concentrations and increased buoyancy turbulence caused by autumnal cooling of the surface boundary layer, diffusive fluxes were much higher in October (average

$\sim 97 \mu\text{mol m}^{-2} \text{d}^{-1}$ , compared to  $7 \mu\text{mol m}^{-2} \text{d}^{-1}$  in May 2012). The increase in methane concentration in the surface water between spring and autumn suggests links between methane accumulation and the annual biological cycle, yet seasonal changes in wind and temperature forcing of methane emission likely play an important modulating role. While the relative importance of biological versus physical controls on methane emission in Lake Lugano awaits further investigations, our study underscores that lakes can act as an important continental source of methane to the atmosphere, even when the lake-internal microbial methane filter in the water column seems to work efficiently.

## 4.2 Introduction

Methane ( $\text{CH}_4$ ) is a powerful greenhouse gas with a global warming potential  $\sim 21$  times that of  $\text{CO}_2$  on a hundred year time horizon (Manne and Richels 2001), accounting for  $\sim 20\%$  of the radiative forcing induced by long-lived greenhouse gases (Wuebbles and Hayhoe 2002; IPCC 2013). Atmospheric methane concentrations have almost tripled since the start of industrialisation (Blasing 2008; Dlugokencky et al. 2009), but the absolute contribution of individual sources to the atmospheric budget is still a matter of debate (Kirschke et al. 2013). Natural sources of atmospheric  $\text{CH}_4$  mainly originate from the anaerobic degradation of organic matter by specialised methanogenic *Archaea* (Liu 2010; Sieber et al. 2010). In lakes and other freshwater bodies, the activity of these microbes often leads to  $\text{CH}_4$  excess in anoxic water layers and sediments.  $\text{CH}_4$  is oxidised by methanotrophic bacteria in oxic surface sediments or in the water column (Rudd et al. 1974; Hanson and Hanson 1996; Blees et al. 2014a, see chapter 2), but a significant fraction of  $\text{CH}_4$  may bypass this

microbial  $\text{CH}_4$  filter (IPCC 2013). When  $\text{CH}_4$  production exceeds microbial  $\text{CH}_4$  consumption, sedimentary porewaters may become supersaturated, and  $\text{CH}_4$  can occur as a free gas, which further reduces its biodegradability. Indeed, lakes are very important sources of  $\text{CH}_4$ , accounting for 6 – 16% of the total natural flux to the atmosphere (Bastviken et al. 2004). Vegetation in littoral zones may furthermore enhance  $\text{CH}_4$  efflux because  $\text{CH}_4$  is transported through the roots, stems and leaves of aerenchymatous plants (Laanbroek 2010). In small and shallow lakes, on average, only ~30% of lacustrine  $\text{CH}_4$  evasion is diffusive, and advective, bubble and plant-mediated transport are more effective. The diffusive component becomes more important with increasing lake surface area and depth (Bastviken et al. 2004). Also, the portion of the surface area that is covered by vegetation at the fringe of a lake decreases with increasing surface area, which additionally reduces the fraction of plant-mediated  $\text{CH}_4$  emission from the lake.

The turbulent diffusive  $\text{CH}_4$  flux from lacustrine water bodies to the atmosphere depends greatly on the surface water  $\text{CH}_4$  concentration, mixing behaviour and on the depth of the lake (Bastviken et al. 2004). During episodic turnover of lakes,  $\text{CH}_4$  efflux can transiently be very high, because  $\text{CH}_4$  stored in anoxic bottom waters reaches the surface in a short time, allowing only incomplete consumption by the methanotrophic microbial community (Schmid et al. 2005; Walter et al. 2007; Schubert et al. 2012). Yet, also in the absence of a significant  $\text{CH}_4$  flux from deeper parts of lacustrine water columns, elevated  $\text{CH}_4$  concentrations in surface waters have been reported (Murase et al. 2005; Hofmann et al. 2010; Grossart et al. 2011), including Lake Lugano (Blees et al. 2014a, see chapter 2). The source of this surface water  $\text{CH}_4$  is not well constrained, but shallow sediments on the lake shores (Murase et al. 2005; Hofmann et

al. 2010), or in situ CH<sub>4</sub> production in anoxic microenvironments (Karl and Tilbrook 1994; Rusanov et al. 2004; Grossart et al. 2011) have been suggested. In analogy to non-methanogenic CH<sub>4</sub> production pathways proposed for marine environments, oxic degradation of methylated substances may also account for CH<sub>4</sub> accumulation in surface waters (Karl et al. 2008; Damm et al. 2010; Carini et al. 2014).

Our knowledge of the dynamics of methane fluxes is often based on point measurements that are extrapolated in space and time. In this study, we investigated the spatiotemporal variability of CH<sub>4</sub> concentrations and C-isotope ratios in surface and subsurface waters of the meromictic northern basin of Lake Lugano, in order to 1) determine spatiotemporal fluctuations of the CH<sub>4</sub> source strength, and 2) gain insight into the possible origin(s) of excess CH<sub>4</sub> in the surface waters.

## **4.3 Methods**

### *4.3.1 Study site*

Lake Lugano is a deep south-alpine lake at an elevation of 271 m above mean sea level. The lake consists of two basins, which are connected through a shallow straight across a natural dam. The northern basin has a maximum water depth of 288 m and a surface area of 27.5 km<sup>2</sup>. Due to the fjord-like bathymetry, the sidewalls of the basin are steep, with little or no accumulation of sediments. This basin has an east-west orientation and is surrounded by mountains, shielding it from the prevailing southern wind directions. As a result of eutrophication, the basin has been meromictic for more than 4 decades, featuring a deep (~135 m) oxic-anoxic interface, with accumulation of CH<sub>4</sub> in the hypolimnion below (Liu et al. 1996; Blees et al. 2014a, see chapter 2).

The annual average wind speed at 10 m above the lake is  $\sim 1.6 \text{ m s}^{-1}$  with little seasonal variation (MeteoSwiss). Nevertheless, peak wind speeds during gusts recorded between October 2011 and October 2012 reached up to  $30 \text{ m s}^{-1}$ .

#### *4.3.2 Sampling*

Sampling campaigns were performed in October 2011, May 2012 and October 2012 (Table 4.1). During each campaign, we collected water samples in 5-L Niskin bottles from 0.4 m water depth throughout the northern basin. A total of 59, 77 and 79 surface water samples were collected in October 2011, May 2012 and October 2012, respectively (Fig. 4.1). Additional samples were taken by hydrocast sampling down to 40 m water depth (0.4, 2.5, 5, 7.5, 10, 12.5, 15, 20, 30 and 40 m) along two transects and at selected sites (Figs 4.2, 4.3, 4.4). At each sampling site, temperature, conductivity,  $\text{O}_2$  concentration, pH and turbidity were measured with a CTD device (Idronaut Ocean Seven 316 Plus, Idronaut S.r.l., Italy). Subsamples for  $\text{CH}_4$  concentration and  $\delta^{13}\text{C}$  measurements were taken directly from the Niskin bottle through silicon tubing and fixed with NaOH in glass vials of 120 mL – 1000 mL (final concentration 1%) (Blees et al. 2014a). A small headspace of 1 – 2% of the sample volume was added to facilitate outgassing of all  $\text{CH}_4$  into the headspace. Bottles were stored upside down until analysis in our home laboratories.

#### *4.3.3 Dissolved methane*

$\text{CH}_4$  concentrations were determined using a gas chromatograph (GC) equipped with a flame ionisation detector (FID), and  $\delta^{13}\text{C}$  values were measured with a GC with a pre-concentration cryo-trap (PreCon, Thermo

Scientific), coupled to an isotope ratio mass spectrometer (GC-IRMS, Isoprime TraceGas) (Blees et al. 2014a). Corrections were made for linearity effects and instrument drift. Stable C-isotope ratios are reported in the common  $\delta$ -notation (in ‰) relative to the Vienna Pee Dee Belemnite standard.  $\delta^{13}\text{C}$  values reported here have an analytical error of  $\pm 1$  ‰.

#### 4.3.4 Flux calculations

Diffusive  $\text{CH}_4$  fluxes ( $F$ ) were calculated according to the boundary layer model of Liss and Slater (1974) (for a review see also Wanninkhof et al. 2009):

$$F = k (C_w - C_{\text{eq}}) \quad \text{Eq. 4.1}$$

where  $k$  is the transfer velocity (see below) and  $C_w$  and  $C_{\text{eq}}$  are the  $\text{CH}_4$  concentration in the surface water (here at 0.4 m depth) and the equilibrium  $\text{CH}_4$  concentration, respectively.  $C_{\text{eq}}$  was calculated following Wiesenburg and Guinasso (1979), based on the average atmospheric  $\text{CH}_4$  concentration (1874 ppbv) in the northern hemisphere (Dlugokencky et al. 2009), lake surface temperature (14 – 21 °C) and salinity (0.3 ‰) as measured with the CTD device. The  $k$ -value, which is determined by wind speed and buoyancy flux (Cole and Caraco 1998; Crusius and Wanninkhof 2003; MacIntyre et al. 2010), was calculated according to:

$$k_{\text{CH}_4} = k_{600} \left( \frac{\text{Sc}_{\text{CH}_4}}{600} \right)^c \quad \text{Eq. 4.2}$$

where  $\text{Sc}$  is the dimensionless Schmidt number, i.e. the ratio between kinematic viscosity of water and the gas diffusion coefficient, which

relates the respective  $k$ -values for different gases.  $k_{600}$  denotes the transfer velocity of CO<sub>2</sub> at 20 °C, corresponding to an Sc of 600, and is used for comparison of different gases (Cole et al. 2010).  $c$  is a wind speed-dependent conversion factor, for which we used  $^{-2/3}$  for  $U_{10} < 3.7 \text{ m s}^{-1}$ , and  $^{-1/2}$  for all other wind speeds (Jähne et al. 1987).  $U_{10}$  stands for the wind speed at 10 m above the surface, in  $\text{m s}^{-1}$ .

For parameterisation of  $k_{600}$  we compared the following three empirical relationships:

1. The bilinear relationship of Crusius and Wanninkhof (C&W) (2003):

$$\text{for } U_{10} < 3.7 \text{ m s}^{-1}: k_{600} = 0.72U_{10} \quad \text{Eq. 4.3}$$

$$\text{for } U_{10} \geq 3.7 \text{ m s}^{-1}: k_{600} = 4.33U_{10} - 13.3 \quad \text{Eq. 4.4}$$

2. The power function by Cole and Caraco (C&C) (1998):

$$k_{600} = 2.07 + 0.215U_{10}^{1.7} \quad \text{Eq. 4.5}$$

3. The relationship given by MacIntyre et al. (2010) for a cooling lake

$$k_{600} = 2.04U_{10} + 2.0 \quad \text{Eq. 4.6}$$

and for a heating lake

$$k_{600} = 1.74U_{10} - 0.15 \quad \text{Eq. 4.7}$$

The MacIntyre relationships (Eqs. 4.6 and 4.7) distinguish between cooling and heating of the surface water, because heating and cooling changes the buoyancy flux. When the surface layer starts losing heat to the atmosphere, the water starts to sink and eddy turbulence will bring water from below with higher CH<sub>4</sub> concentrations to the surface

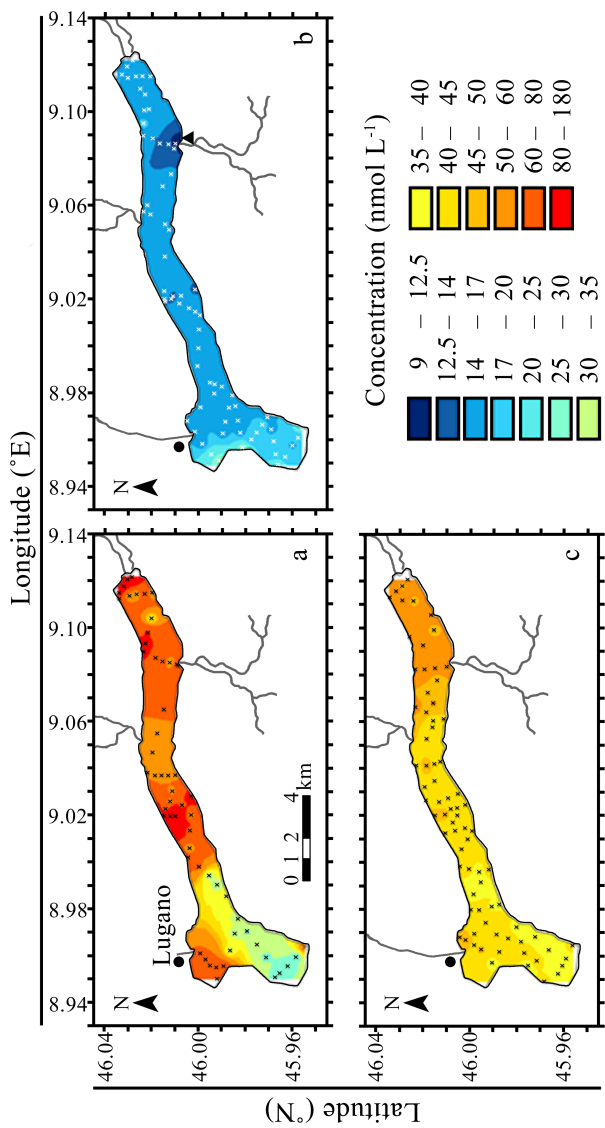


**Figure 4.1** Surface water CH<sub>4</sub> concentration in the northern basin of Lake Lugano determined in October 2011 (a), May 2012 (b) and October 2012 (c). Crosses indicate sampling locations. Tributary streams are shown as grey lines. The river delta where anomalously low CH<sub>4</sub> concentrations were found in May 2012 is indicated with a black triangle in (b), and the city of Lugano is shown as a black dot.

(MacIntyre et al. 2001). Thus, the CH<sub>4</sub> flux from the surface mixed layer to the atmosphere is greater when the surface water is cooling than when it is heating. Although we recognise that heating and cooling cycles also take place on a diurnal basis, we only considered seasonal trends, assuming a heating mode of the lake when monthly average air temperature was higher than surface water temperature (March – August), and a cooling mode when the monthly average air temperature was lower (September – February). Data of wind speeds at 10 m above the lake surface were made available by MeteoSwiss, which operates a measurement station located close to the shore in Lugano. Integration of concentration and flux data was performed in the ArcMap module of the ArcGIS 10 software package (ESRI) by inverse distance squared weighting.

## 4.4 Results

### *4.4.1 Dissolved methane concentration and stable isotope composition*

Surface water CH<sub>4</sub> concentrations were considerably higher during the autumn samplings than in spring. In October 2011, surface water concentrations generally ranged between 26 nmol L<sup>-1</sup> and 96 nmol L<sup>-1</sup> (Fig. 4.1a). During this campaign we only observed higher concentrations at one sampling location close to the shore at a river delta at the eastern end of the basin (132 nmol L<sup>-1</sup>) and at three sampling locations along the Swiss-Italian border on the northern side of the basin (128 – 178 nmol L<sup>-1</sup>). In October 2012, lowest surface water concentrations were ~ 35 nmol L<sup>-1</sup>, in the western part of the basin (Fig. 4.1c), and highest concentrations (~ 60 nmol L<sup>-1</sup>) were found in the eastern part of the lake. Unlike in 2011,

we did not measure exceptionally high concentrations ( $> 100 \text{ nmol L}^{-1}$ ). Surface water concentrations in May 2012 ranged between  $9 \text{ nmol L}^{-1}$  and  $30 \text{ nmol L}^{-1}$  (Fig. 4.1b). Notably, concentration differences between spring and autumn were strongest in the eastern part of the lake (east of  $9.10^\circ\text{E}$ ), i.e. 3 to 5-fold higher in October ( $70 \pm 27 \text{ nmol L}^{-1}$  in 2011 and  $52 \pm 2.6 \text{ nmol L}^{-1}$  in 2012) than in May ( $15 \pm 0.6 \text{ nmol L}^{-1}$ ). In contrast, concentration differences were comparably small in the western part of the lake, close to the town of Lugano (west of  $8.96^\circ\text{E}$ ), i.e. 2-fold higher in October ( $43 \pm 18 \text{ nmol L}^{-1}$  and  $41 \pm 3.1 \text{ nmol L}^{-1}$  in October 2011 and 2012, respectively) than in May ( $19 \pm 4.3 \text{ nmol L}^{-1}$ ).

In autumn, we generally found the highest  $\text{CH}_4$  concentrations close to the surface (Figs. 4.2, 4.3, 4.4), and often we found an additional concentration maximum at the depth of the thermocline, i.e. at  $\sim 15 \text{ m}$  depth. In contrast, no surface maximum was present in May 2012, but again we detected a subsurface maximum at  $15 - 20 \text{ m}$  water depth. The highest  $\text{CH}_4$  concentration in May 2012 ( $62 \text{ nmol L}^{-1}$ ) was found at  $40 \text{ m}$  depth, close to the bottom in the Bay of Lugano (Fig. 4.4b).

In October 2012,  $\text{CH}_4$  in the surface mixed layer was depleted in  $^{13}\text{C}$  relative to  $\text{CH}_4$  from below the thermocline (Figs. 4.2k, 4.3c). Against expectation, the lowest  $\text{CH}_4$  concentrations in the mixed layer were paralleled by the greatest  $^{13}\text{C}$  depletion in the  $\text{CH}_4$ . In contrast,  $\text{CH}_4$  from the water mass below the thermocline (Fig. 4.3c) had the least negative  $\delta^{13}\text{C}$ . Similarly, in January and August 2010,  $\text{CH}_4$  in the surface mixed layer was associated with relatively low  $\text{CH}_4 \delta^{13}\text{C}$  (data not shown).

In order to investigate further whether the conspicuous isotope dynamics within the mixed layer were linked to microbial  $\text{CH}_4$  consumption, we investigated methane oxidation rates with ex situ radio isotope assays (Blees et al. 2014a, see chapter 2) in samples from a

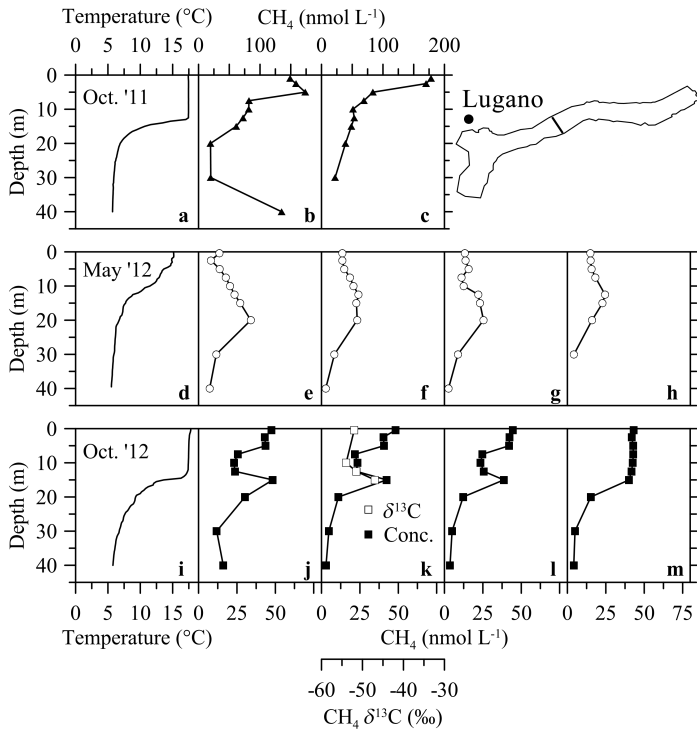


**Figure 4.2** Temperature and CH<sub>4</sub> concentration profiles in the upper 40 m of the water column in north – south transects in the centre of the lake in October 2011 (a-c), May 2012 (d-h) and October 2012 (i-m), and δ<sup>13</sup>C of CH<sub>4</sub> (k, open symbols). The location of the transect is indicated by a black line in the map. The concentration axis for (b) and (c) is shown at the top (up to 200 nmol L<sup>-1</sup>), and for (e-h) and (j-m) at the bottom (up to 75 nmol L<sup>-1</sup>).

hydrocast in the centre of the lake in January 2010 and in October 2011 (at the location of the profile in Fig. 4.2c). Our measurements revealed that CH<sub>4</sub> oxidation rates in surface and subsurface waters were negligible (<0.1% CH<sub>4</sub> turnover d<sup>-1</sup>, i.e. <<0.1 nmol L<sup>-1</sup> d<sup>-1</sup>), without any noticeable depth trends. In agreement with the negligible rates, no Type 1 and Type

2 methanotrophs were observed using Fluorescence In Situ Hybridisation (Blees et al. 2014b, see chapter 3) (data not shown).

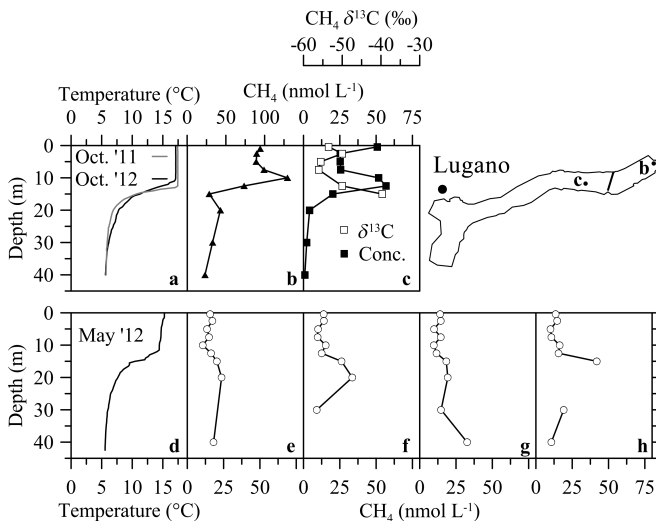


**Figure 4.3** Temperature and CH<sub>4</sub> concentration profiles in the upper 40 m of the water column at isolated stations (a-c) and in a north – south transect (d-h), and δ<sup>13</sup>C of CH<sub>4</sub> (c, open symbols). b: October 2011; c: October 2012; d-h: May 2012. Locations of profiles b and c are indicated with dots, and the transect e-h is indicated as a black line in the map. The concentration axis for (b) goes up to 150 nmol L<sup>-1</sup>, whereas for (c) and (e-h) it goes up to 75 nmol L<sup>-1</sup>.

#### 4.4.2 CH<sub>4</sub> fluxes

Average wind speeds during our sampling campaigns were variable with values between 0.5 m s<sup>-1</sup> (17 October 2012) and 5.5 m s<sup>-1</sup> (13 October 2011) (Table 4.1). Depending on the *k*-value parameterisation according to C&W, C&C or MacIntyre, the Liss and Slater model yielded

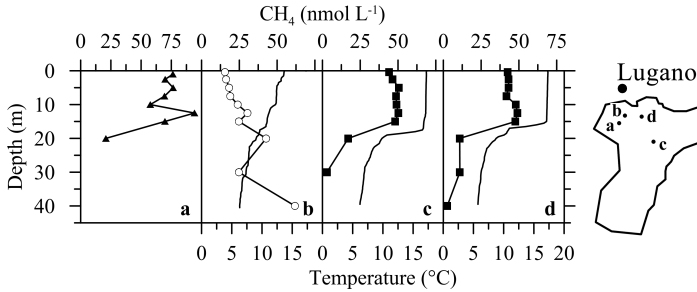


**Figure 4.4** Temperature (lines) and CH<sub>4</sub> concentration (symbols) profiles in the upper 40 m of the water column in the vicinity of Lugano, in October 2011 (a), May 2012 (b) and October 2012 (c, d). Profile locations are indicated in the map on the right. The concentration axis for (a) goes up to 100 nmol L<sup>-1</sup>, whereas for (b-d) it goes up to 75 nmol L<sup>-1</sup>.

diffusive fluxes of CH<sub>4</sub> to the atmosphere of 3 to 168  $\mu\text{mol m}^{-2} \text{d}^{-1}$  (Table 4.1, Fig. 4.5). Extrapolating to the whole-lake scale, the fluxes calculated from discrete concentration measurements translate into a system-flux of 2080 - 4607 mol d<sup>-1</sup> in October 2011, 163 – 466 mol d<sup>-1</sup> in May 2012 and 82 - 968 mol d<sup>-1</sup> in October 2012. Despite the uncertainties associated with  $k$  value parameterisation, flux calculations thus revealed considerable temporal variability in CH<sub>4</sub> emission from the lake surface to the atmosphere, with overall higher methane fluxes during fall (Fig. 4.5). The C&W and C&C relationships were developed from datasets with relatively low wind speeds (5.5 m s<sup>-1</sup>), i.e. lower than wind speeds recorded in Lugano (often >10 m s<sup>-1</sup> and up to 30 m s<sup>-1</sup>, MeteoSwiss). The MacIntyre model, on the other hand, is based on wind data more similar to Lake Lugano, with its variable wind regime, including wind speeds > 10 m s<sup>-1</sup>. Furthermore, the MacIntyre model considers the influence of heating and cooling on the buoyancy flux, which has a profound influence

on the change in efflux between spring and autumn. Given these arguments, we believe that the MacIntyre model yields the most reliable results, and therefore we used this model for the comparison of the three sampling campaigns (Fig. 4.5).

## 4.5 Discussion

### 4.5.1 Modes of $CH_4$ emission

The  $CH_4$  emission flux from lakes can be broadly subdivided into four components: (i) plant-mediated emission in littoral zones, (ii) ebullition, (iii) a storage flux during lake turnover, and (iv) diffusion across the lake surface-atmosphere boundary driven by a partial pressure gradient (Bastviken et al. 2004). (i) As a result of the geometry of the northern basin, comprising steep sidewalls along most of the lake's periphery, the majority of the lacustrine sedimentary deposits are located at great depth. Therefore, the littoral zone, where submerged plants such as reed could grow, is very small relative to the surface area of the lake. This likely reduces the impact of plant-mediated emissions to the total  $CH_4$  budget. (ii) Similarly, a substantial  $CH_4$  flux through ebullition is unlikely in a deep lake such as the northern basin of Lake Lugano, since the probability of bubble formation decreases with increasing hydrostatic pressure (Bastviken et al. 2004). Furthermore, gas exchange between rising bubbles and the surrounding water rapidly decreases the  $CH_4$  concentration in the bubble, which severely limits the potential for  $CH_4$  bubble ebullition (McGinnis et al. 2006). (iii) In lakes that experience a yearly overturn, a storage flux, i.e. release of  $CH_4$  stored in the anoxic hypolimnion, can be important (Bastviken et al. 2004; Schubert et al. 2010). However, in the meromictic northern basin of Lake Lugano, the

**Table 4.1** Average surface water CH<sub>4</sub> concentration ( $\pm 1$  standard deviation), wind speed and calculated daily diffusive fluxes of CH<sub>4</sub> into the atmosphere for the northern basin of Lake Lugano.  $U_{10}$  is the wind speed in m s<sup>-1</sup> at 10 m above the lake surface. Diffusive fluxes were calculated according to the parameterisations of Crusius and Wanninkhof (2003) (C&W), Cole and Caraco (1998) (C&C) and MacIntyre et al. (2010) (MacIntyre).

Date	[CH <sub>4</sub> ] (nM)	$U_{10}$ (m s <sup>-1</sup> )	Average diffusive flux ( $\mu\text{mol m}^{-2}\text{d}^{-1}$ )			Whole lake basin diffusive flux (mol d <sup>-1</sup> )		
			C&W	C&C	MacIntyre	C&W	C&C	MacIntyre
13 Oct. 2011	57 $\pm$ 19	5.5	133	76	168	3664	2080	4607
14 May 2012	16 $\pm$ 2	3.7	7	11	17	202	301	466
15 May 2012		3.2	6	9	14	163	257	384
16 Oct. 2012	45 $\pm$ 5	1.1	7	19	35	181	530	968
17 Oct. 2012		0.5	3	18	25	82	487	689

deep water CH<sub>4</sub> reservoir is decoupled from the surface waters. Indeed, since the onset of meromixis in 1967 (Barbieri and Mosello 1992), the northern basin only mixed fully in the winters of 2004 – 2005 and 2005 – 2006 (Holzner et al. 2009). We consequently argue that plant mediated emission, ebullition and storage flux during lake turnover are unlikely to contribute substantially to CH<sub>4</sub> emission from Lake Lugano's northern basin. Given the arguments above, our results indicate that partial-pressure-gradient-driven CH<sub>4</sub> diffusion across the surface water – atmospheric boundary layer constitutes the prime mechanism of methane emission from Lake Lugano, at least during the sampling campaigns in 2011 and 2012.

#### *4.5.2 Potential sources of surface water CH<sub>4</sub>*

Typically, CH<sub>4</sub> in aquatic systems can be attributed to a biogenic (i.e. microbial methanogenesis in anoxic environments) or, to a lesser extent, a thermogenic (fossil) source. The oxic degradation of methylated substrates was additionally found to contribute to surface water maxima in marine environments (Karl et al. 2008; Damm et al. 2010; Carini et al. 2014). The isotopic composition of CH<sub>4</sub> can be used to trace CH<sub>4</sub> sources and consumption (e.g. Whiticar 1999). Microbial methanogenesis is associated with a strong isotope effect, so that microbial CH<sub>4</sub> is characterised by low  $\delta^{13}\text{C}$  values of <-50‰. Thermogenic CH<sub>4</sub> on the other hand is comparatively <sup>13</sup>C-enriched, with values of -20‰ to -50‰. The low  $\delta^{13}\text{C}$  values of CH<sub>4</sub> in the surface water of Lake Lugano, above the thermocline (between -50‰ and -56‰ in October 2012 (Figs. 4.2k and 4.3c), indicate isotopic disequilibrium with atmospheric CH<sub>4</sub> (-47‰, Dlugokencky et al. 2009) and suggest a biogenic rather than a thermogenic

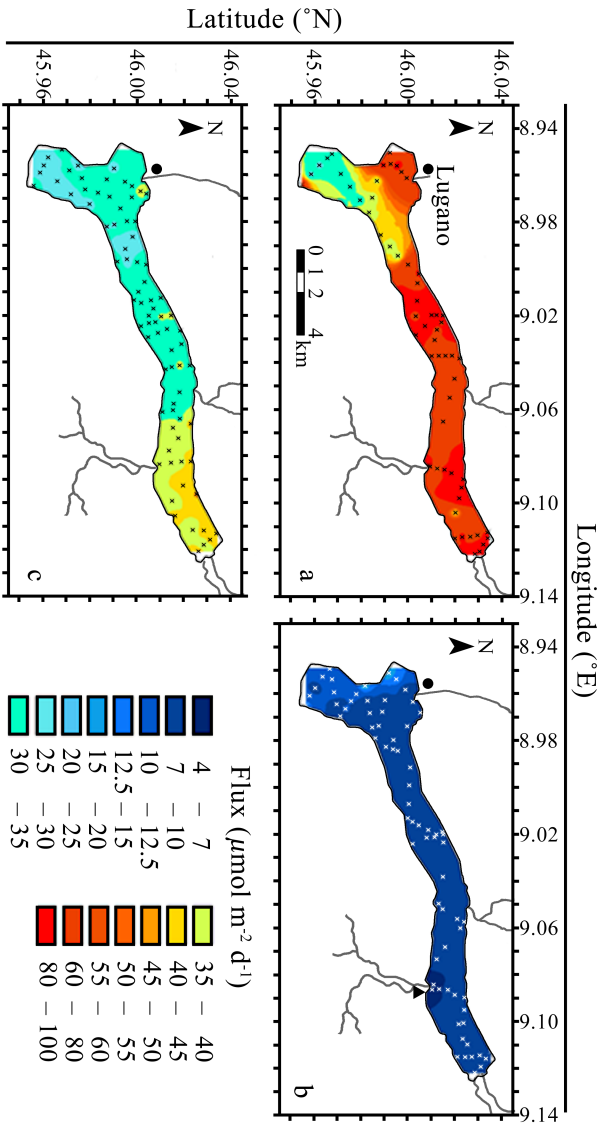


**Figure 4.5** Diffusive fluxes across the water – air boundary layer in October 2011 (a), May 2012 (b) and October 2012 (c). Fluxes were calculated using the transfer velocity according to MacIntyre (2010) and an average wind speed of  $2 \text{ m s}^{-1}$ . Crosses indicate sampling locations. Tributary streams are shown as grey lines. The river delta where anomalously low  $\text{CH}_4$  concentrations were found in May 2012 is indicated with a black triangle in (b), and the city of Lugano is shown as a black dot.

origin. In contrast,  $\delta^{13}\text{C}$  of  $\text{CH}_4$  in the water below the thermocline was distinctly more  $^{13}\text{C}$ -enriched ( $>-40\text{‰}$ ), which is consistent with our previous measurements (Blees et al. 2014a, see chapter 2). Upward-diffusing  $\text{CH}_4$  from the lake bottom is efficiently consumed by aerobic methanotrophs at the permanent redoxcline in 135 m water depth, and only traces of strongly  $^{13}\text{C}$ -enriched  $\text{CH}_4$  escape this microbial filter (Blees et al. 2014a, see chapter 2). Indeed,  $\text{CH}_4$  concentrations in intermediate waters between 135 m and 30 m water depth never exceed  $20 \text{ nmol L}^{-1}$  and  $\delta^{13}\text{C}$ -values are about  $-30\text{‰}$ .  $\text{CH}_4$  accumulation in the surface water of the Lake Lugano North Basin, as well as the generally encountered subsurface peak at the thermocline (Figs. 4.2, 4.3 and 4.4), thus seems to be independent of the deep water  $\text{CH}_4$  reservoir. The surface water concentrations in Lake Lugano's northern basin (between  $26$  and  $178 \text{ nmol L}^{-1}$  in October, and between  $9$  and  $30 \text{ nmol L}^{-1}$  in May) were supersaturated with respect to atmospheric equilibrium ( $\sim 3 \text{ nmol L}^{-1}$ ) and in a range similar to other lakes (e.g. Bastviken et al. 2004; Murase et al. 2005; Schubert et al. 2010; Diem et al. 2012).

Similar  $\text{CH}_4$  concentration maxima have been found previously in other lakes (Murase et al. 2005; Hofmann et al. 2010; Grossart et al. 2011) and in marine surface waters (Karl and Tilbrook 1994; Rusanov et al. 2004; Karl et al. 2008; Damm et al. 2010). The subsurface  $\text{CH}_4$  maximum was explained by lateral turbulent-diffusive transport of sediment-derived, biogenic  $\text{CH}_4$  (Hofmann and Roussy 2002; Murase et al. 2005), by in situ production in anoxic microenvironments (Rusanov et al. 2004; Grossart et al. 2011), or aerobic processes such as decomposition of methylphosphonate and dimethylsulfoniopropionate (Karl et al. 2008; Damm et al. 2010; Carini et al. 2014).

The subsurface  $\text{CH}_4$  peak in the Lake Lugano North Basin could

originate from epilimnetic sediments, particularly in the shallow Bay of Lugano. Turbulence at the sediment-water interface as a result of wind-induced internal waves in lake basins (MacIntyre et al. 1999; Hofmann et al. 2010) can lead to the release of CH<sub>4</sub> from the sediments (Sakai et al. 2002). Such a mechanism has previously been invoked as an explanation for CH<sub>4</sub> accumulation in lake surface water during stratified conditions (Murase et al. 2005). Mean monthly wind speeds 10 m above Lake Lugano were relatively low ( $1.6 \pm 0.2 \text{ m s}^{-1}$  between October 2011 and October 2012, MeteoSwiss), but maximum wind speeds during gusts were as high as  $30 \text{ m s}^{-1}$  in the same period, which indeed could have caused internal waves at the pycnocline. On the other hand, with the exception of the Bay of Lugano and the SW and NE ends of the basin, the shores of Lake Lugano are generally steep. Particularly in the central part of the basin, where we observed elevated subsurface CH<sub>4</sub> concentrations during all sampling campaigns (Fig. 4.2), the sediment cover at the depth of the thermocline is thin, if at all present (unpublished seismic data). It is thus difficult to invoke shallow benthic methanogenesis as the main source of surface water CH<sub>4</sub>. Similarly, tributary rivers, e.g. as suggested by Murase et al. (2005) for Lake Biwa, are an unlikely source of the CH<sub>4</sub> in the upper Lake Lugano water column. Here river inputs are small, and the CH<sub>4</sub> concentration in the river entering the eastern part of the basin was low ( $\sim 4 \text{ nmol L}^{-1}$ ), leading to a plume of lowered CH<sub>4</sub> concentrations in the surface water in front of the outflow (Fig. 4.1b). A more likely source of CH<sub>4</sub> in the surface water of the northern basin of Lake Lugano may be in situ production in the oxic water column, as was found in other lakes (Grossart et al. 2011) and in marine environments (Karl et al. 2008; Damm et al. 2010; Carini et al. 2014). A biologic origin of the CH<sub>4</sub> peak in the subsurface waters is suggested by its low (and, compared to CH<sub>4</sub>

$\delta^{13}\text{C}$ -values at the surface and at the oxycline, anomalous)  $\delta^{13}\text{CCH}_4$ . Nevertheless, the observed C-isotope signatures are ambivalent with regards to the actual source of the biologic  $\text{CH}_4$ . Both  $\text{CH}_4$  from methanogenesis in shallow littoral sediments and anoxic microenvironments likely display similarly low  $^{13}\text{C}/^{12}\text{C}$  ratios. Moreover, the C-isotope effects associated with methylation and de-methylation pathways under oxic conditions are still unknown.

#### *4.5.3 Spatio-temporal variability in $\text{CH}_4$ concentrations in the surface mixed layer*

$\text{CH}_4$  concentrations in the surface waters and the efflux to the atmosphere were highly variable in space and time (Figs. 4.1 and 4.5). On average, surface water concentrations were higher in October (57  $\text{nmol L}^{-1}$  in 2011 and 45  $\text{nmol L}^{-1}$  in 2012) than in May 2012 (16  $\text{nmol L}^{-1}$ ). Based on the depth profiles taken throughout the lake, we calculated an average  $\text{CH}_4$  content of 487  $\mu\text{mol m}^{-2}$  within the mixed layer in May 2012, and 687  $\mu\text{mol m}^{-2}$  in October 2012 (upper 17.5 m of the water column). Given a surface area of 27.5  $\text{km}^2$ , this translates into a total  $\text{CH}_4$  content in this layer of  $14 \times 10^3$  mol (May 2012) and  $19 \times 10^3$  mol (October 2012). In general, microbial methane production is probably higher in late summer / early autumn compared to spring because the water temperature is higher, and increased primary production leads to higher substrate availability for methanogens. Since the pycnocline becomes more pronounced with warming of the surface water, turbulence at the sediment – water interface as a result of internal waves acting on the density interface is also expected to increase (MacIntyre et al. 1999). This increased turbulence would promote the release of sedimentary  $\text{CH}_4$ , which could specifically

explain the accumulation of  $\text{CH}_4$  at the thermocline (Figs. 4.2, 4.3 and 4.4). Similarly, increased biological production in the warmer summer surface waters, in combination with  $\text{O}_2$  consumption through respiration, also increases the number of potential anoxic microenvironments, both in detrital aggregates and in the digestive tracts of zooplankton. Thus, regardless of whether the source of  $\text{CH}_4$  to the surface water in Lake Lugano is sedimentary or located in the surface water itself, the source strength is expected to increase during the summer season.

The observed spatial heterogeneity in  $\text{CH}_4$  concentration, which indicates a spatial imbalance of sources and sinks of  $\text{CH}_4$ , is more difficult to explain. An epilimnetic sedimentary  $\text{CH}_4$  source would probably lead to a concentration decrease with distance from the sedimentary sources, which are restricted to the shallower parts of the basin in the west (Bay of Lugano) and the eastern end. However, in these areas, i.e. the eastern (May 2012, Fig. 4.1b) and western part of the basin (October 2011 and 2012, Fig. 4.1a,c) we encountered comparably low  $\text{CH}_4$  concentrations. Alternatively, the fact that we do not observe a spatial correlation with sedimentary deposits may indicate a water column source that is more evenly distributed laterally, such as methylphosphonate and dimethylsulfoniopropionate degradation.

#### *4.5.4 Absence of $\text{CH}_4$ oxidation in the surface water*

An important factor constraining the efflux of  $\text{CH}_4$  from the surface mixed layer to the atmosphere, besides  $\text{CH}_4$  production leading to  $\text{CH}_4$  excess concentrations (see previous section), is the extent of biological  $\text{CH}_4$  consumption. Since  $\text{CH}_4$  oxidation leaves the residual  $\text{CH}_4$  enriched in  $^{13}\text{C}$  relative to  $^{12}\text{C}$ , such an enrichment in the surface water, coupled to

a concentration decrease, could be regarded as evidence of a microbial CH<sub>4</sub> sink. In October 2012, several profiles showed a distinct CH<sub>4</sub> concentration minimum between the concentration peaks at the thermocline and at the surface (Figs. 4.2j-m, 4.3c). The corresponding  $\delta^{13}\text{C}$  values between -50 and -56‰ (10 m water depth, Fig. 4.2k) stand in contrast to what would be expected for biological consumption (which discriminates against <sup>13</sup>CH<sub>4</sub>) of the CH<sub>4</sub> in the mixed surface layer. Whereas we still lack a plausible explanation for the local CH<sub>4</sub> concentration minimum, the fact that we did not see any characteristic <sup>13</sup>C-isotopic enrichment is consistent with our methane oxidation rate measurements in January 2010 and October 2011, which showed very low ( $\ll 0.1 \text{ nmol L}^{-1} \text{ d}^{-1}$ ) rates within the upper 15 m of the water column without any systematic variation with depth. These results are in agreement with previously reported low rates of CH<sub>4</sub> oxidation in limnetic (Murase et al. 2005) and coastal marine surface waters (Mau et al. 2013), possibly caused by sunlight-inhibition of microbial CH<sub>4</sub> oxidation (Murase and Sugimoto 2005).

#### *4.5.5 Spatio-temporal variability of CH<sub>4</sub> loss from the surface mixed layer*

The calculated diffusive fluxes of CH<sub>4</sub> to the atmosphere (between  $168 \mu\text{mol m}^{-2} \text{ d}^{-1}$  in October 2011 and  $17 \mu\text{mol m}^{-2} \text{ d}^{-1}$  in May 2012; MacIntyre equation, Table 4.1, Fig. 4.5) are low but comparable to other lakes in the northern hemisphere (e.g. Bastviken et al. 2004). The temporal variation in the CH<sub>4</sub> pool in the surface water described above could in part be caused by the differential rates of CH<sub>4</sub> emission. The accumulation of CH<sub>4</sub> in the upper water column in summer is probably aided by an increase in methanogenesis and/or methylation/de-

methylation reactions as the water warms. Since the buoyancy flux in a warming water column is reduced, and the transfer velocity depends on the buoyancy flux (Eqs. 4.6 and 4.7) (MacIntyre et al. 2010), the emission is dampened in spring and early summer, thus reinforcing the accumulation of CH<sub>4</sub> in the near-surface water. On the other hand, in late summer and autumn the cooling water body, with an increased buoyancy flux (at elevated CH<sub>4</sub> concentrations), is prone to emitting more CH<sub>4</sub>. Put another way, CH<sub>4</sub> efflux is retarded during spring and early summer (Fig. 4.5b) when warming of the surface water outweighs nocturnal cooling, and enhanced in autumn (Fig. 4.5a,c) when heat loss from the water to the atmosphere is more important. Indeed, surface water warming and cooling, and therewith the buoyancy flux, show a much more distinct seasonality than do average wind speeds. Also the probability of high wind speeds is similar for all seasons (MeteoSwiss). We thus argue that the observed seasonal variability of surface water CH<sub>4</sub> concentration is driven by temperature-driven differences in the strength of both sources and sinks, underlining that biological as well as physical aspects are relevant for CH<sub>4</sub> fluxes from lake environments to the atmosphere.

## **4.6 Conclusion**

Lake Lugano surface waters are supersaturated with CH<sub>4</sub> with respect to atmospheric equilibrium and thus represent an important source of atmospheric CH<sub>4</sub>. The absence of CH<sub>4</sub> oxidation in the surface waters shows that CH<sub>4</sub> produced in the surface water or in shallow-water sediments is eventually outgassed to the atmosphere. The outgassing of CH<sub>4</sub> seems to undergo distinct seasonal variation, with peak fluxes in autumn and substantially lower fluxes in spring. Annual flux variations

are modulated by seasonal changes in CH<sub>4</sub> production and temperature-related changes in the buoyancy flux associated with the warming and cooling of the surface water during spring and autumn, respectively. The source of the surface water CH<sub>4</sub>, and the exact mechanisms behind observed spatial patterns in surface water CH<sub>4</sub> concentration and fluxes remains unclear, but the lack of any clear correlation with sedimentary deposits tentatively suggests in situ CH<sub>4</sub> production in the oxic water column itself. The low  $\delta^{13}\text{C}$  values of CH<sub>4</sub> in the surface waters and at the thermocline support a biological origin. Since the C-isotope effects of demethylation pathways in the water column are as yet unknown, we cannot rule out these pathways. These isotope effects will have to be elucidated in future work.

## Conclusion and outlook

---

### **5.1 Conclusions and implications**

The studies reported in this PhD thesis were part of a project aimed at a better understanding of carbon and nitrogen dynamics in lake systems. Particularly, I investigated how methane affects the carbon cycle in lacustrine environments. Lake Lugano represents an excellent model system to study this. The markedly different mixing regime between the two basins allows the study of methane oxidation under both meromictic and monomictic conditions in the same lake.

It is increasingly being recognised that carbon mineralisation through microbial methane oxidation can provide an important carbon source for aquatic ecosystems (Bastviken et al. 2003), and possibly even beyond (Kiyashko et al. 2001; Eller et al. 2005a). In chapters 2 and 3 I have made use of compound specific isotope analysis; a powerful tool for the study of carbon flow through a system. Since methane is strongly carbon isotopically depleted, the oxidation of methane in the deep water constitutes a natural isotope labelling experiment. This revealed that methane-derived carbon contributes more than 75% of the organic carbon

in the BNL ecosystem in the southern basin of Lake Lugano (chapter 3). This far exceeds estimates from other lakes (e.g. Bastviken et al. 2003), and shows that the strong methane oxidation at the top of the BNL creates a tight loop in carbon cycling in the deep hypolimnion. Furthermore, compound specific analysis of lipid biomarkers showed that methanotrophs constitute a substantial part of the biomass in the hypolimnetic redox transition zones of both the northern and the southern basin. In the northern basin, more than one third of O<sub>2</sub> consumption is due to the action of methanotrophs, and in the southern basin, methanotrophy alone consumes enough O<sub>2</sub> to drive the expansion of the anoxic BNL, even without consideration of other O<sub>2</sub>-consuming processes. This shows that methanotrophs are major drivers of deep water anoxia in both the meromictic northern and the monomictic southern basin of Lake Lugano. By creating anoxic conditions in the water column, they also act to protect sinking organic matter from oxic degradation, further promoting methanogenesis. Thereby these methanotroph-dominated ecosystems promote their own existence.

#### *5.1.1 Aerobic methane oxidation potentials in anoxic waters – implications for water column (in)stability*

The finding of a community of aerobic methanotrophs deep within the anoxic hypolimnion of the northern basin has profound implications. First, the conspicuous methane concentration profiles and methane <sup>13</sup>C-enrichments in the anoxic water are not necessarily caused by anaerobic oxidation of methane. An alternative explanation – episodic micro-aerobic methane oxidation, as proposed in chapter 2 – may have been overlooked in other studies, possibly leading to erroneous reports of

anaerobic oxidation of methane in freshwater environments. Profiles of concentration and isotopic composition can be powerful tools in the identification of potential sources and sinks, but these sources and sinks must be validated. In Lake Lugano, profiles through the water column indicate a methane sink in anoxic water, but validation by turnover rate incubation under anoxic conditions turned out negative. Furthermore, addition of  $\text{NO}_2^-$ ,  $\text{NO}_3^-$ ,  $\text{Fe(III)}$ ,  $\text{SO}_4^{2-}$  or a mixture of humic acids did not promote methane oxidation. However, incubation of water from the anoxic hypolimnion with  $\text{O}_2$  did increase methane oxidation, leading to the conclusion that  $\text{O}_2$  is the electron acceptor in methane oxidation in the anoxic hypolimnion in Lake Lugano. At first sight, this result seems counterintuitive. However, viewing a lake basin such as the northern basin of Lake Lugano as a system without any exchange between the surface and deep waters may be over-simplistic. In the deep hypolimnion there is no density stratification, and episodic events may bring water from the surface or from the oxic hypolimnion into the anoxic hypolimnion. These episodic events may range from internal waves (seiches) at the redoxcline to turbidity currents induced by floods in tributary rivers. The fact that  $\text{O}_2$  is never observed in the deep water is testament to the strong reducing potential the methanotrophs exert on their environment, and not necessarily to the absence of episodic exchange of water. This calls for an increased awareness of what it means that a water column is stratified – not a static environment, but a dynamic system, in which episodic vertical movement of water can defy the prevailing redox zonation. The year-round presence of a community of aerobic methanotrophs deep within anoxic waters thus shows that redox zonation in the water column of deep lakes can be more complex than the theory predicts.

### *5.1.2 The distribution of methane oxidation potentials in the anoxic hypolimnion*

The lipid biomarker distribution and potential aerobic methane oxidation rates in the profiles through the water column raise an important question: why does the methanotrophic community diminish below 175 m? Sinking of methanotrophs from the permanent redoxcline at 135 m, and the absence of density interfaces in the deep hypolimnion, cannot explain a preferential accumulation at intermediate depths. However, since the source of  $O_2$  is above, and  $O_2$  is expected to be consumed while the oxygenated water travels down through the anoxic hypolimnion, the likelihood of an  $O_2$ -injection in the water between 135 and 175 m depth is higher than that of an appreciable amount of  $O_2$  reaching deeper waters. Especially in the case of turbulence induced by internal waves (seiches), the likelihood of oxygenated water reaching deep anoxic layers decreases markedly with distance from the oxic water. The 175 m depth interval may then demarcate the boundary between relatively regular injections of  $O_2$  and more sparsely oxygenated waters. Additionally, concentrations of hydrogen sulfide, which are low between 135 m and 175 m, may become a limiting factor for methanotrophic growth in deeper waters, as precipitation of  $CuS$  may render the methanotrophs in deeper water copper-limited and unable to synthesise pMMO.

### *5.1.3 Implications of the south basin BNL for methane emission*

Due to the high methane oxidation rates at the redox transition zone at the top of the BNL in the southern basin, during stable stratification of the water column no  $CH_4$  escapes into the oxic water column. However, since no  $CH_4$  oxidation takes place within the BNL and  $CH_4$  accumulates to

high concentrations, large amounts may be emitted to the atmosphere during lake turnover (i.e. the storage factor of methane emission). The amount emitted depends on the dynamics of lake turnover. Prior to complete lake turnover in January 2010, surface water cooling led to mixing of the epilimnion and hypolimnion above the BNL (cf. Fig. 3.1e). Although the BNL was still intact, the CH<sub>4</sub> concentration was lower than in preceding months, and less  $\delta^{13}\text{CH}_4$  depleted (Fig. 3.2b), which supports that methane loss took place through oxidation. As a result, the CH<sub>4</sub> inventory of the water column in January 2010 was only a third of the inventory in October 2009. The increased methane oxidation took place not only at the redoxcline, but within the anoxic BNL, similar to the northern basin (chapter 2). Thus, due to the introduction of O<sub>2</sub> into the BNL, the initial stage of mixing can greatly reduce the CH<sub>4</sub> efflux during full turnover, as CH<sub>4</sub> is oxidised within the BNL. On the other hand, the high O<sub>2</sub> demand of MOx and mixing with anoxic BNL-derived water leaves the surface water O<sub>2</sub> depleted (Fig. 3.1e). During the period of initial mixing, but preceding full turnover in late January 2010, surface water O<sub>2</sub> saturation was < 45%, compared to > 70% in December 2009 and 90% in late March 2010. During full turnover in February 2009, O<sub>2</sub> saturation in the surface water was further reduced to 30%. Slow destruction of the anoxic BNL during winter turnover may thus have a profound seasonal influence on both CH<sub>4</sub> export to the atmosphere and the O<sub>2</sub> inventory in the water column of the southern basin of Lake Lugano.

#### *5.1.4 The lack of methane oxidation in surface waters*

As described in chapter 4, no methane oxidation potential was found

in the photic zone of Lake Lugano. This has important implications for the release of methane into the atmosphere, since without a biological sink in the surface waters, all methane produced in this zone is eventually outgassed to the atmosphere. We observed a similar lack of methane oxidation potential in marine coastal waters around Svalbard (Mau et al. 2013). Some evidence indicates that methane oxidation may be inhibited by sunlight (Murase and Sugimoto 2005), which leaves room for a temporal decoupling of methane production and oxidation (e.g. as suggested by Grossart et al. 2011), with consumption taking place during the dark hours. However, the turnover rate experiments in this study were performed in the dark, and no CH<sub>4</sub> oxidation took place, even after 20 h. Furthermore, in the Lake Biwa example, methane oxidation in water from the surface was only observed after one month of dark incubation (Murase and Sugimoto 2005), suggesting that light has a strong inhibitory effect on the methanotrophic community structure, rather than on the process alone. Thus, all methane released into the surface water of Lake Lugano is eventually emitted to the atmosphere.

## **5.2 Outlook**

The studies reported in chapters 2, 3 and 4 clearly show the importance of methane dynamics for carbon cycling in Lake Lugano. However, several questions remain unanswered, and in the following I will outline suggestions for future work.

In chapter 2, we argue that episodic O<sub>2</sub> injections into the anoxic hypolimnion could sustain the community of aerobic methanotrophs, and explain the distribution of methane concentration,  $\delta^{13}\text{C}$  and lipid

biomarkers. It is not straightforward to verify this hypothesis, since the regular monitoring campaign carried out by SUPSI has never picked up such O<sub>2</sub> intrusions. In order to verify this hypothesis, monitoring of nanomolar O<sub>2</sub> concentrations in the water column is necessary. Such high sensitivity measurements can be carried out with a STOX sensor (Revsbech et al. 2009), or with the system used in chapter 2 (Kirf et al. 2014). Since events that inject O<sub>2</sub>-rich water into the anoxic hypolimnion may follow flood events in tributary rivers (e.g. Lavelli et al. 2002), it may be possible to predict increased chances of such events based on river discharge measurements. Turbidity measurements could further help identify whether the source of O<sub>2</sub> injections is associated with flood-induced turbidity currents.

Methanotrophic biomass in the hypolimnion of the northern basin was found in two distinct depth intervals, rather than in a continuous distribution. The reasons behind the location of the upper peak, at the interface between the oxic water and the methane gradient, are evident. The lower peak in methanotrophic biomass may be determined by the concentration of sulfide and the availability of copper, required for the synthesis of pMMO. However, the methanotrophs would probably be most affected by the availability of copper if they lack sMMO, which could be tested by PCR with mmoX specific primer sets (McDonald et al. 1995). This could also elucidate whether physiological differences might determine the distribution of methanotrophic communities at 135 m and 175 m water depth.

The isotope fractionation factors calculated for methane oxidation in both the northern and southern basin were significantly smaller than

oxidation by pMMO would suggest. This was attributed to a near-complete consumption of the methane inventory. However, it was not explored whether the methanotrophs in the two basins of Lake Lugano express sMMO. Since methane oxidation with sMMO leads to smaller isotope fractionation than with pMMO, this could partially explain the low apparent isotope fractionation factors. Expression of sMMO could be favoured over pMMO when copper concentrations become limiting, which, given the strong production of methanotrophic biomass at the top of the nepheloid layer, could happen during stratified conditions in the deep water of the southern basin. It would therefore be interesting to investigate whether expression of sMMO can be induced (by incubation in the absence of copper), and whether this has an effect on carbon isotope fraction.

The lipid biomarker composition of the benthic nepheloid layer in the southern basin suggests a great contribution of methanotrophs to the total bacterial biomass. Fluorescence In Situ Hybridisation (FISH) cell counts of aerobic methanotrophic bacteria confirmed that up to 30% of cells in the BNL were methanotrophic, and their large cell size corresponds to their great contribution to BNL biomass. Comparison with the lipid biomarker signature of methanotrophs from the northern basin provides a tentative phylogenetic relation to methanotrophs found in other lake systems, but this awaits verification by sequencing of Lake Lugano South Basin methanotroph clones. A comparison with the methanotrophic community in the sediments could then shed more light on the origin of the methanotrophic community in the BNL.

As discussed in chapter 4, the mechanism behind methane supersaturation in the surface water of Lake Lugano remains unresolved. Since large parts of the shoreline of the northern basin are very steep, with little or no space for deposition of sediments, the alternative hypothesis of in situ production of methane in the water column must be considered. Since it is not known what the precursor of methane would be, it is not feasible to design an isotope tracer experiment like the ones used in the methane oxidation studies described in chapters 2 and 3. However, if in situ methane production takes place in the surface water of Lake Lugano, this should be evident in a methane increase over time in incubation vials. These studies should be coupled to molecular studies targeting methanogenic *Archaea*, which may be present in anoxic microenvironments.

The reasons behind the absence of methane oxidation in the surface waters are unclear. A detailed analysis of the microbial community, including both pMMO- and sMMO-bearing methanotrophs, could shed light on the presence or absence of methanotrophs. In this context, the photo-inhibition of methanotrophy should also be investigated by incubation of hypolimnetic water under a range of light conditions. It would be interesting to repeat the long-term incubation experiments that Murase and Sugimoto (2005) carried out with surface water from Lake Biwa, in order to find out whether methane oxidation could take place in the surface water of Lake Lugano, given sufficient dark time.



## Bibliography

---

- Aeschbach-Hertig, W., C. P. Holzner, M. Hofer, M. Simona, A. Barbieri, and R. Kipfer. 2007. A time series of environmental tracer data from deep, meromictic Lake Lugano, Switzerland. *Limnol. Oceanogr.* **52**: 257–273, doi:10.4319/lo.2007.52.1.0257
- Ambrosetti, W., L. Barbanti, and E. A. Carrara. 2010. Mechanisms of hypolimnion erosion in a deep lake (Lago Maggiore, N. Italy). *J. Limnol.* **69**: 3–14, doi:10.4081/jlimnol.2010.3
- Barbieri, A., and R. Mosello. 1992. Chemistry and trophic evolution of Lake Lugano in relation to nutrient budget. *Aquat. Sci.* **54**: 219–237, doi:10.1007/BF00878138
- Barbieri, A., and B. Polli. 1992. Description of Lake Lugano. *Aquat. Sci.* **54**: 181–183, doi:10.1007/BF00878135
- Barbieri, A., and M. Simona. 2001. Trophic evolution of Lake Lugano related to external load reduction: Changes in phosphorus and nitrogen as well as oxygen balance and biological parameters. *Lakes Reservoirs: Res. and Manage.* **6**: 37–47, doi:10.1046/j.1440-1770.2001.00120.x
- Bastviken, D., J. J. Cole, M. L. Pace, and M. C. van de Bogert. 2008. Fates of methane from different lake habitats: Connecting whole-lake budgets and CH<sub>4</sub> emissions. *J. Geophys. Res.* **113**: 1–13, doi:10.1029/2007JG000608
- Bastviken, D., J. J. Cole, M. L. Pace, and L. Tranvik. 2004. Methane emissions from lakes: Dependence of lake characteristics, two regional assessments, and a global estimate. *Global Biogeochem. Cy.* **18**: 1–12, doi:10.1029/2004GB002238

- Bastviken, D., J. Ejlertsson, I. Sundh, and L. Tranvik. 2003. Methane as a source of carbon and energy for lake pelagic food webs. *Ecology* **84**: 969–981, doi:10.1890/0012-9658(2003)084[0969:MAASOC]2.0.CO;2
- Bastviken, D., J. Ejlertsson, and L. Tranvik. 2002. Measurement of methane oxidation in lakes: A comparison of methods. *Environ. Sci. Technol.* **36**: 3354–3361, doi:10.1021/es010311p
- Bastviken, D., L. J. Tranvik, J. A. Downing, P. M. Crill, and A. Enrich-Prast. 2011. Freshwater methane emissions offset the continental carbon sink. *Science* **331**: 50, doi:10.1126/science.1196808
- Beal, E. J., C. H. House, and V. J. Orphan. 2009. Manganese- and iron-dependent marine methane oxidation. *Science* **325**: 184–187, doi:10.1126/science.1169984
- Bianchi, T. S., and E. A. Canuel. 2011. *Chemical biomarkers in aquatic ecosystems*, Princeton University Press.
- Blasing, T. 2008. Recent greenhouse gas concentrations. US Dep. Energy, Carbon Dioxide Inf. Anal. Cent., doi:10.3334/CDIAC/atg.032
- Blees, J., H. Niemann, C. B. Wenk, J. Zopfi, C. J. Schubert, M. K. Kirf, M. L. Veronesi, C. Hitz, and M. F. Lehmann. 2014a. Micro-aerobic bacterial methane oxidation in the chemocline and anoxic water column of deep south-Alpine Lake Lugano (Switzerland). *Limnol. Oceanogr.* **59**: 311–324, doi:10.4319/lo.2014.59.2.0311
- Blees, J., H. Niemann, C. B. Wenk, J. Zopfi, C. J. Schubert, J. S. Jenzer, M. Veronesi, and M. F. Lehmann. 2014b. Bacterial methanotrophs drive the formation of a seasonal anoxic benthic nepheloid layer in an alpine lake. *Limnol. Oceanogr.* **59**: 1410–1420, doi:10.4319/lo.2014.59.4.1410
- Van Bodegom, P. M., F. Stams, L. Mollema, S. Boeke, and P. Leffelaar. 2001. Methane oxidation and the competition for oxygen in the rice rhizosphere. *Appl. Environ. Microbiol.* **67**: 3586–3597, doi:10.1128/AEM.67.8.3586

- Boetius, A., K. Ravenschlag, C. J. Schubert, D. Rickert, F. Widdel, A. Gieseke, R. Amann, B. B. Jørgensen, U. Witte, and O. Pfannkuche. 2000a. A marine microbial consortium apparently mediating anaerobic oxidation of methane. *Nature* **407**: 623–626, doi:10.1038/35036572
- Boetius, A., B. Springer, and C. Petry. 2000b. Microbial activity and particulate matter in the benthic nepheloid layer (BNL) of the deep Arabian Sea. *Deep-Sea Res. II* **47**: 2687–2706, doi:10.1016/S0967-0645(00)00045-X
- Bowman, J. P. 2006. The methanotrophs - The families *Methylococcaceae* and *Methylocystaceae*, p. 266–289. In M. Dworkin, S. Falkow, E. Rosenberg, K.-H. Schleifer, and E. Stackebrandt [eds.], *The prokaryotes*. Springer.
- Bowman, J. P., L. I. Sly, P. D. Nichols, and A. C. Hayward. 1993. Revised taxonomy of the methanotrophs: Description of *Methylobacter* gen. nov., emendation of *Methylococcus*, validation of *Methylosinus* and *Methylocystis* species, and a proposal that the family *Methylococcaceae* includes only the group I methanotrophs. *Int. J. Syst. Bacteriol.* **43**: 735–755, doi:10.1099/00207713-43-4-735
- Bowman, J. P., L. I. Sly, and E. Stackebrandt. 1995. The phylogenetic position of the family *Methylococcaceae*. *Int. J. Syst. Bacteriol.* **45**: 182–185, doi:10.1099/00207713-45-1-182
- Brugnoli, E., and G. D. Farquhar. 2000. Photosynthetic fractionation of carbon isotopes, p. 399–434. In R.C. Leegood, T.D. Sharkey, and S. Von Caemmerer [eds.], *Photosynthesis: Physiology and metabolism*. Kluwer Academic Publishers.
- Bussmann, I., M. Rahalkar, and B. Schink. 2006. Cultivation of methanotrophic bacteria in opposing gradients of methane and oxygen. *FEMS Microbiol. Ecol.* **56**: 331–344, doi:10.1111/j.1574-6941.2006.00076.x

- Canfield, D. E., E. Kristensen, and B. Thamdrup. 2005. The methane cycle, p. 383–418. *In* *Advances in Marine Biology*, doi:10.1016/S0065-2881(05)48010-4
- Carini, P., A. E. White, E. O. Campbell, and S. J. Giovannoni. 2014. Methane production by phosphate-starved SAR11 chemoheterotrophic marine bacteria. *Nat Commun* **5**: 4346, doi:10.1038/ncomms5346
- Chappellaz, J., J.-M. Barnola, D. Raynaud, Y. S. Korotkevich, and C. Lorius. 1990. Ice-core record of atmospheric methane over the past 160,000 years. *Nature* **345**: 127–131, doi:10.1038/345127a0
- Chen, Y.-H., and R. G. Prinn. 2006. Estimation of atmospheric methane emissions between 1996 and 2001 using a three-dimensional global chemical transport model. *J. Geophys. Res.* **111**: D10307, doi:10.1029/2005JD006058
- Cole, J. J., D. L. Bade, D. Bastviken, M. L. Pace, and M. van de Bogert. 2010. Multiple approaches to estimating air-water gas exchange in small lakes. *Limnol. Oceanogr.: Meth.* **8**: 285–293, doi:10.4319/lom.2010.8.285
- Cole, J. J., and N. F. Caraco. 1998. Atmospheric exchange of carbon dioxide in a low-wind oligotrophic lake measured by the addition of SF<sub>6</sub>. *Limnol. Oceanogr.* **43**: 647–656, doi:10.4319/lo.1998.43.4.0647
- Conrad, R. 2007. Microbial ecology of methanogens and methanotrophs. *Adv. Agron.* **96**: 1–63, doi:10.1016/S0065-2113(07)96005-8
- Conrad, R. 2009. The global methane cycle: Recent advances in understanding the microbial processes involved. *Environ. Microbiol. Rep.* **1**: 285–292, doi:10.1111/j.1758-2229.2009.00038.x
- Costello, A. M., and M. E. Lidstrom. 1999. Molecular characterization of functional and phylogenetic genes from natural populations of methanotrophs in lake sediments. *Appl. Environ. Microbiol.* **65**: 5066–5074.

- Crowe, S. A., S. Katsev, K. Leslie, A. Sturm, C. Magen, S. Nomosatryo, M. A. Pack, J. D. Kessler, W. S. Reeburgh, J. A. Roberts, L. González, G. Douglas Haffner, A. Mucci, B. Sundby, and D. A. Fowle. 2010. The methane cycle in ferruginous Lake Matano. *Geobiology* **9**: 61–78, doi:10.1111/j.1472-4669.2010.00257.x
- Crusius, J., and R. Wanninkhof. 2003. Gas transfer velocities measured at low wind speed over a lake. *Limnol. Oceanogr.* **48**: 1010–1017, doi:10.4319/lo.2003.48.3.1010
- Damm, E., E. Helmke, S. Thoms, U. Schauer, E. Nöthig, K. Bakker, and R. P. Kiene. 2010. Methane production in aerobic oligotrophic surface water in the central Arctic Ocean. *Biogeosciences* **7**: 1099–1108, doi:10.5194/bg-7-1099-2010
- Dedysh, S. N., W. Liesack, V. N. Khmelenina, N. E. Suzina, Y. A. Trotsenko, J. D. Semrau, A. M. Bares, N. S. Panikov, and J. M. Tiedje. 2000. *Methylocella palustris* gen. nov., sp. nov., a new methane-oxidizing acidophilic bacterium from peat bogs, representing a novel subtype of serine-pathway methanotrophs. *Int. J. Syst. Evol. Microbiol.* **50**: 955–969.
- Deutzmann, J. S., and B. Schink. 2011. Anaerobic oxidation of methane in sediments of Lake Constance, an oligotrophic freshwater lake. *Appl. Environ. Microbiol.* **77**: 4429–4436, doi:10.1128/AEM.00340-11
- Deutzmann, J. S., S. Wörner, and B. Schink. 2011. Activity and diversity of methanotrophic bacteria at methane seeps in eastern Lake Constance sediments. *Appl. Environ. Microbiol.* **77**: 2573–2581, doi:10.1128/AEM.02776-10
- Diaz, R. J., and R. Rosenberg. 2008. Spreading dead zones and consequences for marine ecosystems. *Science* **321**: 926–929, doi:10.1126/science.1156401
- Diem, T., S. Koch, S. Schwarzenbach, B. Wehrli, and C. J. Schubert. 2012. Greenhouse gas emissions (CO<sub>2</sub>, CH<sub>4</sub>, and N<sub>2</sub>O) from several perialpine and alpine hydropower reservoirs by diffusion and loss in turbines. *Aquat. Sci.* **74**: 619–635, doi:10.1007/s00027-012-0256-5

- Dlugokencky, E. J., L. Bruhwiler, J. W. C. White, L. K. Emmons, P. C. Novelli, S. A. Montzka, K. A. Masarie, P. M. Lang, A. M. Crotwell, J. B. Miller, and L. V. Gatti. 2009. Observational constraints on recent increases in the atmospheric CH<sub>4</sub> burden. *Geophys. Res. Lett.* **36**: L18803, doi:10.1029/2009GL039780
- Dunfield, P. F., and R. Conrad. 2000. Starvation alters the apparent half-saturation constant for methane in the type II methanotroph *Methylocystis* strain LR1. *Appl. Environ. Microbiol.* **66**: 4136–4138, doi:10.1128/AEM.66.9.4136-4138.2000
- Eller, G., P. Deines, J. Grey, H.-H. Richnow, and M. Krüger. 2005a. Methane cycling in lake sediments and its influence on chironomid larval  $\delta^{13}\text{C}$ . *FEMS Microbiol. Ecol.* **54**: 339–350, doi:10.1016/j.femsec.2005.04.006
- Eller, G., L. Känel, and M. Krüger. 2005b. Cooccurrence of aerobic and anaerobic methane oxidation in the water column of Lake Plußsee. *Appl. Environ. Microbiol.* **71**: 8925–8928, doi:10.1128/AEM.71.12.8925
- Eller, G., S. Stubner, and P. Frenzel. 2001. Group-specific 16S rRNA targeted probes for the detection of type I and type II methanotrophs by fluorescence in situ hybridisation. *FEMS Microbiol. Lett.* **198**: 91–97, doi:10.1111/j.1574-6968.2001.tb10624.x
- Elvert, M., A. Boetius, K. Knittel, and B. B. Jørgensen. 2003. Characterization of specific membrane fatty acids as chemotaxonomic markers for sulfate-reducing bacteria involved in anaerobic oxidation of methane. *Geomicrobiol. J.* **20**: 403–419, doi:10.1080/01490450303894
- Etioppe, G., and R. W. Klusman. 2002. Geologic emissions of methane to the atmosphere. *Chemosphere* **49**: 777–789, doi:10.1016/S0045-6535(02)00380-6
- Ettwig, K. F., T. van Alen, K. T. van de Pas-Schoonen, M. S. M. Jetten, and M. Strous. 2009. Enrichment and molecular detection of denitrifying methanotrophic bacteria of the NC10 phylum. *Appl. Environ. Microbiol.* **75**: 3656–3662, doi:10.1128/AEM.00067-09

- Ettwig, K. F., M. K. Butler, D. Le Paslier, E. Pelletier, S. Mangenot, M. M. Kuypers, F. Schreiber, B. E. Dutilh, J. Zedelius, D. de Beer, J. Gloerich, H. J. C. T. Wessels, T. van Alen, F. Luesken, M. L. Wu, K. T. van de Pas-Schoonen, H. J. M. op den Camp, E. M. Janssen-Megens, K.-J. Francoijs, H. Stunnenberg, J. Weissenbach, M. S. M. Jetten, and M. Strous. 2010. Nitrite-driven anaerobic methane oxidation by oxygenic bacteria. *Nature* **464**: 543–548, doi:10.1038/nature08883
- Ettwig, K. F., S. Shima, K. T. van de Pas-Schoonen, J. Kahnt, M. H. Medema, H. J. M. op den Camp, M. S. M. Jetten, and M. Strous. 2008. Denitrifying bacteria anaerobically oxidize methane in the absence of Archaea. *Environ. Microbiol.* **10**: 3164–3173, doi:10.1111/j.1462-2920.2008.01724.x
- Farquhar, G. D., J. R. Ehleringer, and K. T. Hubick. 1989. Carbon isotope discrimination and photosynthesis. *Annu. Rev. Plant Physiol. Plant Mol. Biol.* **40**: 503–537, doi:10.1146/annurev.pp.40.060189.002443
- Forster, P., V. Ramaswamy, P. Artaxo, T. Berntsen, R. Betts, D. W. Fahey, J. Haywood, J. Lean, D. C. Lowe, G. Myhre, J. Nganga, R. Prinn, G. Raga, M. Schulz, and R. van Dorland. 2007. Changes in atmospheric constituents and in radiative forcing, p. 129–234. *In* S. Solomon, D. Qin, M. Manning, Z. Chen, M. Marquis, K.B. Averyt, M. Tignor, and H.L. Miller [eds.], *Climate change 2007: The physical science basis. Contribution of working group I to the fourth assessment report of the Intergovernmental Panel on Climate Change*. Cambridge University Press.
- Gargett, A. E. 1984. Vertical eddy diffusivity in the ocean interior. *J. Mar. Res.* **42**: 359–393, doi:10.1357/002224084788502756
- Grasshoff, K., M. Ehrhardt, K. Kremling, and L. G. Anderson. 1999. *Methods of seawater analysis*, 3rd ed. Wiley-VCH, doi:10.1002/9783527613984
- Grossart, H.-P., K. Frindte, C. Dziallas, W. Eckert, and K. W. Tang. 2011. Microbial methane production in oxygenated water column of an oligotrophic lake. *Proc. Natl. Acad. Sci. U.S.A.* **108**, doi:10.1073/pnas.1110716108

- Guo, L., and H. Santschi. 2000. Sedimentary sources of old high molecular weight dissolved organic carbon from the ocean margin benthic nepheloid layer. *Geochim. Cosmochim. Ac.* **64**: 651–660, doi:10.1016/S0016-7037(99)00335-X
- Hanson, R. S., and T. E. Hanson. 1996. Methanotrophic bacteria. *Microbiol. Rev.* **60**: 439–471.
- Hawley, N., and C. R. Murthy. 1995. The response of the benthic nepheloid layer to a downwelling event. *J. Great Lakes Res.* **21**: 641–651, doi:10.1016/S0380-1330(95)71074-7
- Hawley, N., and R. W. Muzzi. 2003. Observations of nepheloid layers made with an autonomous vertical profiler. *J. Great Lakes Res.* **29**: 124–133, doi:10.1016/S0380-1330(03)70421-3
- Hicks, R. E., P. Aas, and C. Jankovich. 2004. Annual and offshore changes in bacterioplankton communities in the western arm of Lake Superior during 1989 and 1990. *J. Great Lakes Res.* **30**: 196–213, doi:10.1016/S0380-1330(04)70386-X
- Hill, R. 1930. Method for the estimation of iron in biological material. *P. R. Soc. London* **B107**: 205–214, doi:10.1098/rspb.1930.0063
- Hinrichs, K.-U., J. M. Hayes, S. P. Sylva, P. G. Brewer, and E. F. Delong. 1999. Methane-consuming archaeobacteria in marine sediments. *Nature* **398**: 802–805, doi:10.1038/19751
- Hoehler, T. M., M. J. Alperin, D. B. Albert, and C. S. Martens. 1994. Field and laboratory studies of methane oxidation in an anoxic marine sediment: Evidence for a methanogen-sulfate reducer consortium. *Global Biogeochem. Cy.* **8**: 451–463, doi:10.1029/94GB01800
- Hofmann, A., and D. Roussy. 2002. Dissolved silica budget in the North basin of Lake Lugano. *Chem. Geol.* **182**: 35–55, doi:10.1016/S0009-2541(01)00275-3

- Hofmann, H., L. Federwisch, and F. Peeters. 2010. Wave-induced release of methane: Littoral zones as source of methane in lakes. *Limnol. Oceanogr.* **55**: 1990–2000, doi:10.4319/lo.2010.55.5.1990
- Holler, T., G. Wegener, K. Knittel, A. Boetius, B. Brunner, M. M. M. Kuypers, and F. Widdel. 2009. Substantial  $^{13}\text{C}/^{12}\text{C}$  and D/H fractionation during anaerobic oxidation of methane by marine consortia enriched in vitro. *Environ. Microbiol. Rep.* **1**: 370–376, doi:10.1111/j.1758-2229.2009.00074.x
- Holmes, A. J., A. Costello, M. E. Lidstrom, and J. C. Murrell. 1995. Evidence that particulate methane monooxygenase and ammonia monooxygenase may be evolutionarily related. *FEMS Microbiol. Lett.* **132**: 203–208, doi:10.1111/j.1574-6968.1995.tb07834.x
- Holzner, C. P., W. Aeschbach-Hertig, M. Simona, M. Veronesi, D. M. Imboden, and R. Kipfer. 2009. Exceptional mixing events in meromictic Lake Lugano (Switzerland/Italy), studied using environmental tracers. *Limnol. Oceanogr.* **54**: 1113–1124, doi:10.4319/lo.2009.54.4.1113
- Hunkins, K., E. M. Thorndike, and G. Mathieu. 1969. Nepheloid layers and bottom currents in the Arctic ocean. *J. Geophys. Res.* **74**: 6995–7008, doi:10.1029/JC074i028p06995
- Intergovernmental Panel on Climate Change (IPCC). 2007. Changes in atmospheric constituents and in radiative forcing, p. 129–234. *In* S. Solomon, D. Qin, M. Manning, Z. Chen, M. Marquis, K.B. Averyt, M. Tignor, and H.L. Miller [eds.], *Climate change 2007: The physical science basis. Contribution of working group I to the fourth assessment report of the Intergovernmental Panel on Climate Change*. Cambridge University Press.
- Intergovernmental Panel on Climate Change (IPCC). 2013. Carbon and other biogeochemical cycles, p. 465–570. *In* T.F. Stocker, D. Qin, G.-K. Plattner, M. Tignor, S.K. Allen, J. Boschung, A. Nauels, Y. Xia, V. Bex, and P.M. Midgley [eds.], *Climate Change 2013: The physical science basis*. Cambridge University Press.

- Jähne, B., K. O. Münnich, R. Böisinger, A. Dutzi, W. Huber, and P. Libner. 1987. On the parameters influencing air-water gas exchange. *J. Geophys. Res.* **92**: 1937–1949, doi:10.1029/JC092iC02p01937
- Jahnke, L. L., R. E. Summons, J. M. Hope, and D. J. Des Marais. 1999. Carbon isotopic fractionation in lipids from methanotrophic bacteria II: The effects of physiology and environmental parameters on the biosynthesis and isotopic signatures of biomarkers. *Geochim. Cosmochim. Ac.* **63**: 79–93, doi:10.1016/S0016-7037(98)00270-1
- Jalukse, L., I. Helm, O. Saks, and I. Leito. 2008. On the accuracy of micro Winkler titration procedures: A case study. *Accredit. Qual. Assur.* **13**: 575–579, doi:10.1007/s00769-008-0419-1
- Kallmeyer, J., T. G. Ferdelman, A. Weber, H. Fossing, and B. B. Jørgensen. 2004. A cold chromium distillation procedure for radiolabeled sulfide applied to sulfate reduction measurements. *Limnol. Oceanogr.: Meth.* **2**: 171–180, doi:10.4319/lom.2004.2.171
- Karl, D. M., L. Beversdorf, K. M. Björkman, M. J. Church, A. Martinez, and E. F. Delong. 2008. Aerobic production of methane in the sea. *Nat. Geosci.* **1**: 473–478, doi:10.1038/ngeo234
- Karl, D. M., and B. D. Tilbrook. 1994. Production and transport of methane in oceanic particulate organic matter. *Nature* **368**: 732–734, doi:10.1038/368732a0
- Keppler, F., J. T. G. Hamilton, M. Brass, and T. Röckmann. 2006. Methane emissions from terrestrial plants under aerobic conditions. *Nature* **439**: 187–191, doi:10.1038/nature04420
- Kirf, M. K., C. Dinkel, C. J. Schubert, and B. Wehrli. 2014. Submicromolar oxygen profiles at the oxic-anoxic boundary of temperate lakes. *Aquat. Geochemistry* **20**: 39–57, doi:10.1007/s10498-013-9206-7
- Kirschke, S., P. Bousquet, P. Ciais, M. Saunois, J. G. Canadell, E. J. Dlugokencky, P. Bergamaschi, D. Bergmann, D. R. Blake, L. Bruhwiler, P. Cameron-Smith, S. Castaldi, F. Chevallier, L. Feng,

- A. Fraser, M. Heimann, E. L. Hodson, S. Houweling, B. Josse, P. J. Fraser, P. B. Krummel, J.-F. Lamarque, R. L. Langenfelds, C. Le Quére, V. Naik, S. O'Doherty, P. I. Palmer, I. Pison, D. Plummer, B. Poulter, R. G. Prinn, M. Rigby, B. Ringeval, M. Santini, M. Schmidt, D. T. Shindell, I. J. Simpson, R. Spahni, L. P. Steele, S. a. Strode, K. Sudo, S. Szopa, G. R. van der Werf, A. Voulgarakis, M. van Weele, R. F. Weiss, J. E. Williams, and G. Zeng. 2013. Three decades of global methane sources and sinks. *Nat. Geosci.* **6**: 813–823, doi:10.1038/ngeo1955
- Kiyashko, S. I., T. Narita, and E. Wada. 2001. Contribution of methanotrophs to freshwater macroinvertebrates: Evidence from stable isotope ratios. *Aquat. Microb. Ecol.* **24**: 203–207, doi:10.3354/ame024203
- Knittel, K., and A. Boetius. 2009. Anaerobic oxidation of methane: Progress with an unknown process. *Annu. Rev. Microbiol.* **63**: 311–334, doi:10.1146/annurev.micro.61.080706.093130
- Kolb, S., C. Knief, P. F. Dunfield, and R. Conrad. 2005. Abundance and activity of uncultured methanotrophic bacteria involved in the consumption of atmospheric methane in two forest soils. *Environ. Microbiol.* **7**: 1150–1161, doi:10.1111/j.1462-2920.2005.00791.x
- Kool, D. M., B. Zhu, W. I. C. Rijpstra, M. S. M. Jetten, K. F. Ettwig, and J. S. Sinninghe Damsté. 2012. Rare branched fatty acids characterize the lipid composition of the intra-aerobic methane oxidizer “*Candidatus Methyloirabilis oxyfera*.” *Appl. Environ. Microbiol.* **78**: 8650–8656, doi:10.1128/AEM.02099-12
- Kristjansson, J., P. K. Schönheit, and R. K. Thauer. 1982. Different  $K_s$  values for hydrogen of methanogenic bacteria and sulfate reducing bacteria: An explanation for the apparent inhibition of methanogenesis by sulfate. *Arch. Microbiol.* **131**: 278–282, doi:10.1007/BF00405893
- Laanbroek, H. J. 2010. Methane emission from natural wetlands: interplay between emergent macrophytes and soil microbial processes. A mini-review. *Ann. Bot.* **105**: 141–153, doi:10.1093/aob/mcp201

- Lamontagne, R. A., J. W. Swinnerton, V. J. Linnenbom, and W. D. Smith. 1973. Methane concentrations in various marine environments. *J. Geophys. Res.* **78**: 5317–5324, doi:10.1029/JC078i024p05317
- Lavelli, A., G. De Cesare, and J.-L. Boillat. 2002. Numerical 3D modelling of the vertical mass exchange induced by turbidity currents in Lake Lugano (Switzerland). *Proceedings 5th International Conference on Hydro-Science and -Engineering (ICHE-2002) (Reference: LCH-CONF-2002-012 Note: [355])*.
- Lehmann, M. F., S. M. Bernasconi, A. Barbieri, and J. A. McKenzie. 2002. Preservation of organic matter and alteration of its carbon and nitrogen isotope composition during simulated and in situ early sedimentary diagenesis. *Geochim. Cosmochim. Ac.* **66**: 3573–3584, doi:10.1016/S0016-7037(02)00968-7
- Lehmann, M. F., S. M. Bernasconi, J. A. McKenzie, A. Barbieri, M. Simona, and M. Veronesi. 2004. Seasonal variation of the  $\delta^{13}\text{C}$  and  $\delta^{15}\text{N}$  of particulate and dissolved carbon and nitrogen in Lake Lugano: Constraints on biogeochemical cycling in a eutrophic lake. *Limnol. Oceanogr.* **49**: 415–429, doi:10.4319/lo.2004.49.2.0415
- Lehmann, M. F., D. M. Sigman, D. C. McCorkle, J. Granger, S. Hoffmann, G. Cane, and B. G. Brunelle. 2007. The distribution of nitrate  $^{15}\text{N}/^{14}\text{N}$  in marine sediments and the impact of benthic nitrogen loss on the isotopic composition of oceanic nitrate. *Geochim. Cosmochim. Ac.* **71**: 5384–5404, doi:10.1016/j.gca.2007.07.025
- Lieberman, R. L., and A. C. Rosenzweig. 2005. Crystal structure of a membrane-bound metalloenzyme that catalyses the biological oxidation of methane. *Nature* **434**: 177–182, doi:10.1038/nature03311
- Liss, P. S., and P. G. Slater. 1974. Flux of gases across the air-sea interface. *Nature* **274**: 181–184, doi:10.1038/247181a0
- Liu, H. 2010. Taxonomy of methanogens, p. 549–558. *In* K.N. Timmis [ed.], *Handbook of hydrocarbon and lipid microbiology*. Springer.

- Liu, R., A. Hofmann, F. O. Gülaçar, P.-Y. Favarger, and J. Dominik. 1996. Methane concentration profiles in a lake with a permanently anoxic hypolimnion (Lake Lugano, Switzerland-Italy). *Chem. Geol.* **133**: 201–209, doi:10.1016/S0009-2541(96)00090-3
- Lovley, D. R., and M. J. Klug. 1983. Sulfate reducers can outcompete methanogens at freshwater sulfate concentrations. *Appl. Environ. Microbiol.* **45**: 187–192.
- MacIntyre, S., W. Eugster, and G. W. Kling. 2001. The critical importance of buoyancy flux for gas flux across the air-water interface, p. 135–139. *In* M.A. Donelan, W.M. Drennan, E.S. Saltzman, and R. Wanninkhof [eds.], *Gas transfer at water surfaces*. American Geophysical Union, doi:10.1029/GM127
- MacIntyre, S., K. M. Flynn, R. Jellison, and J. Romero. 1999. Boundary mixing and nutrient fluxes in Mono Lake, California. *Limnol. Oceanogr.* **44**: 512–529, doi:10.4319/lo.1999.44.3.0512
- MacIntyre, S., A. Jonsson, M. Jansson, J. Aberg, D. E. Turney, and S. D. Miller. 2010. Buoyancy flux, turbulence, and the gas transfer coefficient in a stratified lake. *Geophys. Res. Lett.* **37**: L24604, doi:10.1029/2010GL044164
- Manne, A. S., and R. G. Richels. 2001. An alternative approach to establishing trade-offs among greenhouse gases. *Nature* **410**: 675–677, doi:10.1038/35070541
- Mariotti, A., J. C. Germon, P. Hubert, P. Kaiser, R. Letolle, A. Tardieux, and P. Tardieux. 1981. Experimental determination of nitrogen kinetic isotope fractionation: Some principles; illustrations for the denitrification and nitrification processes. *Plant Soil* **62**: 413–430, doi:10.1007/BF02374138
- Mau, S., J. Blees, E. Helmke, H. Niemann, and E. Damm. 2013. Vertical distribution of methane oxidation and methanotrophic response to elevated methane concentrations in stratified waters of the Arctic fjord Storfjorden (Svalbard, Norway). *Biogeosciences* **10**: 6267–6278, doi:10.5194/bg-10-6267-2013

- McCave, I. N. 1986. Local and global aspects of the bottom nepheloid layers in the world ocean. *Netherlands J. Sea Res.* **20**: 167–181, doi:10.1016/0077-7579(86)90040-2
- McDonald, I. R., E. M. Kenna, and J. C. Murrell. 1995. Detection of methanotrophic bacteria in environmental samples with the PCR. *Appl. Environ. Microbiol.* **61**: 116–121.
- McGinnis, D. F., J. Greinert, Y. Artemov, S. E. Beaubien, and a. Wüest. 2006. Fate of rising methane bubbles in stratified waters: How much methane reaches the atmosphere? *J. Geophys. Res.* **111**: C09007, doi:10.1029/2005JC003183
- Metcalf, W. W., B. M. Griffin, R. M. Cicchillo, J. Gao, S. C. Janga, H. A. Cooke, B. T. Circello, B. S. Evans, W. Martens-Habbena, D. A. Stahl, and W. A. van der Donk. 2012. Synthesis of methylphosphonic acid by marine microbes: A source for methane in the aerobic ocean. *Science* **337**: 1104–1107, doi:10.1126/science.1219875
- Milucka, J., T. G. Ferdelman, L. Polerecky, D. Franzke, G. Wegener, M. Schmid, I. Lieberwirth, M. Wagner, F. Widdel, and M. M. M. Kuypers. 2012. Zero-valent sulphur is a key intermediate in marine methane oxidation. *Nature* **491**: 541–546, doi:10.1038/nature11656
- Moss, C. W., and M. A. Lambert-Fair. 1989. Location of double bonds in monounsaturated fatty acids of *Campylobacter cryaerophila* with dimethyl disulfide derivatives and combined gas chromatography-mass spectrometry. *J. Clin. Microbiol.* **27**: 1467–1470.
- Murase, J., Y. Sakai, A. Kametani, and A. Sugimoto. 2005. Dynamics of methane in mesotrophic Lake Biwa, Japan. *Ecol. Res.* **20**: 377–385, doi:10.1007/s11284-005-0053-x
- Murase, J., and A. Sugimoto. 2005. Inhibitory effect of light on methane oxidation in the pelagic water column of a mesotrophic lake (Lake Biwa, Japan). *Limnol. Oceanogr.* **50**: 1339–1343, doi:10.4319/lo.2005.50.4.1339

- Naguib, M. 1976. Stoichiometry of methane oxidation in the methane-oxidizing strain M 102 under the influence of various CH<sub>4</sub>/O<sub>2</sub> mixtures. *Z. Allg. Mikrobiol.* **16**: 437–444, doi:10.1002/jobm.3630160604
- Nercessian, O., E. Noyes, M. G. Kalyuzhnaya, M. E. Lidstrom, and L. Chistoserdova. 2005. Bacterial populations active in metabolism of C<sub>1</sub> compounds in the sediment of Lake Washington, a freshwater lake. *Appl. Environ. Microbiol.* **71**: 6885–6899, doi:10.1128/AEM.71.11.6885-6899.2005
- Nichols, P. D., J. B. Guckert, and D. C. White. 1986. Determination of monounsaturated fatty acid double-bond position and geometry for microbial monocultures and complex consortia by capillary GC-MS of their dimethyl disulphide adducts. *J. Microbiol. Meth.* **5**: 49–55, doi:10.1016/0167-7012(86)90023-0
- Niemann, H., and M. Elvert. 2008. Diagnostic lipid biomarker and stable carbon isotope signatures of microbial communities mediating the anaerobic oxidation of methane with sulphate. *Org. Geochem.* **39**: 1668–1677, doi:10.1016/j.orggeochem.2007.11.003
- Niemann, H., M. Elvert, M. Hovland, B. Orcutt, A. Judd, I. Suck, J. Gutt, S. Joye, E. Damm, and K. Finster. 2005. Methane emission and consumption at a North Sea gas seep (Tommeliten area). *Biogeosciences* **2**: 335–351, doi:10.5194/bg-2-335-2005
- Nüsslein, B., K. J. Chin, W. Eckert, and R. Conrad. 2001. Evidence for anaerobic syntrophic acetate oxidation during methane production in the profundal sediment of subtropical Lake Kinneret (Israel). *Environ. Microbiol.* **3**: 460–70, doi:10.1046/j.1462-2920.2001.00215.x
- Panganiban, A., T. Patt, W. Hart, and R. S. Hanson. 1979. Oxidation of methane in the absence of oxygen in lake water samples. *Appl. Environ. Microbiol.* **37**: 303–309.
- Penning, H., P. Claus, P. Casper, and R. Conrad. 2006. Carbon isotope fractionation during acetoclastic methanogenesis by *Methanosaeta*

- concilii* in culture and a lake sediment. Appl. Environ. Microbiol. **72**: 5648–5652, doi:10.1128/AEM.00727-06
- Petit, J. R., J. Jouzel, D. Raynaud, N. I. Barkov, J.-M. Barnola, I. Basile, M. Bender, J. Chappellaz, M. Davis, G. Delaygue, M. Delmotte, V. M. Kotlyakov, M. Legrand, V. Y. Lipenkov, C. Lorius, L. Pépin, C. Ritz, E. Saltzman, and M. Stievenard. 1999. Climate and atmospheric history of the past 420,000 years from the Vostok ice core, Antarctica. *Nature* **399**: 429–436, doi:10.1038/20859
- Posch, T., M. Loferer-Kröbächer, G. Gao, A. Alfreider, J. Pernthaler, and R. Psenner. 2001. Precision of bacterioplankton biomass determination: A comparison of two fluorescent dyes, and of allometric and linear volume-to-carbon conversion factors. *Aquat. Microb. Ecol.* **25**: 55–63, doi:10.3354/ame025055
- Prior, S. D., and H. Dalton. 1985. The effect of copper ions on membrane content and methane monooxygenase activity in methanol-grown cells of *Methylococcus capsulatus* (Bath). *J. Gen. Microbiol.* **131**: 155–163, doi:10.1099/00221287-131-1-155
- Reeburgh, W. S. 2007. Global methane biogeochemistry, p. 1–32. *In* Treatise on Geochemistry: The Atmosphere, doi:10.1016/B0-08-043751-6/04036-6
- Rees, T. D., A. B. Gyllenspetz, and A. C. Docherty. 1971. The determination of trace amounts of sulphide in condensed steam with *NN*-diethyl-*p*-phenylenediamine. *Analyst* **96**: 201–208, doi:10.1039/an9719600201
- Ren, T., J. A. Amaral, and R. Knowles. 1997. The response of methane consumption by pure cultures of methanotrophic bacteria to oxygen. *Can. J. Microbiol.* **43**: 925–928, doi:10.1139/m97-133
- Revsbech, N. P., L. H. Larsen, J. Gundersen, T. Dalsgaard, O. Ulloa, and B. Thamdrup. 2009. Determination of ultra-low oxygen concentrations in oxygen minimum zones by the STOX sensor. *Limnol. Oceanogr.: Meth.* **7**: 371–381, doi:10.4319/lom.2009.7.371

- Roslev, P., and G. M. King. 1994. Survival and recovery of methanotrophic bacteria starved under oxic and anoxic conditions. *Appl. Environ. Microbiol.* **60**: 2602–2608.
- Roslev, P., and G. M. King. 1995. Aerobic and anaerobic starvation metabolism in methanotrophic bacteria. *Appl. Environ. Microbiol.* **61**: 1563–1570.
- Rudd, J. W. M., A. Furutani, R. J. Flett, and R. D. Hamilton. 1976. Factors controlling methane oxidation in shield lakes: The role of nitrogen fixation and oxygen concentration. *Limnol. Oceanogr.* **21**: 357–364, doi:10.4319/lo.1976.21.3.0357
- Rudd, J. W. M., R. D. Hamilton, and N. E. R. Campbell. 1974. Measurement of microbial oxidation of methane in lake water. *Limnol. Oceanogr.* **19**: 519–524.
- Rusanov, I. I., S. K. Yusupov, A. S. Savvichev, A. Y. Lein, N. V. Pimenov, and M. V. Ivanov. 2004. Microbial production of methane in the aerobic water layer of the Black Sea. *Dokl. Biol. Sci. Proc. Acad. Sci. USSR, Biol. Sci. Sect. / Transl. from Russ.* **399**: 493–495, doi:10.1007/s10630-005-0021-1
- Sakai, Y., J. Murase, A. Sugimoto, K. Okubo, and E. Nakayama. 2002. Resuspension of bottom sediment by an internal wave in Lake Biwa. *Lakes Reservoirs: Res. and Manage.* **7**: 339–344, doi:10.1046/j.1440-1770.2002.00200.x
- Schmid, M., M. Halbwachs, B. Wehrli, and A. Wüest. 2005. Weak mixing in Lake Kivu: New insights indicate increasing risk of uncontrolled gas eruption. *Geochem. Geophys. Geosyst.* **6**, doi:10.1029/2004GC000892
- Schönheit, P., H. Keweloh, and R. K. Thauer. 1981. Factor F<sub>420</sub> degradation in *Methanobacterium thermoautotrophicum* during exposure to oxygen. *FEMS Microbiol. Lett.* **12**: 347–349, doi:10.1111/j.1574-6968.1981.tb07671.x
- Schubert, C. J., M. J. L. Coolen, L. N. Neretin, A. Schippers, B. Abbas, E. Durisch-Kaiser, B. Wehrli, E. C. Hopmans, J. S. S. Damsté, S.

- Wakeham, and M. M. M. Kuypers. 2006. Aerobic and anaerobic methanotrophs in the Black Sea water column. *Environ. Microbiol.* **8**: 1844–1856, doi:10.1111/j.1462-2920.2006.01079.x
- Schubert, C. J., T. Diem, and W. Eugster. 2012. Methane emissions from a small wind shielded lake determined by eddy covariance, flux chambers, anchored funnels, and boundary model calculations: A comparison. *Environ. Sci. Technol.* **46**: 4515–22, doi:10.1021/es203465x
- Schubert, C. J., F. S. Lucas, E. Durisch-Kaiser, R. Stierli, T. Diem, O. Scheidegger, F. Vazquez, and B. Müller. 2010. Oxidation and emission of methane in a monomictic lake (Rotsee, Switzerland). *Aquat. Sci.* **72**: 455–466, doi:10.1007/s00027-010-0148-5
- Schubert, C. J., F. Vazquez, T. Lösekann-Behrens, K. Knittel, M. Tonolla, and A. Boetius. 2011. Evidence for anaerobic oxidation of methane in sediments of a freshwater system (Lago di Cadagno). *FEMS Microbiol. Ecol.* **76**: 26–38, doi:10.1111/j.1574-6941.2010.01036.x
- Shrestha, M., W.-R. Abraham, P. M. Shrestha, M. Noll, and R. Conrad. 2008. Activity and composition of methanotrophic bacterial communities in planted rice soil studied by flux measurements, analyses of *pmoA* gene and stable isotope probing of phospholipid fatty acids. *Environ. Microbiol.* **10**: 400–412, doi:10.1111/j.1462-2920.2007.01462.x
- Sieber, J. R., M. J. McNerney, C. M. Plugge, B. Schink, and R. P. Gunsalus. 2010. Methanogenesis: Syntrophic metabolism, p. 337–355. *In* K.N. Timmis [ed.], *Handbook of hydrocarbon and lipid microbiology*. Springer, doi:10.1007/978-3-540-77587-4\_22
- Sieburth, J. M., and P. L. Donaghay. 1993. Planktonic methane production and oxidation within the algal maximum of the pycnocline: Seasonal fine-scale observations in an anoxic estuarine basin. *Mar. Ecol.-Prog. Ser.* **100**: 3–15.
- Sigman, D. M., R. Robinson, A. N. Knapp, A. van Geen, D. C. McCorkle, J. A. Brandes, and R. C. Thunell. 2003. Distinguishing between water column and sedimentary denitrification in the Santa Barbara

- Basin using the stable isotopes of nitrate. *Geochem. Geophys. Geosyst.* **4**, doi:10.1029/2002GC000384
- Sivan, O., M. Adler, A. Pearson, F. Gelman, I. Bar-Or, S. G. John, and W. Eckert. 2011. Geochemical evidence for iron-mediated anaerobic oxidation of methane. *Limnol. Oceanogr.* **56**: 1536–1544, doi:10.4319/lo.2011.56.4.1536
- Spinrad, R. W., R. J. van Zaneveld, and J. C. Kitchen. 1983. A study of the optical characteristics of the suspended particles in the benthic nepheloid layer of the Scotian Rise. *J. Geophys. Res.* **88**: 7641–7645, doi:10.1029/JC088iC12p07641
- Tamura, K., D. Peterson, N. Peterson, G. Stecher, M. Nei, and S. Kumar. 2011. MEGA5: Molecular evolutionary genetics analysis using maximum likelihood, evolutionary distance, and maximum parsimony methods. *Mol. Biol. Evol.* **28**: 2731–2739, doi:10.1093/molbev/msr121
- Tavormina, P. L., W. Ussler, J. A. Steele, S. A. Connon, M. G. Klotz, and V. J. Orphan. 2013. Abundance and distribution of diverse membrane-bound monooxygenase (Cu-MMO) genes within the Costa Rica oxygen minimum zone. *Environ. Microbiol. Rep.* **5**: 414–423, doi:10.1111/1758-2229.12025
- Thunell, R. C., D. M. Sigman, F. Muller-Karger, Y. Astor, and R. Varela. 2004. Nitrogen isotope dynamics of the Cariaco Basin, Venezuela. *Global Biogeochem. Cy.* **18**: GB3001, doi:10.1029/2003GB002185
- Tiano, L. 2013. Microbial respiration and gene expression as a function of very low oxygen concentration. Ph.D. thesis. Aarhus University.
- Treude, T., A. Boetius, K. Knittel, K. Wallmann, and B. B. Jørgensen. 2003. Anaerobic oxidation of methane above gas hydrates at Hydrate Ridge, NE Pacific Ocean. *Mar. Ecol.-Prog. Ser.* **264**: 1–14, doi:10.3354/meps264001
- Trotsenko, Y. A., and J. C. Murrell. 2008. Metabolic aspects of aerobic obligate methanotrophy. *Adv. Appl. Microbiol.* **63**: 183–229, doi:10.1016/S0065-2164(07)00005-6

- Tsutsumi, M., T. Iwata, H. Kojima, and M. Fukui. 2011. Spatiotemporal variations in an assemblage of closely related planktonic aerobic methanotrophs. *Freshwater Biol.* **56**: 342–351, doi:10.1111/j.1365-2427.2010.02502.x
- Valentine, D. L., and W. S. Reeburgh. 2000. New perspectives on anaerobic methane oxidation. *Environ. Microbiol.* **2**: 477–484, doi:10.1046/j.1462-2920.2000.00135.x
- Vigano, I., H. van Weelden, R. Holzinger, F. Keppler, A. McLeod, and T. Röckmann. 2008. Effect of UV radiation and temperature on the emission of methane from plant biomass and structural components. *Biogeosciences* **5**: 937–947, doi:10.5194/bg-5-937-2008
- Wainright, S. C. 1990. Sediment-to-water fluxes of particulate material and microbes by resuspension and their contribution to the planktonic food web. *Mar. Ecol.-Prog. Ser.* **62**: 271–281, doi:10.3354/meps062271
- Walter Anthony, K. M., P. Anthony, G. Grosse, and J. Chanton. 2012. Geologic methane seeps along boundaries of Arctic permafrost thaw and melting glaciers. *Nat. Geosci.* **5**: 419–426, doi:10.1038/ngeo1480
- Walter, K. M., L. C. Smith, and F. S. Chapin. 2007. Methane bubbling from northern lakes: Present and future contributions to the global methane budget. *Philos. Trans. A. Math. Phys. Eng. Sci.* **365**: 1657–1676, doi:10.1098/rsta.2007.2036
- Wanninkhof, R., W. E. Asher, D. T. Ho, C. Sweeney, and W. R. McGillis. 2009. Advances in quantifying air-sea gas exchange and environmental forcing. *Ann. Rev. Mar. Sci.* **1**: 213–244, doi:10.1146/annurev.marine.010908.163742
- Warneck, P. 2000. Chemistry of the troposphere: The methane oxidation cycle, p. 157–210. *In* *Chemistry of the Natural Atmosphere*. Academic Press.
- Wartiainen, I., A. G. Hestnes, I. R. McDonald, and M. M. Svenning. 2006. *Methylobacter tundripaludum* sp. nov., a methane-oxidizing

- bacterium from Arctic wetland soil on the Svalbard islands, Norway (78° N). *Int. J. Syst. Evol. Microbiol.* **56**: 109–13, doi:10.1099/ijs.0.63728-0
- Wenk, C. B., J. Blees, J. Zopfi, M. Veronesi, A. Bourbonnais, C. J. Schubert, H. Niemann, and M. F. Lehmann. 2013. Anaerobic ammonium oxidation (anammox) bacteria and sulfide-dependent denitrifiers coexist in the water column of a meromictic south-alpine lake. *Limnol. Oceanogr.* **58**: 1–12, doi:10.4319/lo.2013.58.1.0001
- Wenk, C. B., J. Zopfi, J. Blees, M. Veronesi, H. Niemann, and M. F. Lehmann. 2014. Community N and O isotope fractionation by sulfide-dependent denitrification and anammox in a stratified lacustrine water column. *Geochim. Cosmochim. Ac.* **125**: 551–563, doi:10.1016/j.gca.2013.10.034
- Whiticar, M. J. 1999. Carbon and hydrogen isotope systematics of bacterial formation and oxidation of methane. *Chem. Geol.* **161**: 291–314, doi:10.1016/S0009-2541(99)00092-3
- Whiticar, M. J., and E. Faber. 1986. Methane oxidation in sediment and water column environments – Isotope evidence. *Org. Geochem.* **10**: 759–768, doi:10.1016/S0146-6380(86)80013-4
- Whittenbury, R., K. C. Phillips, and J. F. Wilkinson. 1970. Enrichment, isolation and some properties of methane-utilizing bacteria. *J. Gen. Microbiol.* **61**: 205–218, doi:10.1099/00221287-61-2-205
- Wieland, E., P. Lienemann, S. Bollhalder, A. Lück, and P. H. Santschi. 2001. Composition and transport of settling particles in Lake Zurich: Relative importance of vertical and lateral pathways. *Aquat. Sci.* **63**: 123–149, doi:10.1007/PL00001347
- Wiesenburg, D. A., and N. L. Guinasso. 1979. Equilibrium solubilities of methane, carbon monoxide, and hydrogen in water and sea water. *J. Chem. Eng. Data* **24**: 356–360, doi:10.1021/je60083a006
- Wuebbles, D. J., and K. Hayhoe. 2002. Atmospheric methane and global change. *Earth-Sci. Rev.* **57**: 177–210.

- Wüest, A., W. Aeschbach-Hertig, H. Baur, M. Hofer, R. Kipfer, and M. Schurter. 1992. Density structure and tritium-helium age of deep hypolimnetic water in the northern basin of Lake Lugano. *Aquat. Sci.* **54**: 205–218, doi:10.1007/BF00878137
- Zaikova, E., D. A. Walsh, C. P. Stilwell, W. W. Mohn, P. D. Tortell, and S. J. Hallam. 2010. Microbial community dynamics in a seasonally anoxic fjord: Saanich Inlet, British Columbia. *Environ. Microbiol.* **12**: 172–191, doi:10.1111/j.1462-2920.2009.02058.x
- Zehnder, A. J. B., and T. D. Brock. 1979. Methane formation and methane oxidation by methanogenic bacteria. *Time* **137**: 420–432.
- Zopfi, J., T. G. Ferdelman, B. B. Jorgensen, A. Teske, and B. Thamdrup. 2001. Influence of water column dynamics on sulfide oxidation and other major biogeochemical processes in the chemocline of Mariager Fjord (Denmark). *Mar. Chem.* **74**: 29–51, doi:10.1016/S0304-4203(00)00091-8

## Acknowledgments

---

This dissertation chronicles an important part of my life: the years I spent in Basel on my PhD research, my coming of age as a researcher. However, it does not do justice to the people around me and behind me, who guided and supported me. Because one does not pursue a PhD alone. Foremost I wish to express my intense gratitude to my supervisors, Moritz Lehmann and Helge Niemann. You provided a professional and social atmosphere in the group of which other PhD students are rightly jealous. I could always count on your thorough and constructive criticism. It has not always been an easy ride, but I have learned much, and whatever I may lack as a researcher now is certainly not through your lack of trying!

Both Helge and Moritz have constantly supported my development as a scientist. From the very beginning Helge has taught me rigorous planning of field campaigns, anticipating the unexpected, and getting the most out of any campaign. He also introduced me to a great number of people, and it was through his contacts in Bremen that I was able to perform the initial  $^{14}\text{C}$ -tracer experiments. Moritz encouraged me to present my work at conferences from early on. He also made it possible for me to attend the Microbial Diversity summer course at the Marine Biological Laboratory in Woods Hole, which has radically changed and broadened my outlook on biogeochemistry and geomicrobiology. I could not have wished for better supervisors, and I will sorely miss their support and constructive criticism.

I am particularly grateful to my external co-examiner, and the external

expert, Tim Eglinton and Helmut Bürgmann, who both did not hesitate to be on my thesis committee.

Studying methanotrophic bacteria, even a geochemist cannot get around some microbiology, and here I have to give credit to Jakob Zopfi. Jakob has supported me both with his expertise and by organising that I could use the laboratory infrastructure in Neuchâtel. Here, I also wish to thank Pilar Junier, who provided Christine and me with space in her laboratory, and who always made us feel welcome and at home.

Christine Wenk deserves a special place in my acknowledgments for the important part she played. We worked together on a joint project, investigating methane and nitrogen dynamics in Lake Lugano. This means we could easily and freely share and discuss data, and plan sampling campaigns together. It has been a great four years working with you on the lake, in the lab, and in the office.

I did most of the methane concentration measurements, and all methane isotope measurements that are part of this dissertation at the EAWAG in Kastanienbaum, in the laboratory of Carsten Schubert. I wish to thank Carsten for providing that opportunity. In the laboratory in Kastanienbaum, I received the greatest support from Gijs Nobbe. Gijs, bedankt voor al je hulp, en voor de goeie sfeer in het lab. Het was altijd mooi een stukje Holland in hartje Zwitserland te hebben. Het was me een eer en een genoegen in jouw lab te kunnen werken.

Especially during the first half of my time as a PhD student, I had the opportunity to work in the laboratory at the Max Planck Institute for Marine Microbiology in Bremen. I am very grateful to Antje Boetius for

providing this opportunity. This dissertation would have been impossible without it. In the lab, I could not have wished for someone better than Gabi to show me around, support me, and generally have lots of laughs with. Thank you Gabi, for the great time in Bremen.

In the lab in Bremen I also met Susan Mau, in the sort of chance encounter that is so important in science. It was very nice how we got along instantly, from the first sampling in the frozen pond outside the MPI to this day. The cruise to Spitsbergen was an amazing opportunity, both scientifically and personally, and I am grateful to Susan, Ellen Damm and Michael Schlüter, for allowing me to come on that cruise. Michael Schlüter and Torben Gentz also deserve special mention for coming all the way to Lugano with their in situ MIMS. It is unfortunate that it didn't work out, but the fourth chapter of this dissertation was born out of that campaign.

I wish to express my sincerest gratitude to Bo Thamdrup. With his STOX measurements on incubation vials, we could accurately determine the O<sub>2</sub> consumption rate, and the time required for anoxia to establish in incubations. This was crucial for the experiments described in chapter 2. I also wish to thank Mathias Kirf, who accurately determined the depth of the interface between the oxic and anoxic waters in the northern basin of Lake Lugano, and the extent of the zone of sub-micromolar oxygen concentrations. The joint campaigns on Lake Lugano were a fruitful cooperation, and great fun.

The research described between these covers relies heavily on fieldwork campaigns on Lake Lugano. Without the constant and tireless work and support of Mauro Veronesi, Marco Simona and Stefano Beatrizotti this would have been impossible. They are the main reason why I always loved going to Lugano, to collect yet another batch of

samples. I have fond memories of the long days on the lake, which are among the best of my time as a PhD student.

In Basel, the home lab, Mark Rollog and Marianne Caroni kept the various labs running, and I could always count on their support. Of course, Mark, I also wish to thank you here for the countless beers, whether homebrew or other, and the good times both at and after work. We have always had a great social atmosphere in the group, and I would like to thank my former office mate Yael, and my office mates of the next generation Lea and Yuki, for the pleasant and open atmosphere in the office. I also thank Matthias, Jan Paul, Gregor, Stefan, Emiliano, Axel, Dörte and Caitlin for the good times, sometimes just a chat, a cup of coffee and a laugh.

Thanks are also due to Markus Erne, who is currently writing his BSc thesis about surface water methane concentrations in Lake Lugano and its emission to the atmosphere. The trips we made to Lugano have been very productive, and on top of that great fun. It was great to work with you, Markus.

Every saga has a beginning... And so this saga began, before I even considered coming to Basel. Lipid biomarker research and compound specific isotope analysis have been the cornerstones of my PhD work, but I was initiated into these fields during my MSc studies in Bremen, under the guidance of Solveig Bühring. I cannot begin to imagine where I would be if it hadn't been for her, and I can safely say that Solveig is the mother of the scientific me. Thank you Solveig, for the confidence you've shown in me, not only during my brief time in Bremen, but also all these years since.

The people mentioned above have all been important to my work and my life over the past years. However, none of that would have mattered if it weren't for the unwavering support I have always enjoyed from my parents. Pap, mam, er zijn geen woorden die kunnen beschrijven hoeveel ik aan jullie te danken heb. Zonder jullie constante steun zou ik hier nu niet zitten om het dankwoord van mijn proefschrift te schrijven. Met gepaste trots, en met de erkenning dat ik op de schouders van reuzen sta, treed ik in de voetsporen van mijn vader.

My family has always been a great support to me, and that is not in the least due to the greatest big sister a little brother could wish for. Even though you're far away, you have been instrumental in getting me here.

I am immensely grateful to my friends, old and new, who have kept me sane by providing much-needed distractions, and sometimes simply by putting things in perspective. Your friendship is a great gift. I couldn't have done this without you. In this sense I especially wish to thank the other JRR. Three more people stand out because they have been with me, even if not in a physical sense, since the beginning of my academic career. Rogier, thank you for skiing, climbing and whisky; David, it's been some long years, but we all go the same way home. And the third... I must have forgotten, but I thank St. Paddy in his name.

Basel, June 2013